New functions for an archaeal translation factor

Flavia Bassani

Supervisor: Prof. Anna La Teana

PhD Program

Biomolecular Sciences: XV Cycle

Università Politecnica delle Marche

2017

3.3.2016

Summary

Protein synthesis is a process conserved among the three primary domains of life, in which the genetic information is translated into working proteins.

The translational machinery has been extensively studied in bacteria and eukaryotes, whereas the archaeal one is still poorly characterized, therefore a better understanding of the translation process in Archaea could help to clarify several aspects, which have been conserved during the evolution.

In this regards the structural and functional study of translation factors, with high homology between archaea and eukaryotes, is important to determine not only their role in protein synthesis but also to help understand their role in physiological and pathological cellular processes.

The aim of this thesis is to shed light on the archaeal protein aIF5A, a translation factor highly conserved and essential in eukaryotes and archaea, whose requirement in protein synthesis remains elusive.

The eukaryotic eIF5A and the bacterial ortholog EF-P, post-translationally modified through a distinct pathway, were identified as initiation factors, but subsequent studies highlight their implication in translation elongation.

Recently it was also reported the involvement of the eukaryotic eIF5A in translation termination, however the function of the archaeal homologue is still unknown, as well as its post-translational modification.

The gene appears to be essential and the modification seems to be important, since at least its inhibition in some Archaea causes a rapid and reversible arrest of growth.

Significant studies have been carried out in the Euryarchaeota kingdom, in which it was shown for the first time that aIF5A has RNA degrading activity *in vitro* and can be modified via an alternative modification pathway.

Information on the archaeal aIF5A in *Chrenarchaeota*, which appears to be closely related to eukaryotes, is extremely limited and in order to fill this gap we investigate the role of the protein in the model organism *Sulfolobus solfataricus* (Sso), highlighting unreleased features of this factor.

The first part of the thesis focuses on the subcellular localization of the protein and the identification of its post-translational modification.

The fractionation of *Sulfolobus solfataricus* whole-cell extract on sucrose density gradients allowed us to determine the behavior and localization of aIF5A.

Whilst the expression of the protein in Sso followed by affinity purification and mass spectrometry analysis enable the detection of the post-translational modification.

The second part of the thesis is aimed at identifying interacting partners (proteins and RNAs) of Sso-aIF5A, providing new hints of the protein involvement in several cellular processes.

Taken together our evidences suggest the probable involvement of aIF5A in mRNA stability/turnover and its multifunctional role, which in *Sulfolobus* can be modulated by the hypusination itself or by the structural conformation of the protein.

Contents

List of Figures

List of Tables

1. Introduction

Decoding the evolutionary history, translation is one of the most conserved cellular processes, although each of the three primary domains has elaborated specific variants of some steps; the elongation phase is essentially invariant in all cells, whereas translation initiation, termination and ribosome recycling, have specific features [1].

The translation initiation process is one of the most delicate moment of protein synthesis due to two fundamental events, the recognition of the mRNA start codon and the setting of the correct reading frame.

The selection of the start codon by the ribosome entails the play of accessory proteins called translation initiation factors (IFs).

Due to their crucial role in the translation process, most of them have been functionally characterized, in particular the eukaryal and bacterial ones.

The only ambiguous protein, which might have been improperly included among the initiation factors, is the translation initiation factor IF5A, homologous between Eukarya and Archaea and with an orthologue, EF-P, in Prokaryotes.

1.1. The eukaryotic translation factor eIF5A

1.1.1. Structural features and hypusination

The eukaryotic translation factor eIF5A is a small protein (17 kDa) highly conserved and essential.

The protein consists of two distinct domains: the N-terminal domain (SH3-like domain) composed of six β-strands, which fold into a partially open β-barrel, and the C-terminal domain, which is formed by 3–5 β-strands and 0–2 α-helices and resembles an OB-fold domain.

Multiple alignment of eIF5A amino acid sequences shows a strong conservation, in particular, in the N-terminal domain.

This is conserved among the three primary domains, and conservation is especially evident in the region surrounding the lysine residue at position 50 (Lys 50) that is the site of a unique post-translational modification: hypusination.

The hypusine residue resides in the long unstructured loop, between strands β3 and β4, which protrudes from the N-terminal domain [2].

The eukaryal eIF5A exists as a dimer, not only *in vitro* but also *in vivo*, independently of the presence of the hypusine residue or the ribosome, but dependently on RNA [3]. RNase treatment of the affinity-purified protein eIF5A in yeast, followed by size-exclusion chromatography, leads to the disruption of the dimer *in vitro*.

The oligomeric state of the protein does not depend on electrostatic interactions and disulfide bridges, in agreement with a previous study [4], which suggested that hypusine is necessary for eIF5A dimerization *in vitro*; however this discrepancy may be due to different experimental conditions.

This region is positively charged for the presence of the hypusine residue, whereas the overall content of acidic residues is concentrated in the C-terminal domain.

The eukaryotic translation factor eIF5A is the sole protein known that contains the unique polyamine-derived amino acid, hypusine [Nε-(4-amino-2-hydroxybutyl) lysine], discovered in 1971 [5].

Polyamines are synthesized via highly regulated pathways and these small aliphatic molecules are involved in a myriad of cellular processes, as cations they can bind to nucleic acids and promote cellular proliferation and signaling.

This residue was initially called “hypusine” according to the structure that consist of two moieties, hydroxyputrescine and lysine, and its biosynthesis is accomplished by two distinct enzymatic steps (figure 1).

In the first reaction, the enzyme deoxyhypusine synthase (DHS) transfers the 4-amino butyl moiety of spermidine (synthesized in the L-arginine metabolism) to the ε-amino group of one specific lysine residue (Lys50 for the human protein) of the protein precursor to form the deoxyhypusine residue.

The second enzyme deoxyhypusine hydroxylase (DOHH) subsequently hydroxylates this intermediate to form the hypusine residue and mature form of eIF5A [2, 6].

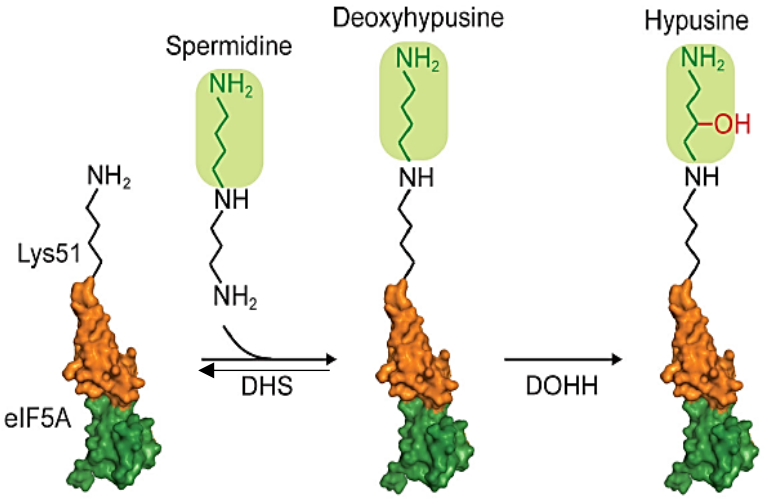

Figure 1. Post-translational modification pathway for the eukaryal eIF5A *[2].*

Many insights about the essential protein eIF5A and its modification arise from experimental evidence in *Saccharomyces cerevisiae*.

The DHS enzyme is essential, since the null mutation in the single copy *ydhs* gene results in the loss of cell viability in yeast and, upon depletion of deoxyhypusine synthase, cessation of growth is accompanied by a marked enlargement of cells, suggesting a defect in cell cycle progression or in cell division [7].

The enzyme exhibits an absolute specificity toward its protein substrate but also a very narrow specificity toward spermidine and few of its closely related compounds (homospermidine, aminopropyl cadaverine, cis- and trans-unsaturated spermidine, and N8-methyl- and N8-ethyl spermidines) [6].

The deoxyhypusine synthesis occurs in four steps and in the first one the NAD cofactor is required for the dehydrogenation of spermidine to dehydrospermidine. In the second part of the reaction the dehydrospermidine 4-aminobutyl moiety is cleaved and transferred to the ε-amino group of a lysine residue, present in the active site, to form a covalent enzyme-imine intermediate.

This was demonstrated by trapping it into a stable enzyme-substrate adduct after $NaBH_3CN$ reduction of the mixture containing the enzyme, [1,8-^{3}H] spermidine, NAD and the deoxyhypusine was the labeled component identified.

Thus is now clear that the acceptor of the amino-butyl group is a lysine residue of the enzyme (Lys329 for the human DHS). Substitutions of this particular residue lead to a totally inactive human enzyme and also *S. cerevisiae*'s growth is impaired if the Lys350 of the DHS active site is mutated [8].

In the third step the 4-aminobutyl moiety is transferred to the ε-amino group of a specific lysine of eIF5A, and this imine intermediate is finally reduced to form the deoxyhypusine residue by the enzyme-bound NADH.

An alternative butylamine acceptor of eIF5A lysine is putrescine, which can be converted into homospermidine from spermidine, despite the deoxyhypusine synthesis is the preferred pathway of the DHS reaction.

All the DHS-catalyzed reactions are reversible and this was experimentally validated using a radiolabeled 4-aminobutyl group, which can be transferred to anyone of the three acceptors, eIF5A lysine, putrescine or 1,3-diaminopropane leading to the synthesis of deoxyhypusine, homospermidine or spermidine, respectively [9].

N1-guanyl-1,7-diaminoheptane (GC7) is the most effective inhibitor of deoxhypusine synthase GC7 [10], which leads to anti-proliferative effects, even in human cancer cell lines. The spermidine homolog GC7 inhibits the first step of the hypusination pathway by occluding the DHS binding site for spermidine [11], however, apart from the enzyme inhibition, other effects on cell growth cannot be excluded.

The discovery of this inhibitor was also useful for determining the crystal structure of the human recombinant deoxyhypusine synthase in its ternary complex with the cofactor NAD and the GC7 inhibitor [12, 13].

The human DHS is a tetramer composed of four identical subunits of 40 kDa, two tightly associated dimers and four spermidine-binding sites in each dimer interface.

Deoxyhypusine hydroxylase (DOHH), which completes the modification of eIF5A, through hydroxylation, is also highly conserved among the eukaryotic kingdom.

Although the DHS enzyme has been extensively studied, experimental evidences about DOHH are still limited.

The human DOHH is a α-helix-rich protein (302 amino acids, 32 KDa) characterized by metal-chelating sites in the interior concave structure (diiron core) and belongs to a family of HEAT-repeat-containing proteins [14].

Studies in mammalian cells revealed that the cloned human *dohh* gene is active and the co-expression of the eIF5A precursor, DHS and DOHH is required to obtain the hypusinated eIF5A [15]. The yield of this process is greater than the yield of deoxyhypusinated eIF5A in bacteria co-expressing eIF5A, suggesting that hydroxylation of deoxyhypusine to hypusine blocks this back reaction stabilizing the hypusine.

Moreover the knock-out of *dohh* in mouse was accompanied by the loss of both the hypusine and deoxyhypusine forms of eIF5A [16].

The crystal structure of DOHH is now available and further studies maybe directed towards the identification of selective inhibitors.

It is relevant to mention that the *dohh* gene seems to be essential only in higher multicellular eukaryotes, in fact it does not appear to be essential in *S. cerevisiae*, since the null strain shows only a slow growth phenotype [17].

This may explain also the absence of the *dohh* gene in *Trichomonas vaginalis* genome and the peculiar post-translational modification of the eIF5A precursor in this organism. Hypusination, in this protozoan parasite, occurs thanks to the catalytic activity of a single bifunctional enzyme (TvDHS), which performs both the DHS and DOHH reactions [18]. TvDHS is a mixture of DHS and DOHH features, it has a tetrameric structure and contains a HEAT-motif in each monomer, which let this enzyme also capable of hydroxylase activity.

1.1.2. The role of the eukaryal eIF5A in translation

The eukaryotic factor eIF5A was identified for the first time in the late 1970s during the isolation of translation stimulatory factors from fractionated rabbit reticulocyte lysates [19, 20].

IF-M2Bα, renamed eIF-4D and then eIF5A was isolated from ribosomal high-salt washes and this suggest since the beginning an involvement in translation.

The synthesis of methionyl-puromycin (Met-Pmn) is a classical assay used to characterize initiation factors, in which 80S initiation complexes are assembled *in vitro* and translation is monitored tracing the radioactivity of the radiolabeled methionine, that is transferred from the Met-tRNA in the P site to the puromycin, which mimics the aminoacyl-tRNA in the ribosomal A site.

The eukaryotic factor eIF5A was initially identified as a translation initiator factor that stimulates the Met-Pmn synthesis, facilitating the formation of the first peptide bond and promoting the transition from the initiation to the elongation phase [20].

The Met-Pmn synthesis is a translation initiation step that also reports on elongation activity, anyhow the factor eIF5A was ineffective in any other assay used to characterize translation initiation (*e.g.* binding of initiator Met-tRNA/mRNA to ribosomes).

Subsequent studies in the yeast *Saccharomyces cerevisiae* definitively established that eIF5A plays a role in translation, showing effects in total protein synthesis and polysome profiles upon depletion of the gene.

In *S. cerevisiae* the *tif51a* and *tif51b* genes encode for two proteins that share >60% identity with the human eIF5A and their expression is reciprocally regulated by oxygen.

In one study, the *tif51a* gene, regulated by the galactose promoter, resides in a cassette together with protein-destabilizing elements which rapidly deplete the protein of interest within a single generation; shifting the culture from galactose to glucose, eIF5A depletion causes 4-fold decrease in translation rates [21].

Another approach exploited eIF5A temperature-sensitive mutant and showed that the protein can impairs translation elongation. Once the culture is shortly shifted to the restrictive temperature the inactivation of eIF5A leads to an increase in the average ribosomal transit time and polysome retention [22].

In support of the theory that links eIF5A to translation elongation studies in yeast reported the protein association with ribosomes and polysomes in whole-cell extracts and with the elongation factor eEF2 [23].

Consistent with these findings Gutierrez and coworkers recently reported that the eukaryal protein eIF5A plays a critical role in translation elongation and in particular in translation of polyproline motifs [24]. They developed a set of dual-luciferase reporter constructs in which the 5' *Renilla* luciferase and 3' firefly luciferase open reading frames (ORFs) were separated by ten consecutive codons for each of the twenty amino acids and the activity in the bifunctional *Renilla*-firefly luciferase fusion protein was measured in wild-type eIF5A and the temperature-sensitive eIF5A-S149P mutant yeast strains.

As mentioned before reduced levels of eIF5A impair the growth at semi permissive temperature (33°C) and causes the retention of polysomes in the absence of cycloheximide, suggesting a general translation elongation defect in the strain.

In this dual-luciferase assay, if eIF5A has an impact in the translation of specific amino acids motifs, it is possible to observe a change of the luciferase activity in the temperature mutant strain, when grown at the semipermissive temperature.

What experimentally came out is that only the expression of the reporter, which contains proline codons, is impaired in eIF5A mutant, so the protein promotes translation of polyproline motifs rescuing stalled ribosomes.

This latter aspect was digged more in details in the same study through the toe-printing analysis of eukaryotic ribosomes translating polyproline sequences: the lack of eIF5A leads to the ribosome stall with a diproline codon bound to the P-site and a single Pro codon in the A site.

The analysis of *Saccharomyces cerevisiae* proteome reveals that almost 10% of proteins contains at least one tripeptide motif and the expression of some of them was tested by Gutierrez *et al*. to confirm their data.

Likewise the translation of several yeast polyproline-containing proteins (Ldb17, Eap1, Vrp1) was reduced *in vivo* in eIF5A mutant strains and the hypusine modification of eIF5A is needful for an efficient polyPro synthesis *in vitro*. The same authors proposed a probable scenario of eIF5A bound to the 80S ribosomes confirmed by subsequent structural studies [25].

The cryo-electron microscopy reconstruction of eIF5A in the yeast 80S ribosome (figure 2) showed that the protein is located in the ribosomal subunits interface assuming an L-shape tRNA-like structure.

eIF5A binds between the P and the E sites placing the hypusine side chain near the diprolyl-tRNA in the peptidyl transferase center (PTC) of the ribosome, where it facilitates peptide bond formation.

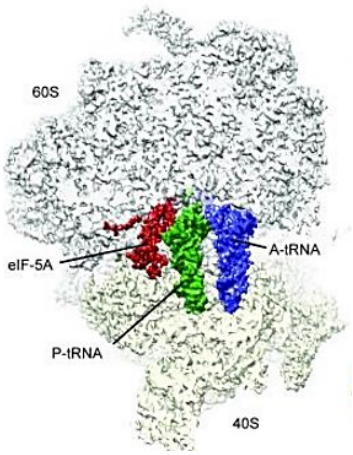

Figure 2. Cryo-EM structure of eIF5A bound to the yeast 80S ribosome *[25].*

In particular, eIF5A recognizes ribosomes that are stalled, and binds in such a way that the hypusine residue interacts with the A76 of the CCA-end of the P-tRNA; this interaction stabilizes the P-tRNA in the optimal geometry for the peptide bond formation.

A recent study described the structure of eIF5A within a rotated state of the 80S ribosome, proposing a dynamic scenario. The protein can interact with the L1-stalk and with helix H69 of the 25S rRNA, implying that eIF5A affinity for the ribosome may depend on the ribosome conformation and its recruitment or release is coupled to the dynamic motions in the ribosome [26].

The structural evidence that eIF5A binds to the E site of the ribosome stabilizing the peptidyl-tRNA urged the curiosity to investigate other probable involvements of the protein in the ribosomal peptidyl transferase center.

A very recent study uncovered for the first time a role for eIF5A in translation termination and a role in elongation broader than previously reported [27].

To asses this the depletion of eIF5A in yeast was carried out through the fusion of the protein with a mini auxin-inducible degron (mAID) tag which, in the presence of auxin, ubiquitinates the mAID- eIF5A fusion protein for proteasome degradation [28].
This allowed them to avoid the alteration of the transcriptional landscape that occurs in temperature-sensitive mutants, providing a good reproducibility without global changes in gene expression introduced by the temperature shift.
The depletion of eIF5A increases the fraction of ribosomes in polysomes and the ribosome profiling revealed a higher ribosome occupancy in the 5'-end relative to the 3'-end, consistent with a general elongation defect as previously discussed.
More in detail the ribosome occupancy on individual genes showed many strong pauses in eIF5A-depleted cells at positions that do not encode only for polyproline motifs and the computational analysis confirmed that eIF5A stimulates translation elongation in many peptide contexts, certainly not limited to proline stretches.
The involvement of eIF5A in translation termination derived from *in vivo* profiling data, in which the ribosome occupancy at stop codons and in the 3' UTR is higher in the depleted strain and from the stimulation of peptidyl-tRNA hydrolysis by eRF1 *in vitro*.
Taken together these observations suggest that ribosomes interact with eIF5A mainly throughout the elongation and termination phases of translation.

1.1.3. Implications of the eukaryal eIF5A in physiological and pathological cellular processes

The role of eIF5A in the translation process has been widely discussed but, due to its abundance in the cell, the eukaryal protein is also involved in various cellular and RNA-related processes, arousing significant physiological and pathological effects.
Studies on the immunodeficiency virus (HIV) reveal that eIF5A is an RNA binding protein.
In particular the protein can facilitate the nucleocytoplasmic transport of viral mRNAs through the RRE (Rev responsive elements) or IRES (iron responsive elements) binding and stimulates their translation initiation events, contributing to human immunodeficiency virus type 1 and human T cell leukemia virus type 1 replication [29].

In this regard, the hypusinated eIF5A is also required for nuclear export and translation of iNos-encoding mRNA, which are crucial steps during the inflammatory damage of islet β cells in the diabetic disease; eIF5A depletion as well as the inhibition of hypusination prevents hyperglycemia in diabetic mouse models [30].

Using SELEX (systematic evolution of ligands by exponential enrichment), it was also possible to show that eIF5A RNA binding is sequence-specific, in fact the SELEX-enriched RNA shares two conserved motifs (UAACCA, AAAUGU) and the binding is hypusine dependent [31]. Later on the same authors combined the affinity co-purification with the differential display, termed SNAAP, and identified *in vivo* the potential physiological RNA targets of eIF5A in HeLa cells [32].

eIF5A-interacting RNAs founded encode proteins such as ribosomal L35a, plasminogen activation inhibitor mRNA-binding protein, NADH dehydrogenase subunit and ADP-ribose pyrophosphatase and some hypothetical proteins.

However to establish if the interaction of eIF5A with this selected groups of RNA may be related to the regulation of their metabolism further analysis are required.

A first hint comes from the predicted structures of these RNAs that exhibit extensive secondary structures containing structural elements, such as hairpins and internal loops [33]. In particular, the C-terminal domain of eIF5A shares a structural similarity with CspA, a putative RNA chaperone and it may functions as an RNA chaperone during translation of a small class of mRNA with extensive secondary structures.

Even in this case studies on temperature-sensitive yeast mutants revealed important information. At the restrictive temperature, eIF5A mutants displayed mRNA decay defects, like the accumulation of NMD-targeted mRNAs, suggesting a direct role of eIF5A in mRNA degradation [34, 35].

Other evidences from the depleted budding yeast suggested an important role for eIF5A and its unique amino acid residue in the control of the cell cycle and proliferation. High-copy genes, involved in cell-wall integrity and actin cytoskeleton polarization, are suppressed in the yeast temperature-sensitive eIF5A mutant, and a similar defect is observed in yeast cells depleted of spermidine and spermine [36].

Even in mammalian cells, several authors observed that the use of hypusine inhibitors, like GC7, lead to the cell proliferation inhibition.

It is obvious from these findings that there is also a correlation between the eukaryal protein and its possible involvement in cancer.

Most mammalian cells and tissues normally express predominantly the *eif5a1* gene and the isoform protein eIF5A1, however only in certain tissues, such as testis and brain another isoform has been identified, eIF5A2, suggesting a tissues specific expression of *eif5a2* gene [6].

A high amplification of the *eif5a2* gene was reported in human ovarian cancer cells [37] and the eIF5A2-isoform is significantly upregulated in mouse embryonic livers and several cancer cell lines, such as the human hepatocellular carcinoma (HCC) cell lines [38] and colorectal (SW-480) cancer line [39].

Turning again to eIF5A RNA-mediated processes, the protein may promotes cell proliferation facilitating the translation of specific, growth-promoting mRNAs, which support DNA replication and hyperproliferation of tumor cells [40].

The considerable therapeutic interest in the eukaryal eIF5A is now directed towards the identification of selective targets, such as the inhibition of hypusination, since it has been shown already that the inhibitor GC7, together with usual chemotherapeutic agents, causes an additive effect in the treatment of cancer cells [41]. Related to this the inhibition of hypusination or the accumulation of eIF5A precursor led to cell apoptosis and this effect was useful in the treatment of mice multiple myeloma, through a net reduction of eIF5A levels by siRNA nanoparticles [42].

eIF5A silencing by RNAi is also particularly interesting in the treatment of malaria that still remains a great problem of public health. Schizonts, transgenic for the enzymes argonaute and dicer, were transfected with a siRNA construct of eIF5A and the parasitemia in rodents decreased within a couple of days [43].

1.2. The bacterial elongation factor EF-P

1.2.1. Structural features and post-translational modification

Identified in 1975 [44], EF-P, the bacterial ortholog of the eukaryal eIF5A, is a small protein (21 kDa) which consists of three β-barrel domains with an overall shape that resembles the L-shape of the tRNA molecule (figure 3).

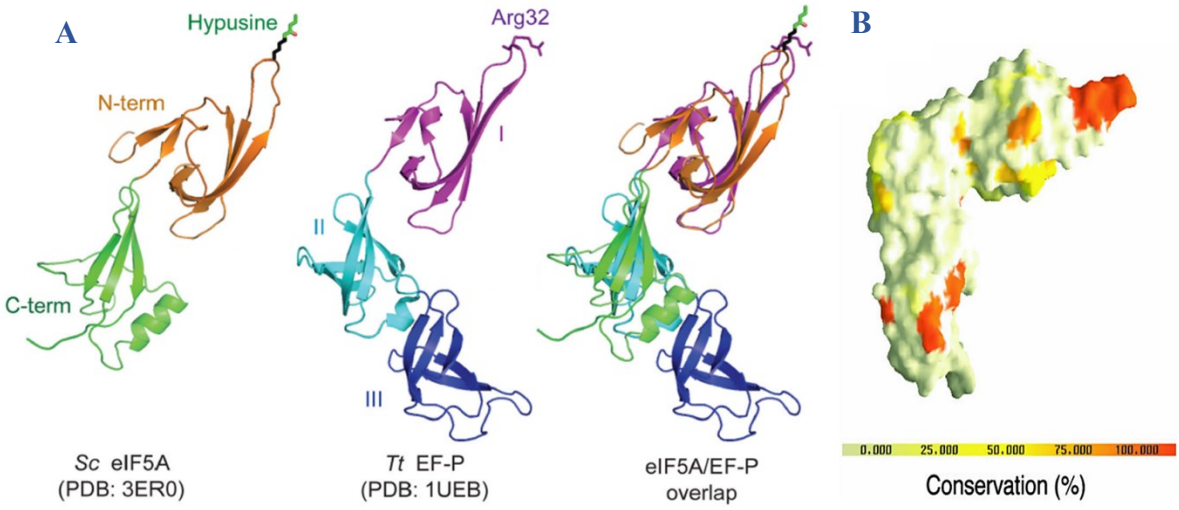

Figure 3. Comparison of eukaryal eIF5A and bacterial EF-P structures. (A) Superimposed structure of *Saccharomyces cerevisiae* eIF5A and *Thermus thermophilus* EF-P [2]. (B) Amino acid residues conserved in T. thermophilus EF-P and *M. jannaschii* aIF5A [45].

One arm of the L contains domain I and II, whereas the other one is formed by domain II and III, which probably originated from a single domain by a duplication event, since they share the same topology [45].

EF-P is an acidic protein (pI = 4.6) and the overall surface is negatively charged, however it has a patch of basic residues in the conserved tip of the N-terminal domain I and in the C-terminal domain III.

The latter one shows a typical OB-fold and is probably favorable for nucleic acid binding, due to the presence of positively charged residues, whereas the negatively charged domain II does not.

Intriguingly both N-terminal and C-terminal domain of the eukaryal eIF5A have the same topology of the N-terminal domain I and domain II of EF-P respectively (figure 3) and, besides their structures are superimposable, these domains share also the same internal flexibility. In addition SAXS analysis of the dimeric yeast eIF5A showed that the molecular envelope has the same topology of EF-P [4].

The alignment of the bacterial EF-P and the eukaryal counterpart eIF5A underlines that around the eukaryal hypusinated Lys50 resides the highest conservation of residues, however neither DHS nor DOHH homologs has been identified in bacteria [6] and in some species the Lys residue in EF-P is replaced by Arg (figure 3).

Nevertheless EF-P undergoes different post-translational modifications that are present in some species, but not in all bacteria.

One of this has been found for the first time in *E.coli* by mass spectrometry analysis of the native EF-P, that revealed a modified Lys34 which contributes an extra mass of ~144 Da [46].

Subsequent studies in *E.coli* and *Salmonella sp.* uncovered the β-lysinylation modification pathway that occurs in three steps and requires three enzymes YjeK, YjeA and YfcM [47-49].

This pathway is predicted to proceed first with the conversion of α-lysine to β-lysine by YjeK, which is a lysine aminomutase. Next the lysyl-tRNA synthetase YjeA transfers, in an ATP-dependent manner, a β-lysine to the ε-amino group of a specific lysine (Lys34 on *E. coli* EF-P).

The evidence that the isomerization of the α-lysine is the first event of the β-lysinylation arouse from biochemical analysis in which the β-lysine was a preferred substrate for the lysyl-tRNA synthetase YjeA than was α-lysine [50]. In the last step, recently discovered, YfcM hydroxylates the lysine residue (figure 4).

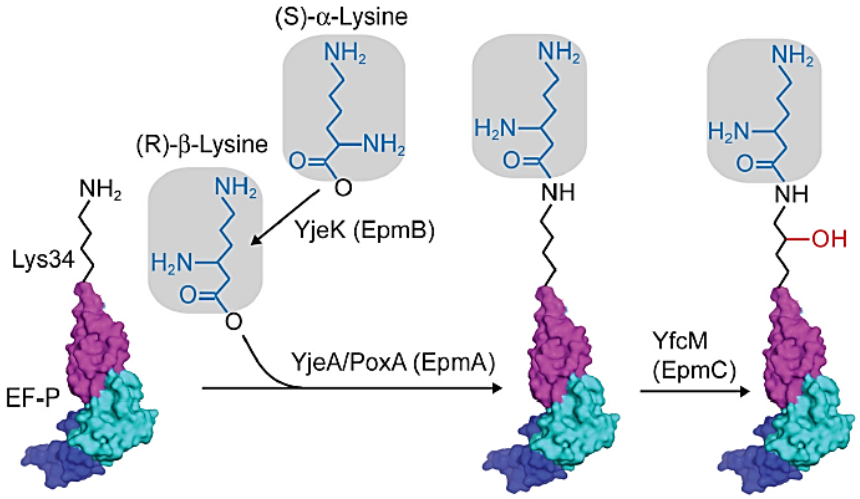

Figure 4. β-lysinylation patway of EF-P *[2].*

The β-lysinylation is necessary for EF-P function in species that contain this modification but not much is known about the protein hydroxylation, despite the loss of *yfcM* in *E. coli* did not affect bacterial growth or antibiotic sensitivity [51].

However this modification pathway is restricted to only one-third of known bacterial genomes and the substitution of the modified lysine by arginine in several bacteria (*e.g. Thermus thermophilus, Pseudomonas aeruginosa, Neisseria meningitidis, Shewanella oneidensis*) leads to the recent discovery of other two modification strategies.

The rhamnosyl modification pathway was described and extensively studied first in *Pseudomonas aeruginosa* and *Shewanella oneidensis.*

A 2'-deoxy-thymidine-β-L-rhamnose is attached on the conserved arginine of EF-P by a glycosyltransferase (EarP) and this is the only glycosylation on arginine known in bacteria, that is also essential for the function of a translation factor [52].

The study of this alternative modification is clinically relevant since it was shown for *Pseudomonas aeruginosa* that the depletion of EarP leads to a defect of growth, decrease in motility and a greater susceptibility toward certain antibiotics.

Another modification was identified in the Gram-positive bacterium *Bacillus subtilis* and consists of a 5-aminopentanol moiety attached to Lys32 of EF-P [53].

Although EF-P and the β-lysinylation have a general housekeeping role in Gram-negative bacteria, the modification in *Bacillus subtilis* plays a role in the synthesis of proteins required for swarming motility.

1.2.2. Function of the elongation factor P

Despite several parallelisms with the eukaryal factor eIF5A, EF-P is not an essential protein, even if described as essential in *E.coli* and was initially identified as an elongation factor.
It was isolated from fractionating cellular components and at the very beginning was assessed the biochemical activity to stimulate formylmethionyl-puromycin peptide (fMet-Puro) synthesis and the production of some fMet-tRNAi initiator dipeptides [44].
However based on the predominant abundance in the post-ribosomal supernatant and the differential peptide-bond stimulation, which depends on the aminoacyl moiety of the acceptor and not only on the presence of fMet-tRNAi [54], EF-P was proposed to be an elongation factor.
The crystal structure analysis of *Thermus thermophilus* EF-P bound to the 70S ribosome (figure 5) leads to a better understand of the protein effect in translation [55].
EF-P resides in the interface of 30S and 50S subunits, between the P and the E site.
EF-P domains I and II, which are superimposable to the N-terminal and C-terminal domains of the eukaryal eIF5A, as mentioned before, interact with the D loop and acceptor stem of tRNA respectively in the ribosome PTC; EF-P domain III binds near the anticodon tRNA stem loop, close to the 30S subunit.
EF-P domain II comes also into direct contact with L1 ribosomal protein, which is involved in tRNA translocation and release.

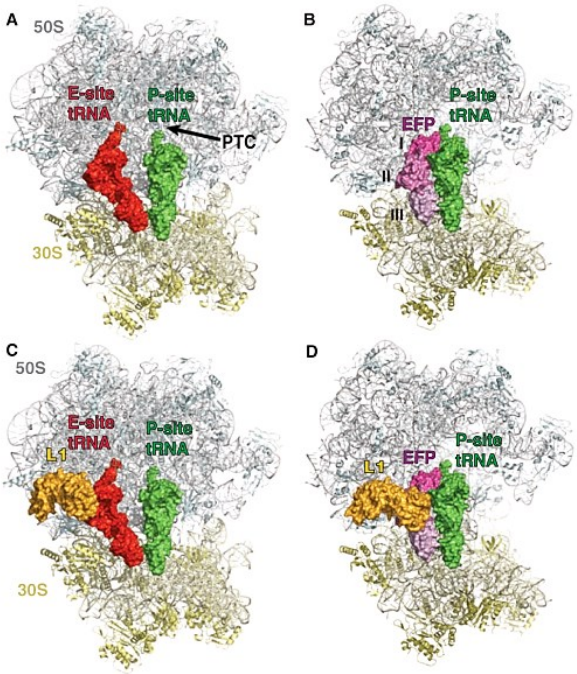

Figure 5. Crystal structure of EF-P bound to the ribosome. (A) E- and P-site tRNAs bound to the 70S ribosome. (B) EF-P and P-site tRNA–binding in the 70S ribosome. (C) E-site tRNA, P-site tRNA and ribosomal protein L1bound to the 70S ribosome. (D) L1 movement from its location in (C), due to the presence of EF-P together with P-site tRNA in the 70S ribosome [55].

In this reconstituted 70S complex the modified residue (β-lysinylated or rhamnosylated) of the bacterial protein resides near the amino acid attached to the 3'-CCA end of tRNA in the P site.

Looking at the structure is evident that EF-P competes with the tRNA in the E-site but its recruitment during translation, relying only on structural data, is difficult to explain.

Interestingly further studies help to address this question, since it was shown that EF-P has a specialized role in translation elongation.

First of all mutants of EF-P, YjeA and YjeK cause the accumulation of polysomes [51], underlying their involvement in translation elongation and the ribosome profiling analysis in *Δefp* strains identified regions of pausing motifs where the ribosome stalled and failed to translate [56].

Previous studies solidified the EF-P role in translation elongation showing that the protein enhanced the synthesis of proteins containing consecutive proline codons [57, 58].

Ude et al. proved that the translation of one of these proteins, CadC, is impaired in strains lacking EF-P or its modifying enzymes, and the mutation of proline codons restored the expression.

Doerfel and coworkers confirmed *in vitro* the stimulatory effect of EF-P in the synthesis of polyproline containing peptides, enhanced by the β-lysyl-lysine modification.

Taken together all these evidences explain the recruitment of EF-P on the ribosome, which is dependent on the conformation/composition of the peptide in the active site and exit tunnel [59] and the involvement of the bacterial protein in the specialized translation of a certain subset of mRNAs.

Anyhow the number of proteins containing polyP, PPG or other stalling motifs is higher in eukaryotes and this could explain why the eukaryal eIF5A is an essential protein, while the bacterial EF-P is not.

It is now clear that EF-P and its post-translational modification play an essential role in the translation of native proteins containing polyproline or stalling motifs and their deletion leads to pleiotropic effects. These proteins are involved in several cellular processes such as bacterial fitness, cell motility, virulence, susceptibility to hyperosmotic conditions, stress resistance and that is the reason why the study of EF-P and its modification pathway is particularly relevant in the antibacterial therapy field.

Curiously, it was reported very recently that EF-P, beyond the support in the translation elongation of polyproline motifs, has also a role in maintaining coupled transcription and translation, when potential terminators (Rho-dependent terminators or hairpin dependent) are transcribed downstream [60].

To asses this fluorescent reporters containing a polyproline motif upstream of either a Rho-dependent terminator or the intrinsic hairpin one were used and it was detected a significant increase in termination efficiency in *Δefp* cells.

Further experiments could be directed to the identification of other factors that safeguard coupling between transcription and translation, but also to a better understand of global effects in genes expression due to the EF-P-altered transcription.

1.3. The archaeal translation factor aIF5A

1.3.1. Protein synthesis in Archaea

Among the primary domains of life, Bacteria, Archaea and Eukarya, much has been discovered concerning the fascinating process of translation, the archaeal one dials a medley of bacterial, and eukaryal features.

Starting from the translation initiation the main differences result from the structure of the archaeal mRNA, which can be polycistronic or monocistronic, Shine - Dalgarno (SD) motifs are present only in a minority of cases and in some species transcripts lack a 5' untranslated region (5'UTR).

These latest ones, named "leaderless" mRNAs, can be considered ancestral forms of mRNAs and are very abundant in some archaeal species such as halophiles (72% in *Haloferax volcanii*) and extreme thermopiles of the Crenarcheota branch (69% *Sulfolobus solfataricus*).

It is known for the thermophilic archeon *Sulfolobus solfataricus* that the 30S subunit alone is unable to interact with a leaderless mRNA, which requires the presence of tRNAi, conversely it can contact directly a leadered mRNA endowed with ShineDalgarno (SD) motif in stable binary complex.

This underlines that Archaea such as *Sulfolobus* can routinely use two distinct mechanisms for translational initiation [61].

The overall size of Archaeal ribosomal subunits is similar to the bacterial one, despite archaeal ribosomes are more protein-rich (68 in total).

Of this set, 34 ribosomal proteins are conserved in all three groups, but the archaeal and eukaryotic homologs are more similar to each other.

Exclusively Archaea and Eukaryotes share the remaining 33 ribosomal proteins and only one is unique to Archaea.

Therefore, the archaeal ribosome can be viewed as a smaller version of the eukaryal particle in terms of protein composition [62].

The selection of the start codon by the ribosome requires the functional involvement of translation initiation factors (IFs).

Archaea and Eukaryotes possess more translation factors in common than with the Bacteria, and primary sequences of these factors are more similar between those of Archaea and Eukaryotes, than the bacterial homologs.

A list of shared and domain specific IFs is presented in table 1 [63].

ARCHAEA	BACTERIA	EUKARYA
aIF1A	IF1	eIF1A
aIF2	IF2	eIF5B
(aIF5A	EFP	eIF5A)
aIF1/aSUI1	YCiH (only some)	eIF1/SUI1
aIF2		eIF2
aIF6		eIF6
	IF3	
		eIF3
		eIF5
		eIF2B
		eIF4F

Table 1. Universal translation initiation factors *[63].*

Starting from the archaeal pre-initiation complex the initiator tRNA, which carries an unformylated methionine, is escorted to the 30S ribosomal P site by the heterotrimeric factor aIF2 [64].

Despite archaeal mRNAs lack the 5'-end 7-methyl-G modification is important to mention that a recent study proved the existence of an archaeal "capping" system. It has been shown that both the complete trimer aIF2 and the isolated γ subunit bind to the 5' end of mRNAs, protecting them from degradation [65, 66].

Another archaeal initiation factor bound to the small 30S subunit is aIF1 (aSUI1), which facilitates the binding of the initiator tRNA and mRNA to the ribosome [67].

Once the codon–anticodon recognition occurs aIF2–bound GTP is hydrolyzed and aIF2 leaves the ribosome, probably with aIF1 and aIF1A (figure 6).

The last one is known as an homologue of the eukaryal eIF1A, but its function has not been determined yet.

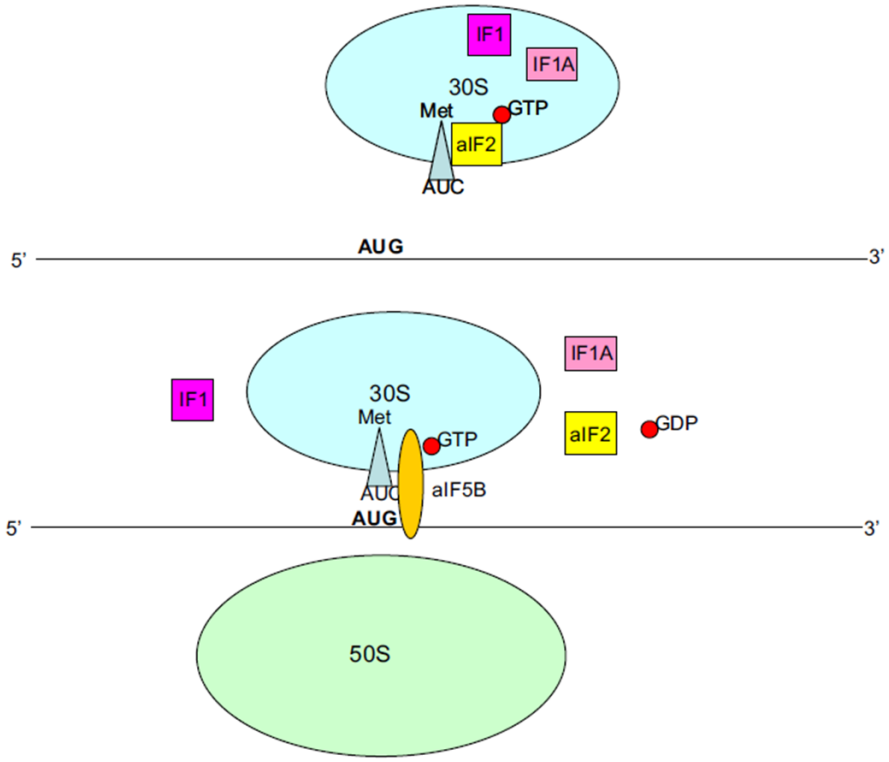

Figure 6. Model of translation initiation in Archaea *[63].*

The initiation event ended with the joining of the 50S subunit promoted by the archaeal factor aIF5B, which is responsible also in stabilizing the tRNAi in the P site [68].

Lastly, a ribosome anti-association factor aIF6 has been characterized and is known to bind specifically the 50S ribosomal subunit hindering the formation of the 70S [69].

Its binding and release is currently being investigated as many others translation factors, like aIF5A, whose function remains still elusive.

1.3.2. Structural features of the archaeal factor aIF5A

Structural information of the archaeal protein aIF5A were available since 1992, when the small protein (15kDa) was isolated from the aerobically grown crenarchaeon *Sulfolobus acidocaldarius* [70].

A strong conservation of residues, surprisingly high in the N-terminal domain around the corresponding eukaryal hypusine site, suggests from the beginning a common ancestry of the archaeal protein and the eukaryotic factor eIF5A.

The crystallographic structure of the archaeal protein aIF5A from *Pyrococcus horikoshii* has been determined [71] and the striking similarity of the euryarchaeal protein with its eukaryotic counterpart is even more evident.

The β-rich structure is composed of two distinct domains, the N-terminal domain is a SH3-like barrel motifs and the C-terminal domain folds in an OB-fold (figure 7A). The N-terminal domain consists of a 3_{10}-helix, six stranded anti-parallel highly twisted β-sheets and a long hairpin loop, in which the K37 is supposed to be post-translational modified.

The C-terminal domain comprises two short α-helices and five anti-parallel β-sheets.

A flexible peptide linker connects the two domains, which embrace a hydrophobic core and contacts between them are established by hydrogen bonds.

Regarding the electrostatic potential of the archaeal protein, the N-terminal domain, as well as the interface of the two domains, are positively charged, whereas the C-terminal domain is negatively charged. Based on this the authors speculated that the archaeal aIF5A acts as a bimodular protein, interacting with nucleic acids in the concave surface and in the flexible loop, and with protein partners in the C-terminal domain.

The amino acid sequence alignment of aIF5A from *Pyrococcus horikoshii* with two euryarchaeal homologs and eukaryotic homologues shows that the overall structure of the protein displays significant similarity and high sequence conservation within the N-domain, while the C-domain is less conserved (figure 7B).

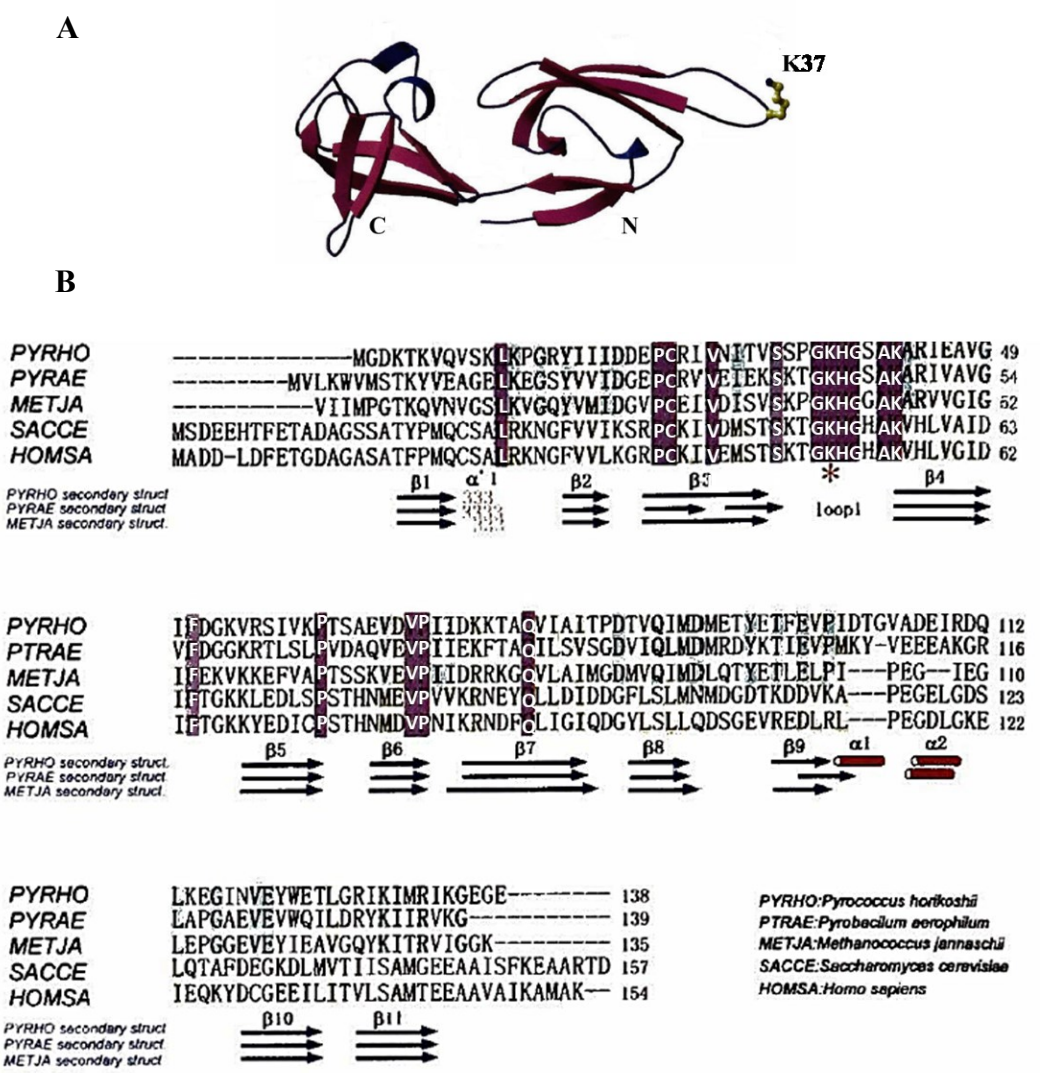

Figure 7. Structural features of the archaeal protein aIF5A. (A) Crystal structure of *Pyrococcus horikoshii* factor aIF5A (PDB ID: 1IZ6). (B) Amino acid sequences alignment (CLUSTAL W) and secondary structure elements (DSSP program) of aIF5A protein from *Pyrococcus horikoshii, Pyrobaculum aerophilum, Methanococcus jannaschii, Saccharomyces cerevisiae, Homo sapiens*. Identical residues are white and the eukaryotic modified K50 is marked by an asterisk [71].

1.3.3. Post-translational modification of the archaeal factor aIF5A

From its discovery, the characterization of the archaeal factor aIF5A was mainly addressed to the identification of the post-translational modification, since a functional assay, like the *in vitro* initiation complex, cannot be built up.

Almost ten years after the discovery of the eukaryotic translation factor eIF5A, the archaeal homologue was isolated from aerobic crenarchaeota and euryarchaeota archaea [72] and chromatographic methods assessed that the archaeal protein from *Sulfolobus acidocaldarius*, *Halobacterium cutirubrum* and *Thermoplasma acidophilum* is hypusinated. This is phylogenetic relevant to the lysine modification, which could originate in the archaeal kingdom or in the common ancestor of archaea and eukaryotes.

A subsequent study revealed that several species, not only aerobic, in the archaeal kingdom are able to synthesize protein-bound deoxyhypusine and/or hypusine (figure 8) [73].

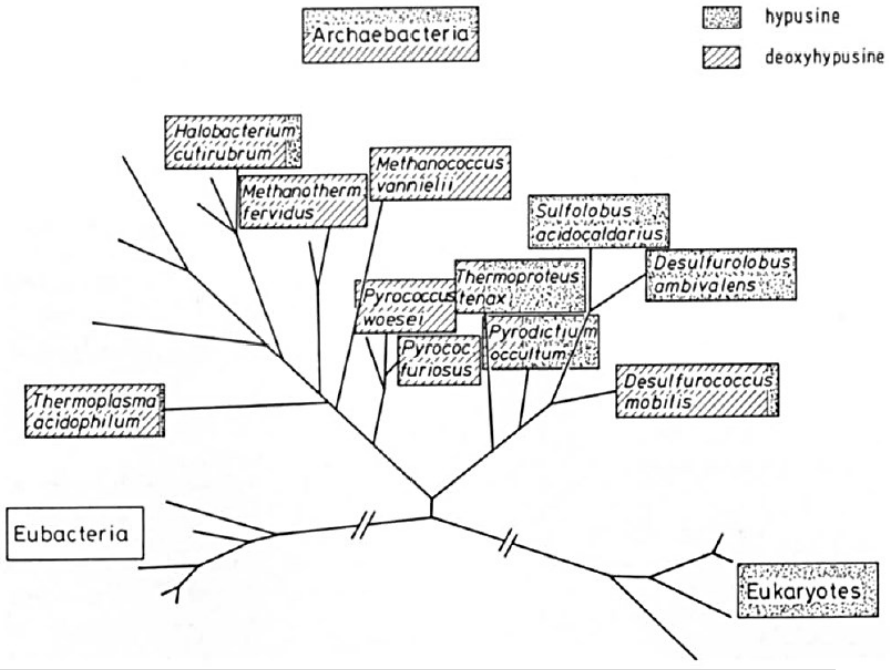

Figure 8. Hypusine and deoxyhypusine modification in the archaeal kingdom. The number of dots and dashes in each box is proportional to deoxyhypusine or hypusine content [73].

Deoxyhypusine is mainly present in strictly anaerobic thermophilic archaea (*Thermoproteus tenax, Pyrodietium oecultum* and *Desulfurolobus ambivalens*), however the hypusine modification was found also in anaerobic Thermoproteales, suggesting that deoxyhypusine could be an intermediate of the hypusine pathway as in eukaryotes. From this finding the question about an alternative hydroxylation step is obvious, since there is no possibility for anaerobic organisms to perform an oxygenation.

Bartig D *et al*. suggested that a dehydrogenation followed by bond hydratation may occur, likewise the hydroxylation of fatty acid chains during the β-oxidation. Nevertheless, no deoxyhypusine was detected in *Sulfolobales* and is still an open question if these organisms develop, in aerobic mode, an oxygen way of deoxyhypusine hydroxylation.

Another crucial issue of the hydroxylation step, related to the lack of information about the archaeal protein and its modification pathway, arose when the hypusine residue was identified in Archaea.

To date no DOHH is found in any archaeal genomes or proteomes, whereas DHS homologs has been identified in all sequenced archaeal genomes.

It is worth to elucidate the archaeal post-translational modification, starting from the characterization of the archaeal DHS and the analysis of its substrate.

Indeed this was the approach of a recent study in which it was shown that aIF5A is totally deoxyhypusinylated in the euriarchaeon *Haloferax volcanii*, through an alternative pathway [74].

The analysis of *Hfx. volcanii* intracellular polyamines revealed that agmatine is the more abundant in all growth stages, the DHS enzyme is not able to transfer the 4-aminobutyl moiety from spermidine to aIF5A and is not inhibited by the known DHS inhibitor GC7.

In addition the essential agmatinase-like gene clusters, in *Hfx. Volcanii*, with the *dhs* gene and the agmatinase enzyme may have a role in the modification pathway.

Based on this data the authors proposed a model in which the *Hfx. volcanii* DHS transfers directly the aminobutyl group from agmatine to aIF5A and the agmatinase enzyme finally hydrolyzes the agmatine moiety of the mature deoxyhypusine protein.

The effect of the inhibitor GC7 was also investigated in members of the genus *Sulfolobus* and for the first time, several hints on the physiological role of the archaeal hypusinated protein were provided [75].

The growth of four different archaeal species and a bacterial one was analyzed during GC7 treatment, which was effective on all archaea tested but not on the bacterium *E. coli* (table 2).

Species	Growth at 100 μM GC_7	Growth at 1,000 μM GC_7
S. acidocaldarius	+	−
S. solfataricus	+++	−
H. halobium	+++	−
H. mediterranei	+++	−
E. coli	+++	++

Table 2. Effect of the inhibitor GC7 on the archaeal and bacterial growth. +++, normal growth; ++, slight effect; +, strong effect; -, no measurable growth [75].

The insensitivity of *E.coli* is consistent with the absence of the *dhs* gene in bacterial genomes, despite a strong inhibition and a reversible arrest of growth was observed in *Sulfolobus acidocaldarius*, even at low concentration of GC7.

A previous analysis of the polyamine content in sulfur-dependent archaea [76] revealed that there is a high amount of spermidine, norspermidine and norspermine, however spermidine is the most abundant and this can be one explanation of the strong inhibition by GC7 in *Sulfolobus acidocaldarius*.

More in detail the inhibitor causes the arrest of growth at the end of the D period (G2), that occurs prior to cell division, but no changes in *S.acidocaldarius* cell morphology were detectable. The authors suggested that these physiological effects may be due to the presence of unmodified aIF5A, which is unable to synthetize a subset of proteins directly involved in cell cycle progression.

The possibility that the GC7 inhibitor can have targets others than DHS enzyme, causing thus a general effect in the cell, cannot be excluded.

However, these findings paved the way for future studies, which can be directed towards the functional characterization of the protein aIF5A in sulfur-metabolizing archaea, that are closely related to eukaryotes.

Nowadays very little is known about the role of the archaeal aIF5A, even though a comprehensive analysis of initiation factors in *Haloferax volcanii*, attempted through single gene deletion mutants, showed that aIF5A gene is essential [77].

While the involvement of this factor during the protein synthesis is still unknown, just in *Halobacterium sp*., a completely novel activity of aIF5A was discovered.

Wagner et al. showed for the first time that aIF5A from *Halobacterium sp.* NRC-1 has RNA-degrading activity *in vitro*, which has not been reported for its eukaryotic homologue [78]. The biochemical characterization revealed that the cleavage is not dependent on the hypusination, but requires charged residues in the N-terminal and C-terminal domain and occurs preferentially between adenine and cytosine, within single stranded regions.
The *Halobacterium sp.* aIF5A is also able of RNA binding *in vitro* but, unlike the cleavage, the hypusine residue is needful to stabilize the RNA-protein complex.
In the same study, the authors tested also the ribonucleolytic activity of the eukaryotic eIF5A *in vitro* and showed for this the hypusine-dependent RNA degrading activity.
Moreover the RNA-cleavage by *Halobacterium sp.* aIF5A may depends on the oligomeric state of the protein, thus further studies should be aimed to identify its potential interacting partners.

1.4. Aim of the thesis

There is rather limited knowledge on the archaeal factor aIF5A, therefore we aim to characterize this protein in the model organism *Sulfolobus solfataricus*.
We investigate about the subcellular localization of the protein, focusing, in particular on the interaction with ribosomal particles, in order to clarify whether the archaeal factor aIF5A is involved in the protein synthesis.
We investigated about the post-translational modification of aIF5A in *Sulfolobus solfataricus* and the structural and functional features of the enzymes that are involved in this pathway.
Concomitantly we seek to identify all protein interacting partners and characterize the functional interplay between aIF5A and RNA molecules.
Our goal is to discover whether the function of the archaeal factor aIF5A is confined to the protein synthesis or it is also involved in other physiological processes.

2. Materials and Methods

Materials: all chemicals used were of analytical grade from Sigma-Aldrich and were used as received without any further purification.

2.1. Expression of ORF Sso0970 in *E.coli* and purification of Sso-aIF5A

The ORF Sso0970 was PCR-amplified from *S. solfataricus* P2 genomic DNA using a forward primer containing an NcoI site (5′- GCAACCATGGGCATAACGTACACG -3′) and a reverse primer containing a BamHI site (5′- GCGCGGATCCCTTAACCCTAACTATT -3′).

100 ng of genomic DNA was used as a template for the PCR (table 3), performed with Phusion High-Fidelity PCR Master Mix (Thermo Fisher Scientific) and 10 μM primers were added to the reaction mixture.

	TEMPERATURE	TIME	CYCLES
Initial denaturation	98 °C	5’	1X
Denaturation	98 °C	30’’	30X
Annealing	50 °C	30’’	
Elongation	72 °C	30’’	
Final extension	72 °C	10’	1X

Table 3. PCR program for the amplification of ORF 0970 from Sulfolobus solfataricus P2 genomic DNA.

The amplification product, purified with the PCR purification kit (Quiagen), was cleaved with NcoI and BamHI and inserted into the corresponding sites of plasmid pETM11 (a kind gift from Dr. Roberto Spurio, University of Camerino), then the recombinant pETM11-aIF5A expression plasmid was propagate in *E.coli* DH5.

The recombinant plasmid was extracted using a mini-prep kit (QIAprep Spin Miniprep Kit, Quiagen), sequenced and used to transform *Escherichia coli* ROSETTA (DE3)/ pLysS cells.

Concentrations of PCR products and plasmids were determined with a NanoDrop 2000c spectrophotometer device.

The cloned aIF5A gene encoded a protein that consists of six histidine residues in the N-terminal position, a peptide linker of ten amino acids and the specific cleavage site (ENLYFQ) for the Tobacco Etch Virus (TEV) protease.

2 l LB medium containing 34 µg/ml chloramphenicol, 25 µg/ml kanamycin and 100 µg/ml ampicillin were inoculated and grown at 37 °C until an OD_{600} of 0.7, then the culture was induced by adding 0,5 mM IPTG. After 3 hours cells were harvested, pelleted, resuspended in 20 ml of lysis buffer (50 mM Tris-HCl pH 7.4, 150 mM NaCl, 15 mM imidazole, 1mM PMSF, 10 mM β-mercaptoethanol, 10 µg/mL DNase I, 0.1% Triton X-100, 25 µg/mL lysozyme) and incubated for 20 min on ice.

Cells were lysed by sonication and the lysate was clarified by centrifugation at 25.000 g for 30 min at 4°C.

The supernatant was incubated with 500 µl of pre-equilibrated Ni-NTA Agarose resin (Quiagen) overnight at 4 °C, to allow the binding of the His-tagged Sso- aIF5A.

The lysate and the beads was transferred to Poly-Prep chromatography columns (Bio-Rad, Hercules, CA, USA) and washed with 30 mL buffer (50 mM Tris-HCl pH 7.4, 500 mM NaCl, 40 mM imidazole). The protein aIF5A was eluted in 2 ml elution buffer (50 mM Tris-HCl pH 7.4; 150 mM NaCl; 250 mM imidazole) and the eluate was dialyzed overnight at 4 °C in dialysis buffer (50 mM Tris-HCl pH 7.4, 150 mM KCl, 5% glycerol).

The concentration of aIF5A was determined by the Bradford assay and the purity was assessed by SDS-PAGE, followed by coomassie-blue and silver staining; aliquots of the protein were stored at –80 °C.

An aliquot of the purified protein was incubated with the TEV protease to remove the His-tag. The TEV protease was added in a 1:50 ratio (TEV/protein aIF5A) and they were incubated overnight at room temperature in TEV incubation buffer (50 mM Tris-HCl pH 7.4, 0.5 mM EDTA, 1mM DTT).

The TEV protease contains a His-tag, therefore, to purify the cleaved protein aIF5A, 500 µl of Ni-NTA Agarose beads were added and the reaction was incubated overnight at 4 °C.

The protein of interest, present in the flowthrough, was collected and a small aliquot was analyzed by SDS-PAGE, followed by coomassie-blue staining.
Part of the protein, without His-tag, was used for the production of polyclonal antibodies in rabbit, using the speedy 28-day program, provided by Eurogentec, Belgium.
Different dilutions (1:1000, 1:5000, 1:10000) of anti-Sso aIF5A were tested for the detection of the recombinant Sso- aIF5A, expressed and purified in *E.coli*, by western blot analysis.

2.2. Expression of ORF Sso0967 in *E.coli* and purification of Sso-DHS

ORF Sso0967 was amplified by PCR using 100 ng genomic DNA of *S. solfataricus* P2 using two pairs of oligonucleotides for cloning the gene in two different plasmids:

1- forward 5'GCGGCCATGGTAAATAGAGAGGAC3' (NcoI restriction site)
2- reverse 5'CCGGGATCCTTAGCTTAATAAAGACG-3' (BamHI restriction site)
3- forward 5'AAAAGCATGCGCATAAATAGAGAGGACTTGTTAAAAAACCC3' (SphI restriction site)
4- reverse 5'AAAAGGATCCGCTTAATAAAGACGCGGCCAAAATAGG3' (BamHI restriction site).

ORF Sso0967 amplified with primers 1 and 2 was cloned in pETM11 and the N-terminal His-tagged DHS was expressed in *Escherichia coli* ROSETTA (DE3)/ pLysS, using the same protocol described above for Sso- aIF5A.
ORF Sso0967 amplified with primers 3 and 4 was cloned in the plasmid pQE-70 (Quiagen) which adds a C-terminal His-tag to the recombinant protein.
The C-terminal His-tagged DHS protein was purified with the same protocol described above, with the exception of the TEV cleavage, impossible to perform with this expression plasmid.

2.3. Western blot analysis

Proteins were separated by SDS-PAGE using standard protocols [79] and transferred by Semi-dry Western blotting onto a 0,2 μm nitrocellulose membrane (GE Healthcare). Blotting

was performed at 15V for 20 min in transfer buffer (25 mM Tris, 192 mM glycine, 0.1% (w/v) SDS, 20% (v/v) methanol).

Suitable protocols, for each antibody used, are summarized in table 4.

<table>
<tr><th>Blocking solution
1h, R.T.</th><th>Primary antibody, (in the corresponding blocking solution) overnight, 4°C</th><th>Wash n°1
(3 x 5')</th><th>Secondary antibody, (in the corresponding blocking solution)
1h, R.T.</th><th>Wash n°2
(4 x 5')</th><th>Detection solution</th></tr>
<tr><td rowspan="2">TBS + 0,1% Tween 20, 5% milk</td><td>anti-SsoaIF5A
(1:10000)</td><td rowspan="3">TBS + 0,1% Tween 20</td><td rowspan="4">anti-rabbit IgG HRP conjugate
(1:20000)</td><td rowspan="3">TBS + 0,1% Tween 20</td><td rowspan="4">Enhanced chemiluminescent reagent (SuperSignal West Pico PLUS, Thermo Scientific)</td></tr>
<tr><td>anti-SsoaIF6
(1:10000)</td></tr>
<tr><td>TBS + 0,1% Tween 20, 3% BSA</td><td>anti-hypusine
(1:2000)</td></tr>
<tr><td rowspan="2">TBS, 5% milk</td><td>anti-Sso2509
(1:5000)</td><td rowspan="2">TBS</td><td>TBS + 0,05% Tween 20</td></tr>
<tr><td>anti-SsoaIF2γ
(1:5000)</td></tr>
</table>

Table 4. Western blot probing protocols. All solutions are in TBS buffer (20 mM Tris HCl pH 7.6, 150 mM NaCl)

The chemiluminescent signal was detected using the Chemidoc detection system (Biorad).

2.4. Preparation of *Sulfolobus solfataricus* cell extract

Sulfolobus solfataricus P2 was aerobically grown in Brock's medium [80], supplemented with 0.2% NZamine and 0.2% sucrose, at 75 °C, pH 3.0.

During exponential growth, at an OD_{600} of 0.8, cells were harvested, pelleted and stored at -80°C. 1,5g (wet weight from 1L culture) of cells was disrupted by grinding [81], with 3g of alumina, using a sterile cold mortar on ice.

1ml of ribosome extraction buffer (20 mM Tris/HCl pH 7.4, 40 mM NH_4Cl, 10 mM $MgAc_2$, 1 mM DTT, 2.5 µg/ml DNase I) was gradually added and the cell lysate was shortly centrifuged to remove the alumina and cell debris.

Then two centrifugation steps at 26000 g for 30 min at 4°C were performed and the supernatant, crude cell extract S30, was collected.
Part of it was centrifuged at 45000 rpm (Beckman TLA-100.3 rotor) for 2h in order to obtain the S100 supernatant, rich in enzymes and factors.
The crude ribosomes pellet was resuspended in high salt buffer (20 mM Tris/HCl pH 7.4, 500 mM NH_4Cl, 10 mM $MgAc_2$, 2 mM DTT) and gently layered on the surface of a 18% sucrose cushion.
Ribosomes were centrifuged at 45000 rpm (Beckman TLA-100.3 rotor) for 3h at 4°C and at the end of this step the supernatant HSW was collected, whereas the salt- washed ribosomal fraction was resuspended in extraction buffer.
The protein concentration in S30, S100, HSW and salt-washed ribosomes fractions was determined by Bradford assay. These fractions were analyzed by western blot, with anti-SsoaIF5A antibody, to determine the sub-cellular localization of the protein.

2.5. Fractionation of *Sulfolobus* S30 exctract programmed for translation on linear sucrose gradients

Sulfolobus solfataricus S30 lysates (500µg total proteins) were pre-incubated at 75°C for 10 min and then programmed for protein synthesis.
In vitro translation reaction contained, in a final volume of 50 µl: 10 mM KCl, 20 mM Triethanolamine-HCl (TEA) pH 7, 18 mM $MgCl_2$, 3 mM ATP, 1 mM GTP, 1,5 µg of bulk *S. solfataricus* tRNA, amino acid mixture 0,1mM (concentration related to each of the 20 essential amino acids), 4 µg of an *in vitro* transcribed mRNA (Sso2375 mRNA).
The reaction was incubated for 30 min at 75 °C, then 2% formaldehyde was added and after an incubation on ice for 1h. A control sample containing only the S30 extract was incubated with 2% formaldehyde for 1h on ice.
Both samples were layered on a 10%-30% linear sucrose density gradient using 14 ml centrifuge tubes [82].
After a centrifugation step, at 23000 rpm (Beckman SW40Ti rotor) for 17 h at 4°C, 500 µl fractions were collected by continuously monitoring absorbance at 260 nm.

Samples were TCA precipitated (10% of TCA), loaded on 15% SDS-polyacrylamide gels and analyzed by western blot analysis with anti-SsoaIF5A serum.
As a loading control anti-SsoaIF6 was used, in order to detect fractions which correspond to the large 50S subunit [69].

2.6. Construction of plasmids pMJO5-SsoaIF5A and transformation of *Sulfolobus solfataricus* PH1-16 cells

The Sso-aIF5A gene (Sso0970) was amplified by PCR (protocol in table 3) from 100 ng of *Sulfolobus solfataricus* genomic DNA using two pairs of oligonucleotides in order to create two version of the cloned aIF5A gene: an N-terminal and a C-terminal His-tagged.
Sso-aIF5A N-terminal His tagged:

- forward primer containing an NcoI site and the 6xHis tag coding sequence (5′-AAAACCATGGAACATCACCATCACCATCACAGCATAACGTACACGACCGTC -3')
- reverse primer containing an EagI site (5′-AAAACGGCCGTTACTTAACCCTAACTATTTTCTC-3′).

Sso-aIF5A C-terminal His tagged:

- forward primer containing an NcoI site (5′-AAAACCATGGACAGCATAACGTACACGACCGTC-3')
- reverse primer containing an EagI site and the 6xHis tag coding sequence (5′-AAAACGGCCGTTAGTGATGGTGATGGTGATGCTTAACCCTAACTATTTTCTCC-3′).

The PCR was performed with Phusion High-Fidelity PCR Master Mix (Thermo Fisher Scientific) supplied with 10 μM primers, using the same protocol shown in table 3.
The productiom of the His-tagged protein aIF5A, in *Sulfolobus solfataricus*, was achieved using the pMJ05-based vector system [83].
First the PCR products were purified with the PCR purification kit (Quiagen), cleaved with NcoI and EagI and inserted in two different entry vectors, pSVA5 (arabinose inducible promoter) and pSVA11 (tf55α constitutive promoter).

Resulting plasmids pSVA5-SsoaIF5A N-termHis, pSVA5-SsoaIF5A C-termHis, pSVA11-SsoaIF5A N-termHis and pSVA11-SsoaIF5A C-termHis were sequenced and propagated in *E.coli* TOP10.

Recombinant plasmids were extracted using a mini-prep kit (QIAprep Spin Miniprep Kit, Quiagen), sequenced and digested, together with the shuttle vector pMJ05, with AvrII and EagI. Fragments were purified from agarose gel (QIAquick Gel Extraction Kit, Quiagen), and ligated into the corresponding sites of plasmid pMJ05.

This gave rise to plasmids, pMJ05 (ptf55)-SsoaIF5A N-termHis, pMJ05 (ptf55)-SsoaIF5A C-termHis, pMJ05 (AraP)-SsoaIF5A N-termHis, pMJ05 (AraP)-SsoaIF5A C-termHis used to transform *E.coli* TOP10.

Since pMJ05 is a huge plasmid (21868bp), which can be easily expelled, the cell recovery, after the heat-shock, was carried out for 2h at 25 °C and plates of transformants were leaved at room temperature for 2 days.

Plasmids were extracted and sequenced with pMJ05 specific primers [84], forward 5'-GGATGCTAAACAACTATTCAAACTG-3' and reverse 5'-GTTGTGTGGAATTGTGAGCGGATAA-3', to assess that each construct is in frame.

300 ng of each plasmid was used for electroporation of *Sulfolobus solfataricus* PH1-16 (Δ*pyrEF*) [85] and cells were recovered for 3 days in uracil medium and then selected in medium without uracil for other 3 days. Finally cells were plated in glass Petri dishes containing Brock's media, supplemented with 0,2% w/v sucrose, 0,2% NZamine, Gelrite (0,7% w/v) solidified.

Once grown single colonies were inoculated in liquid medium without uracil, genomic DNA was isolated and the presence of the recombinant plasmid was confirmed using the pMJ05 specific primers previously reported.

Glycerol stocks of positive clones were made and their growth was monitored for 5 days in order to see if there is an effect due to aIF5A expression.

As controls Sso PH1-16, Sso PH1-16 [pMJ05 (ptf55)-empty plasmid] and Sso PH1-16 [pMJ05 (AraP)-empty plasmid] were grown in parallel.

The two strains in which aIF5A gene is under control of the inducible arabinose promoter, were induced at a certain OD_{600nm}, as described below.

2.7. Synthesis of His-tagged Sso-aIF5A and purification of the recombinant protein in *Sulfolobus solfataricus*

Sulfolobus solfataricus strains PH1-16 [pMJ05 (ptf55)- aIF5A N-terminal His], PH1-16 [pMJ05 (ptf55)- aIF5A C-terminal His], were grown at 75 °C in 1l Brock's medium (composed of Brock's salts and supplemented with 0.2% NZamine, 0.2% sucrose pH 3.0) and harvested when they reached an OD_{600nm} of 0.8.

Since ptf55 is a heat-inducible promoter of the thermosome α subunit, these cultures, at an OD_{600nm} of 0.8, were also shifted to 88°C for one day and then pelleted.

Sso strains PH1-16 [pMJ05 (AraP)- aIF5A N-terminal His], PH1-16 [pMJ05 (AraP)- aIF5A C-terminal His] were grown in the same condition above described until they reached an OD_{600nm} of 0.8.

Cells were pelleted, washed twice with water, induced in 1l (OD_{600nm} start: 0.2) Brock's medium (supplemented with 0.2% NZamine and 0.2% D-arabinose) and harvested when they reached again an OD_{600nm} of 0.8.

Pelleted cells were lysed in 20 ml of lysis buffer (50 mM Tris-HCl pH 7.4, 150 mM NaCl, 15 mM imidazole, 10 mM β-mercaptoethanol, 1mM PMSF) by sonication and the lysate was centrifuged at 25,000 g for 30 min at 4°C.

For all expression strains and control strains [pMJ05 (ptf55)-empty plasmid]/Sso PH1-16 [pMJ05 (AraP)-empty plasmid], lysates (100ng total proteins) were fractionated on SDS–PAGE gel 15%.

The presence of the recombinant His-tagged aIF5A was revealed by western blot analysis and quantified with the Image Lab Software from Bio-Rad; data were normalized using aIF6 as a reference protein, revealed with the specific antibody.

Clarified lysates were incubated with 300 µl of pre-equilibrated Ni-NTA agarose resin (Qiagen), overnight at 4 °C. The lysates with beads were transferred to Poly-Prep chromatography columns (Bio-Rad, Hercules, CA, USA) and washed with 30 ml of washing buffer (50 mM Tris-HCl pH 7.4, 500 mM NaCl, 40 mM imidazole).

Proteins were eluted with 1ml elution buffer (50 mM Tris-HCl, pH 7.4, 150 mM NaCl, 250 mM imidazole). 1/10 of each eluate was concentrated using 3K Amicon® Ultra-0.5 centrifugal filter devices and loaded on SDS-PAGE gel 15%, coomassie-blue stained.
The rest of each eluate was dialyzed in buffer (50 mM Tris-HCl pH 7.4, 150 mM KCl, 5% glycerol), concentrated with the same device and aliquots of proteins were stored at –80 °C.

2.8. Determination of the *Sulfolobus solfataricus* aIF5A intact mass by LC-MS

10µl (0,5mg/ml) of factor aIF5A C-terminal His-tagged, produced in *Sulfolobus solfataricus* PH1-16, was analyzed by LC-MS in order to assess its intact mass and the eventual presence of post-translational modifications.
As a control we also analyzed the recombinant protein Sso-aIF5A synthesized in *E.coli* (the His-tag was removed by TEV protease cleavage), which is not modified.
High performance liquid chromatography was performed on a Dionex Ultimate 3000 HPLC (Thermo Fisher Scientific) system configured with the Chromeleon 6.0 software (Thermo Fisher Scientific). Proteins were reduced in 100 mM DTT for 30 minutes at room temperature and then separated on an Aeris Widepore C4 column (3.6 µm particle size, dimensions 2.1 x 150 mm, Phenomenex) running a six minutes step gradient from 10% up to 70% acetonitrile in 0.1% formic acid.
The working temperature was set at 50 °C and the flow rate at 300 µl/min.
The LC-system was coupled online to the quadrupole-time of flight-mass spectrometer Synapt G2-Si (Waters), operated via the MassLynx V 4.1 software package, using a Z Spray ESI source (Waters). Mass spectra were acquired in the m/z range from 500-2000, at a scan rate of 1 sec and the mass spectrometer was calibrated with a MS spectrum of [Glu1]-Fibrinopeptide B human (Glu-Fib) solution.
Acquired data were analyzed with the MaxEnt algorithm to reconstruct the uncharged average protein mass.

2.9. Structural analysis of the recombinant Sso-DHS by Static Light Scattering

Analytical Size-Exclusion Chromatography and Multiangle Laser Static Light Scattering SEC was performed with a Superdex S200 10/300 GL increase column (GE Healthcare) equilibrated in a buffer containing 20 mM Tris-HCl pH 7.5 and 150 mM NaCl.

Separations were performed at rTC with a flow rate of 0.5 ml/min by HPLC (Agilent Technologies 1260 infinity).

The *E.coli* recombinant proteins Sso-DHS (C-terminal His-tagged) and Sso-aIF5A (without His-tag) were pre-incubated at 65°C for 10 min and 100µl were injected at a concentration of 1.5 mg/ml.

On-line MALLS detection was performed with a miniDawn Treos detector (Wyatt Technology Corp., Santa Barbara, CA) using a laser emitting at 690 nm and by refractive index measurement using a Shodex RI-101 (Shodex).

2.10. *In vitro* hypusination assay

The *in vitro* hypusination assay was performed testing different amounts of the recombinant Sso-DHS (pre-incubated 10 min at 65°C), 200 pmol and 1200 pmol respectively, in presence of 400 pmol of the recombinant Sso-aIF5A produced in *E.coli* (the N-terminal His-tag was cleaved), 2mM spermidine, 2mM nicotinamide adenine dinucleotide (NAD^+), 2mM $MgCl_2$, 50mM glycine-NaOH buffer pH 9.4, 150 mM KCl and 1mM DTT in a final volume of 30 μl.

We also tested different incubation times (1h, 2h, and overnight) at 65°C, checking after each incubation the integrity of the proteins by SDS-PAGE.

The intact mass of the resulting protein, after the *in vitro* hypusination, was detected by LC-MS, using the experimental procedure previously reported.

2.11. Identification of Sso-aIF5A protein interacting partners by LC-MS/MS

Proteins that were affinity co-purified with Sso-aIF5A N-terminal His-tagged, from 1l culture of *Sulfolobus* PH1-16 [pMJ05 (ptf55-aIF5A)], were detected by LC-MS/MS.

During the affinity purification several proteins stick to the matrix in a non-specific way, thus we performed a mock purification, using 1l culture of *Sulfolobus* PH1-16 [pMJ05-(ptf55)-empty plasmid] and we analyzed also this eluate by LC-MS/MS, in order to identify only proteins that are clearly enriched in Sso-aIF5A eluate.

Proteins purified from these two strains present in 1/10 of the eluate were denatured in 4M urea, 50 mM ammonium bicarbonate (ABC), before reducing the disulfide bonds in 10 mM dithiothreitol for 30 minutes at room temperature.

Free thiols were alkylated with 20 mM iodoacetamide in the dark and the solution was then diluted with 50 mM ABC to 1M urea. Proteins were digested over night at 37° C with trypsin (Promega, Trypsin Gold), 1:50 trypsin/protein ratio, the digestion was stopped with trifluoroacetic acid and peptides were desalted on custom-made C18 Stage Tips [86].

Tryptic digests were separated on an Ultimate 3000 RSLC nano-flow chromatography system (Thermo Fisher Scientific), using a pre-column for sample loading (PepMapAcclaim C18, 2 cm × 0.1 mm, 5 µm, Dionex-Thermo-Fisher) and a C18 analytical column (PepMapAcclaim C18, 50 cm × 0.75 mm, 2 µm, Dionex-Thermo-Fisher), applying a linear gradient from 2% up to 35% acetonitrile in 0.1% formic acid at a flow rate of 230 nl min^{-1} over 120 min.

Eluting peptides were analyzed on a Q Exactive HF Orbitrap mass spectrometer (Thermo Fisher Scientific), equipped with a Proxeon nanospray source (Thermo Fisher Scientific), operated in a data-dependent mode. Survey scans were obtained in a mass range of 380–1,650 m/z with lock mass on, with a resolution of 120.000 at 200 m/z.

The 10 most intense ions were selected with an isolation width of 2 Da, fragmented in the HCD cell at 27% collision energy and the spectra were recorded at a resolution of 30000.

Peptides with a charge of +1, and higher than 6 were excluded from fragmentation, the peptide match and exclude isotope features were enabled and selected precursors were dynamically excluded from repeated sampling for 30 s.

Raw data were processed using the MaxQuant software package (version 1.5.5.1, www.maxquant.org) [87] and searched against the uniprot *Sulfolobus solfataricus* database (www.uniprot.org).

The search was performed with full trypsin specificity and a maximum of two missed cleavages. Cysteine Carbamidomethylation (CAM) of residues was set as fixed, oxidation of methionine, N-terminal protein acetylation as variable modifications and all other parameters were set to default.

Results were filtered at a protein and peptide false discovery rate of 1% and LFQ (label free quantification) was used to quantify proteins relatively between the two samples.

2.12. Co-Immunoprecipitation assay

E.coli recombinant proteins Sso-aIF5A and Sso-2509 (purified as previously described [88]), were used in the Co-IP, performed with anti-Sso2509 serum (provided by Prof. Udo Bläsi lab, MFPL, Wien).

70 pmol of purified proteins were either incubated alone or together, in 200 µl Co-IP buffer (50 mM Tris–HCl pH 6.0, 100 mM KCl; 5% glycerol, 1 mM $MgCl_2$ and 0.1% Triton X-100), for 10 min at 65°C. 15 µl of anti-Sso2509 serum was added and samples were leaved for 1 h on ice.

Dynabeads® Protein G beads (Thermo Fisher Scientific) were equilibrated in Co-IP buffer, 10 µl were then added to each reaction and samples were incubated overnight at 4°C.

Immunocomplexes were captured by a magnetic device and after washing (three times with 1ml Co-IP buffer), proteins were eluted with 45µl of sodium dodecyl sulfate (SDS)-loading buffer, boiling beads for 10 min and analyzed by western-blotting using anti-SsoaIF5A and anti-2509 specific antibodies.

2.13. aIF2 release by Sso-2509 & Sso-aIF5A

aIF2 releasing assay was performed according to the published procedure [88], in addition a short form of the model 2508 mRNA, prepared as previously described [65], was used.

100 pmol of 5′-P3-end 2508sh RNA were ligated with 300 pmol biotinylated oligonucleotide 5′-CAGGTGGCACTTTTCGGG (biotin)-3′ using T4-RNA-ligase (Thermo Fisher Scientific) and the ligation mixture was purified with illustra MicroSpin G-50 Columns (GE-Healthcare).

50 pmol of biotinylated 2508sh RNA was bound to 50 µl of pre-equilibrated Dynabeads® Straptavidin beads (Thermo Fisher Scientific), in a final volume of 200 µl (50mM Tris-HCl pH 7,4, 1M NaCl, 0.5 mM EDTA, 0.05% Tween 20), overnight at 4°C.

50 pmol of aIF2-α, -β, -γ, pre-incubated at 65°C for 10 min, were added to RNA-coated beads, pre-equilibrated with binding buffer (50mM Tris-HCl pH 6.0, 100mM KCl, 5% glycerol, 1 mM $MgCl_2$, 0.05% Tween 20).

The binding was performed for 2h at 4°C, then the unbound proteins in the supernatant (S) were collected and the beads were washed six times with 1 ml of binding buffer.

The last wash fraction (W) was precipitated with 10% TCA in order to ensure that unbound aIF2/aIF2γ was removed completely.

The immobilized complex was resuspended in 200 µl of binding buffer alone, in the presence of Sso-2509 (50 pmol), Sso-aIF5A (50 pmol) and Sso-2509 together with Sso-aIF5A (50 pmol each) respectively and incubated for 30 min at 65°C. For each reaction supernatants (S) were collected and precipitated with 10%TCA, beads were washed six times with binding buffer, than last washes were collected and also TCA precipitated.

Proteins that are still attached to the beads (B) were eluted boiling samples for 10 min in 30 µl sodium dodecyl sulfate (SDS)-loading buffer.

Proteins were separated by SDS-PAGE, gel 12,5% and the presence of aIF2γ in all fractions was determined by western blot analysis, using anti-aIF2γ specific antibody.

2.14. Glycerol density gradients

5-15% linear glycerol gradient were prepared in extraction buffer (20 mM Tris/HCl pH 7.4, 40 mM NH4Cl, 10 mM MgAc2, 1 mM DTT), using 14 ml centrifuge tubes.
500 µg (total proteins) of *Sulfolobus solfataricus* P2 S30 extract was prepared as previously described, disrupting cells by grinding, pre-incubated at 65°C for 10 min and then layered on the gradient.
In parallel 500 µg (total proteins) of *Sulfolobus solfataricus* P2 S30 extract, pre-incubated at 65°C for 10 min, was treated with 5µl of micrococcal nuclease (New England Biolabs) and then layered on the gradient.
We also fractionated on glycerol gradients 200 µl of a protein mixture containing myoglobin (17kDa) 5mg/ml, ovalbumin (44 kDa) 10mg/ml and conalbumin (76 kDa) 5mg/ml.
After a centrifugation step, at 36000 rpm (Beckman SW40Ti rotor) for 17 h at 4°C, 500 µl fractions were collected by continuously monitoring absorbance at 260 nm.
Samples were TCA precipitated (10% of TCA), loaded on 12,5% SDS-polyacrylamide gels and analyzed by western blot analysis. Half protein amount in each fraction was blotted with anti-SsoaIF5A antibody and the other half with the eukaryotic anti-hypusine antibody (ABS1064, Merck Millipore).
Fractions from the gradient of protein standards were separated by SDS-PAGE on a 12,5% gel, stained with coomassie-blu.

2.15. Isolation of RNA substrates affinity co-purified with Sso-aIF5A and RNA_{Seq}

The eluate obtained after the affinity purification, using the lysate from 4l Sso PH1-16 [pMJ05 (ptf55)- aIF5A C-terminal His] and from 4l Sso PH1-16 [pMJ05 (ptf55-empty plasmid)] were used to extract the co-purifying RNA.
Cells were grown in the same condition previously reported and harvested in the logarithmic phase (OD_{600nm} of 0.8).

The affinity purification was also carried out following the procedure mentioned before, but all buffers were prepared in DEPC-water and the salt content in the wash buffer was reduced to 300mM.

To assess if other proteins were co-eluted with Sso-aIF5A, 10 µl of each eluates were analyzed by SDS-PAGE, gel 15% and the purity judged by silver staining.

RNA co-purified in the two eluates was extracted by Phenol/Chloroform, precipitated and resuspended in 50µl of DEPC-water. Samples were treated with DNase I (RNase-free, Roche) and a control PCR was performed to confirm complete degradation of chromosomal DNA.

The primers used forward 5'- TTGGGATCGAGGGCTGAAAC-3' and reverse 5'-CTCACCCCTCTCCTACTCGG-3', amplified a short part of 16S rRNA gene (133 nt at the 3'-end).

The quality and the quantity of the RNA samples was determined with the Agilent 2100 Bioanalyzer (Agilent Technologies) and the RNA 6000 Pico Kit (Agilent Technologies). cDNAs libraries were constructed using the SMART-Seq v4 Ultra Low Input RNA Kit (Clontech) and a total of 50 bp single end sequence reads were generated by the next generation sequencing facility at the Vienna Biocenter Core Facilities GmbH (VBCF), member of Vienna Biocenter (VBC), using the Illumina HiSeq 2000 platform.

Adaptor sequences were removed with cutadapt [89] from the raw reads and the mapping of the samples against the *S. solfataricus* P2 reference genome (NC_002754) was performed with segemehl (http://www.bioinf.uni-leipzig.de/Software/segemehl/).

Reads for coding regions and for non-coding regions were counted using BEDtools [90], normalized to transcripts per million (TPM) and processed for automatic visualization with Vienna NGS toolbox [91].

For a comparison of transcripts levels, bound to either Sso-aIF5A or co-eluted in the mock control, we used a threshold of four-fold difference in the TPM values to select ncRNAs and eight-fold difference to select mRNAs.

2.16. RNA cleavage assay

Sso-aIF5A (His tag removed by the cleavage with the TEV protease) purified from *E.coli* and Sso-aIF5A C-terminal His tagged purified from *Sulfolobus solfataricus* PH1-16 [pMJ05 (ptf55-aIF5A)] were incubated with different RNA substrates.
2508sh mRNA was *in vitro* transcribed as described before [65], similarly to 0118 mRNA and 0175 mRNA that were prepared using *S. solfataricus* chromosomal DNA as template and the following oligonucleotides (forward primers contain the T7 promoter sequence): 5′-TAATACGACTCACTATAGGTTGCTACAACTAATGATGAAAG-3' (Fp_0118), 5'-TTACGCTATTGAAGCCAGC-3' (Rp_0118), 5'-TAATACGACTCACTATAGGATGATTAAGATGGTTATTGTCG-3' (Fp_0175), 5'-TCACAGTAATTTTAGATCACCC-3' (Rp_0175).

2.16.1. Native polyacrylamide gel electrophoresis

Sso-aIF5A purified from *E.coli*, pre-heated 10 min at 65°C, was incubated for 15 min at 65°C with 100 pmol of 2508sh mRNA (pre-denatured at 85 °C for 5 min).
Reactions with different ratios 2508sh mRNA/aIF5A (1:1, 1:5, 1:10) were incubated in a volume of 10 µl containing 20mM Tris-HCl pH 7.4, 5mM $MgCl_2$, 50 mM KCl, 1 mM DTT, and 5% glycerol in a final volume of 10µl.
As control we used the 2508sh mRNA directly loaded and the RNA incubated in the reaction buffer for 10 min at 65°C.
2 µl 85% glycerol was added, then samples were loaded on a 8% polyacrylamide gel, the electrophoresis was carried out at 90 V and 4°C for 4 hours using Tris-Borate-EDTA (TBE) pH 8.3 as running buffer and the gel was stained with toluidine blue.

2.16.2. Denaturing urea polyacrylamide gel electrophoresis

RNA substrates were first denatured for 5 min at 85°C and then incubated with *Sulfolobus* proteins performing different reactions, using a reaction buffer containing 10 mM HEPES pH 8.0, 100 mM KCl, 5 mM β-mercaptoethanol, 5% glycerol.

Sso-aIF5A purified from *E.coli* (pre-heated 10 min at 65°C) was incubated at 65°C with 300 pmol of 2508sh mRNA (ratio RNA/aIF5A 1:7) in reaction buffer and as a control we used the RNA alone in the same buffer for 30 min at 65°C.

Samples of 10µl (50 pmol of 2508sh RNA each) were withdrawn every 5 min for 30 min in total.

This protocol was also applied for other two reactions, one at 37°C using Sso-aIF5A purified from *E.coli* (not pre-heated) and the second one at 65°C with Sso Deoxyhypusine synthase purified from *E.coli* (pre-heated 10 min at 65°C).

Sso-aIF5A purified from *E.coli* (pre-heated 10 min at 65°C) was also incubated at 65°C, for 15 min, with 50 pmol of 0118 mRNA (ratio RNA/aIF5A 1:7) in reaction buffer; as a control we loaded directly the RNA substrate and we also performed a reaction with the sole RNA in the same buffer for 15 min at 65°C.

This last assay was performed also using two other RNA substrates 0118 mRNA and 0175 mRNA respectively.

Lastly we performed the RNA degradation assay using Sso-aIF5A C-terminal His tagged purified from *Sulfolobus solfataricus* (pre-heated 10 min at 65°C) and the native Sso-aIF5A, purified according the published protocol related to *Sulfolobus acidocaldarius* aIF5A [70] (kindly provided by Dr. Alice Romagnoli, Università Politecnica delle Marche, Italy). Proteins were pre-heated 10 min at 65°C and incubated at 65°C for 30 min, with 10 pmol of 2508sh mRNA (ratios RNA/aIF5A 1:4, 1:8, 1:16) in reaction buffer.

This mixture was separated on a denaturing gel together with the RNA substrate directly loaded and the RNA after the incubation at 65°C for 30 min, in reaction buffer.

An additional control in this last assay consisted in the incubation, at 65°C for 30 min, of 2508sh mRNA with the eluate of the mock purification, used for the RNAseq analysis.

The volume of the mock eluate in the reaction corresponded to the volume of Sso-aIF5A used in the sample with the ratio RNA/protein 1:16.

All reactions were performed in a final volume of 10 µl and then an equal volume of RNA loading dye was added. Samples were incubated at 65°C for 10 min and loaded on a denaturing (8M urea) polyacrylamide 8% gel.

The electrophoresis was carried out at 20 mA for 1h, using Tris-Borate-EDTA (TBE) as running buffer.

2.17. Zymogram assay

The *in vitro* transcribed 2508sh mRNA from *S. solfataricus* P2 was incubated, in DEPC water, at 50°C for 5 minutes and added to the gel (15% SDS polyacrylamide gel) at a concentration of 0.15 mg/ml before it was cast.

3 µg of the native Sso-aIF5A, 5 µg of the recombinant Sso-aIF1A, produced and purified in *E.coli* (kindly provided by Dr. Alice Romagnoli, Università Politecnica delle Marche, Italy) and as a positive control 1 ng of bovine pancreatic RNase A (70856, Merck Millipore) were loaded on the gel.

The gel was incubated overnight in 25% isopropanol on a shaking platform at room temperature.

The following renaturing and incubation steps were carried out at room temperature as previously described [92]: 2 x 15 min, 6 M guanidine chloride (GnCl) in incubation buffer (IB; 5 mM HEPES at pH 7, 10mM KCl, 10 mM $Mg[OAc]_2$); 15 min, 3 M GnCl in IB; 15 min, 1.5 M GnCl in IB; 15 min, 0.75 M GnCl in IB; 15 min, 0.375 M GnCl in IB; 15 min, 0.1 M GnCl in IB; 15 min, IB; 90 min, IB at 65°C.

The gel was stained with ethidium bromide and the degradation was detected using the Chemidoc detection system (Biorad).

3. Results

3.1. Production and purification of Sso-aIF5A in *E.coli*

The synthesis of extremophilic proteins mainly exploits commonly used mesophilic expression systems, which successfully enable their characterization for technological or scientific ends.

Nowadays the optimization of currently used hosts, like *E.coli*, provided new strategies that prevent limitations with respect to codon bias and protein folding issues.

We decided to start from the cloning and synthesis of Sso-aIF5A in *E.coli*, in order to obtain a consistent amount of protein, useful for subsequent experiments and for the production of antibodies, which allowed the detection of the archaeal native factor.

The gene coding for the hypothetical translation factor aIF5A (SSO-aIF5A) (ORF Sso0970) was PCR amplified from *Sulfolobus solfataricus* P2 genomic DNA, cloned in the plasmid pETM-11 and expressed in *E.coli* ROSETTA (DE3)/ pLysS.

To clone the gene of interest the mutation of the second amino acid, serine to glycine, was necessary to design the primers sequence.

In yeast, the second residue (Serine) is phosphorylated [93], however mutation of this residue has no effect on cell growth and the unphosphorylated protein shows an activity, in stimulating Met-Pmn synthesis, comparable to wt, suggesting that this residue is not essential for the factor function.

A 2l culture was induced by IPTG, after 3h of induction the recombinant protein was purified from the cell lysate by affinity chromatography and the procedure yielded 20 mg of Sso-aIF5A, which looked pure even after silver staining (figure 9).

Sso-aIF5A produced in *E.coli* is a protein of 157 amino acids, with an estimated molecular mass of 15kDa and a theoretical isoelectric point of 6.

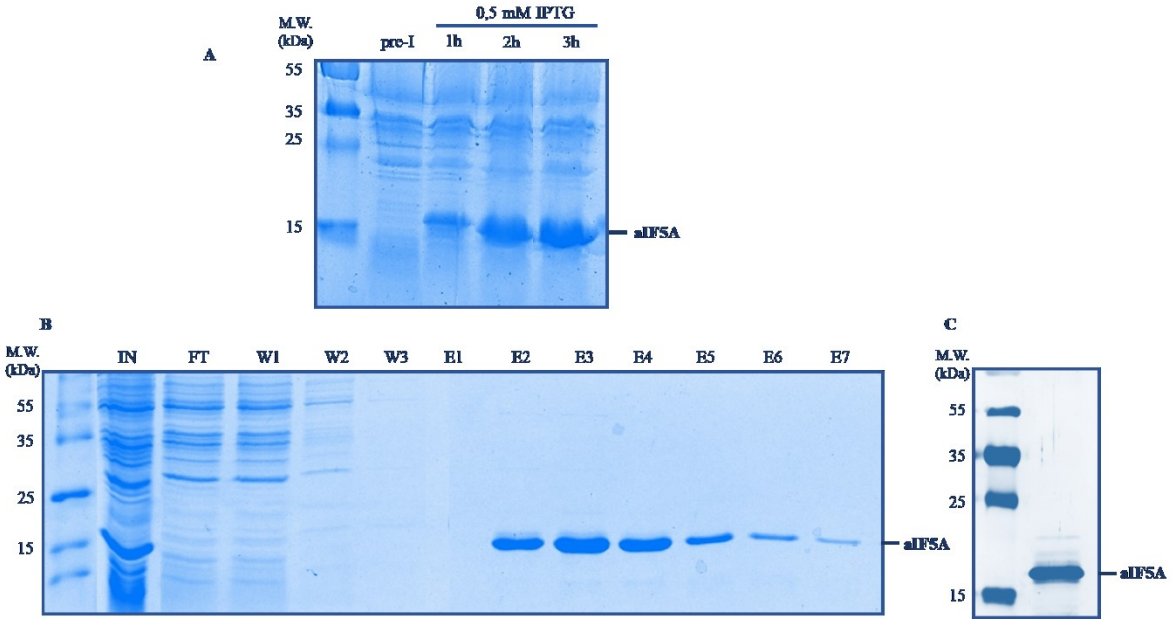

Figure 9. Production and purification of Sso-aIF5A in E.coli. (A) Test of Sso-aIF5A production, pre-I: lysate before IPTG induction, 1h, 2h, 3h: lysates after IPTG induction; 0,5 OD600 of cells each lane, 15% SDS-polyacrilamide gel, comassie stained (B) Purification of Sso-aIF5A by affinity purification. Loaded amount in percent of total fractions were input (IN) 0,001% of the cell lysate, flowthrough (FT) 0,001%, washes (W) 2% each lane, eluate (E) 1% each lane; 15% SDS-polyacrilamide gel, coomassie-blue stained. (C) Sso-aIF5A affinity purified, 15% SDS-polyacrilamide gel, silver stained.

The purified protein was subjected to His-tag cleavage by TEV protease and used to produce rabbit polyclonal antibodies.

A series of western blot analysis was performed to check the sensitivity and the specificity of the antibodies: different dilutions of the antibody were tested against different amounts of the recombinant Sso-aIF5A in western blot analysis.

Results in Fig.10 show that a 1:10.000 dilution is effective in recognizing the protein and the limit of detection is around 0,3 pmol.

Based on these results the antibody was used to probe a *Sulfolobus* cell lysate to verify the capacity of the antibody to recognize also the native protein and to exclude any cross-reactivity (figure 10C)

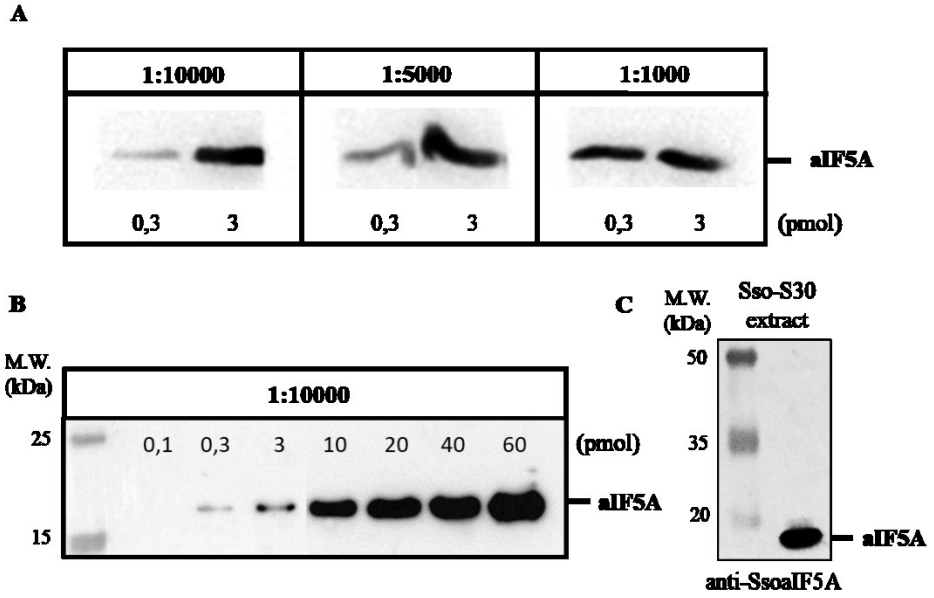

Figure 10. Performance of the polyclonal antibody in the detection of the recombinant Sso-aIF5A. Different amounts of aIF5A were loaded on 15% SDS-polyacrylamide gel and analyzed by western blot analysis with anti-SsoaIF5A antibody. (A) Test of three different antibody dilutions, 1:1000, 1:5000, 1:10000. (B) Sensibility of anti-SsoaIF5A, using a dilution 1:10000, in the detection of the recombinant protein aIF5A. (C) Western blot analysis with anti-SsoaIF5A on 40 µg total proteins of *Sulfolobus solfataricus* P2 S30 extract.

3.2. Subcellular localization of Sso-aIF5A

In order to start clarifying the functional role of the protein we fractionated *Sulfolobus solfataricus* P2 cell lysates and analyzed the different fractions by western blot using the specific anti-Sso-aIF5A to localize the native protein.

Results are presented in Fig. 11.

The protein appears to be abundant in the crude S30 extract and localized mainly in post-ribosomal fractions, in fact most of it is detected in the S100 supernatant, while a tiny amount remains in the ribosomal high salt wash (HSW), were proteins tightly bound to the ribosomes are present.

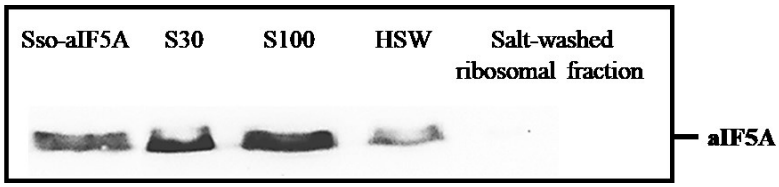

Figure 11. Cellular localization of the native Sulfolobus solfataricus aIF5A. Proteins were separated on 15% SDS-polyacrylamide gel and aIF5A was detected using anti-SsoaIF5A antibody. Sso-aIF5A: 5 pmol of Sso-aIF5A, expressed and purified in *E.coli*; crude S30 extract: 20 μg total proteins; supernatant S100: 20 μg total proteins; ribosomal high salt was HSW: 50 μg total proteins; Salt-washed ribosomal fraction: 100 pmol.

In order to clarify the involvement of aIF5A in the translation process we proceeded analyzing the localization of the protein in cell lysates which have been programmed for protein synthesis.

To this end *S. solfataricus* cell lysates were incubated in the presence of exogenous mRNA and all other components necessary for translation, fixed with formaldehyde and then fractionated on a 10%–30% sucrose gradient, the ribosome profile was determined monitoring absorbance at 260nm (figure 12).

A control sample of a lysate non programmed for translation was analyzed as well.

The fractions were subjected to western blot analysis and probed with anti-Sso-aIF5A antibodies.

S. solfataricus ribosomes are known to dissociate during centrifugation [81], therefore 70S monosomes or polysomes are not detectable in the control sample. 70S associate more stably only during translation and become detectable upon fixation with formaldehyde.

Results from the control sample (figure 12A) confirmed what previously observed, Sso-aIF5A is present exclusively in the top low-molecular-weight fractions and it is not associated with ribosomal subunits.

Analysis of the lysate programmed for translation (figure 12B) shows instead that when ribosomes are involved in mRNA translation, even though most of aIF5A protein is still present in the top fraction, a portion becomes ribosome bound is detected in the 30S, 50S and 70S fractions.

As a control the presence of aIF6, which is known to be stably bound to the large ribosomal subunits, was probed [69].

This result is the first indication that an archaeal aIF5A protein participates in the process of protein synthesis.

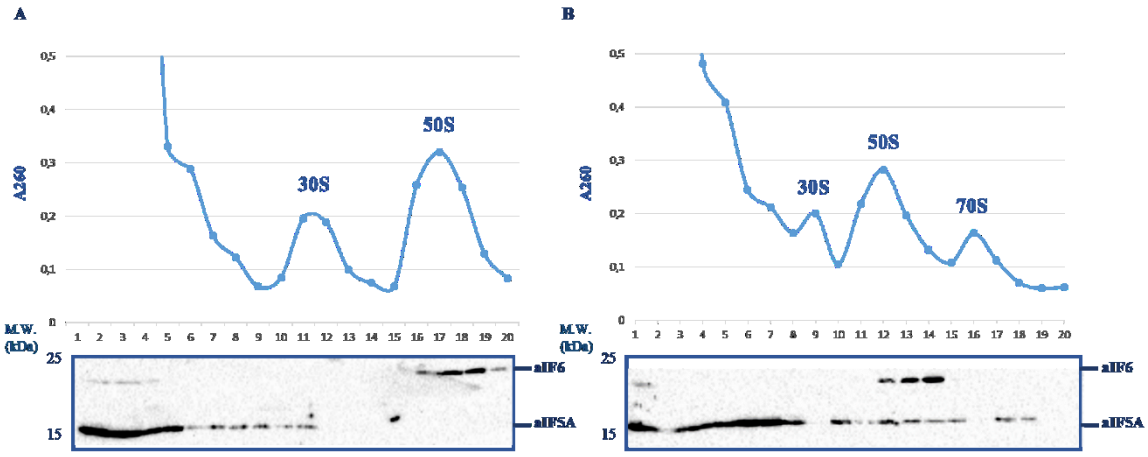

Figure 12. Fractionation of Sulfolobus solfataricus S30 extract and localization of Sso-aIF5A. *(A)* Density gradient fractionation of 500 µg (total proteins) *Sulfolobus solfataricus* P2 S30 extract. (B) Density gradient fractionation of 500 µg *Sulfolobus solfataricus* P2 S30 extract programmed for translation and fixed with formaldehyde. The number of fractions is shown in white and proteins in each fraction were separated on 15% SDS-polyacrylamide gel and analyzed by immunoblot, using anti-SsoaIF5A and anti-aIF6 polyclonal antibodies.

To gain more insight into the functional role of aIF5A in translation and to investigate other possible functions of the protein, it would be extremely important the possibility to perform *in vitro* experiments.

To this end, the availability of the recombinant protein in its active, hypusinated, form is an absolute requirement.

Therefore, having obtained large amount of the protein from *E. coli* in its unmodified version, we sought to obtain the modified protein in *Sulfolobus*.

3.3. Production of His-tagged Sso-aIF5A proteins in *Sulfolobus solfataricus*

It is conceivable that extremophilic recombinant proteins retain their properties, post-translational modifications and structural conformation in genetically and environmentally native hosts.

Therefore, to provide some insights about the functional role and the possible post-translational modification of Sso- aIF5A we cloned and produced it in the native host.

The protein aIF5A was synthesized in *Sulfolobus solfataricus* PH1-16 (Δ*pyrEF*), cloning the gene (P2 ORF Sso0970) in the expression plasmid pMJ05 [83] and mutating the second amino acid serine in leucine (as previously discussed this should not affect the protein function).

Four different constructs were created: the His-tag was introduced at both the N-terminus and the C-terminus position and each of the construct was inserted under the control of two different promoters, the inducible arabinose promoter and constitutive one ptf55.

The four strains and the respective controls were inoculated in the appropriate medium and the growth was followed by monitoring the OD at 600 nm (figure13).

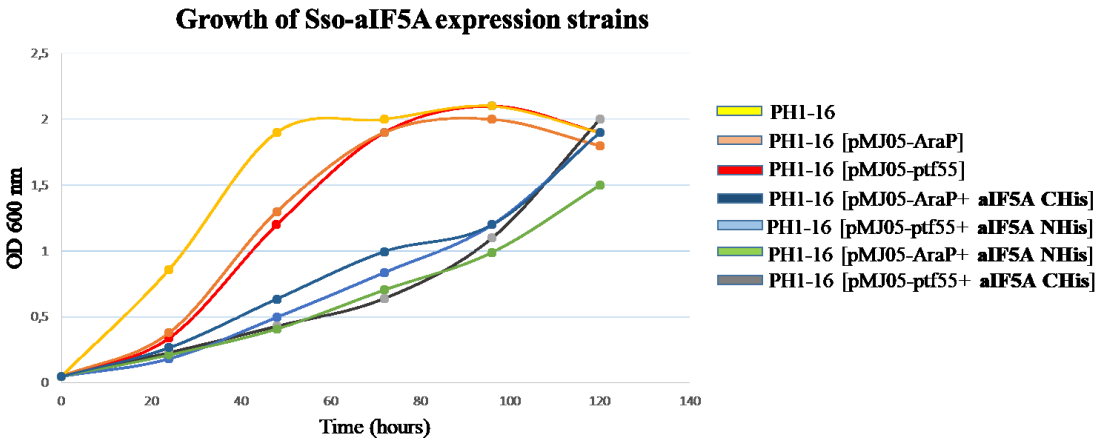

Figure 13. The synthesis of aIF5A in Sulfolobus solfataricus causes a dramatic slow-down of growth. *Sulfolobus solfataricus* PH1-16 strains: the growh of expression strains (blue, light blue, green and grey) slowed down during the exponential phase, compare to control strains (yellow, orange and red).

A slowing down of the growth rate was clearly observed in all four strains containing the recombinant plasmids, compared to the control, an indication that the overproduction of the protein might have a toxic effect.

To verify the synthesis of the protein, cell lysates from all strains were analyzed by western blot with anti-SsoaIF5A serum to detect both the native aIF5A and the recombinant His-tagged protein.

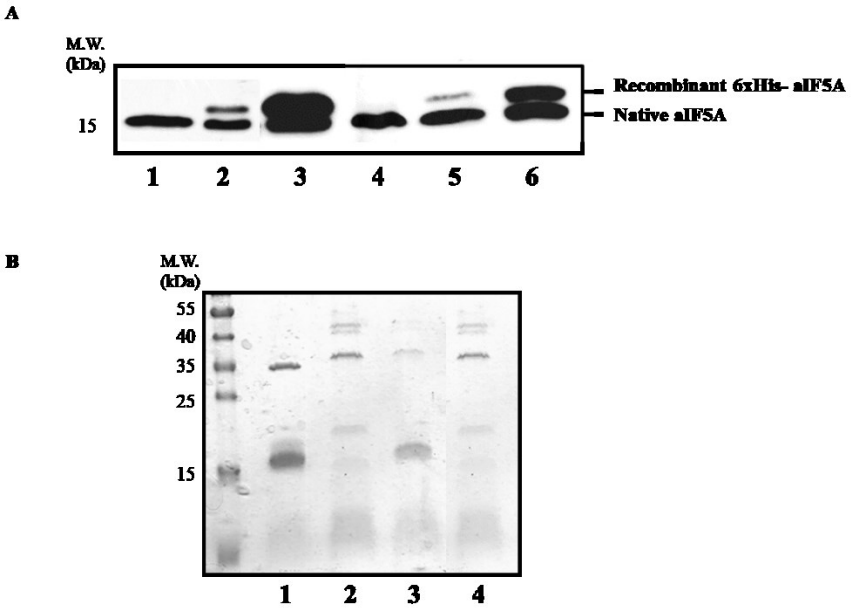

Figure 14. Production of aIF5A in Sulfolobus solfataricus. **(A)** Test of Sso-aIF5A production in *Sulfolobus solfataricus* PH1-16. 100 µg (total proteins) of control/expression strains lysates (OD_{600nm} 0,8) were separated on SDS-PAGE gel 15% and the western blot analysis with anti-SsoaIF5A serum allowed the detection of either the native aIF5A and recombinant His-tagged protein respectively. Lane 1: native aIF5A in the control strain PH1-16 [pMJ05-ptf55]; lane 2: native aIF5A and recombinant N-terminal His-tag in the expression strain PH1-16 [pMJ05-ptf55]; lane 3: native aIF5A and recombinant C-terminal His-tag in the expression strain PH1-16 [pMJ05-ptf55]; lane 4: native aIF5A in the control strain PH1-16 [pMJ05-AraP]; lane 5: native aIF5A and recombinant N-terminal His-tag in the expression strain PH1-16 [pMJ05-AraP]; lane 6: native aIF5A and recombinant C-terminal His-tag in the expression strain PH1-16 [pMJ05-AraP]. **(B)** Sso-aIF5A proteins affinity purified, separated on SDS-PAGE gel 15%, coomassie-blue stained. Lane 1: aIF5A C-terminal His tagged (pMJ05-ptf55); lane 2: aIF5A N-terminal His tagged (pMJ05-ptf55); lane 3: aIF5A C-terminal His tagged (pMJ05-AraP), lane 4: aIF5A N-terminal His tagged (pMJ05-AraP).

The results, showed in figure 14A, have been quantified and the intensity of each band estimated by Bio-Rad's Image Lab software.

The recombinant protein was present in all four strains but we can observe clear differences in the expression level of the protein especially depending on the position of the His-tag with C-terminal His-tagged proteins showing a more abundant production.

In particular the highest yield was achieved in *Sulfolobus* PH1-16 [(pMJ05-ptf55) aIF5A C-terminal His-tagged] (figure 14A lane 3) where a 3-fold overproduction of the recombinant protein, compared to the native protein level, was observed.

In both cases the constructs bearing the *ptf55* promoter gave rise to higher expression levels (figure 14A, 2 vs 5 and 3 vs 6).

The strain with the highest expression was also subjected to heat induction of the *ptf55* promoter but no significant increase in the level of the protein was detected (data not shown).

All four different version were affinity purified and the eluates loaded on SDS-Page as shown in figure 14B.

Sso- aIF5A C-terminal His-tagged, as expected, expressed from both promoters, was obtained in higher yield.

In addition the two version of the protein looked much pure than the eluate of Sso- aIF5A N-terminal His-tagged, where several proteins were co-eluted with the protein of interest figure 15B, compare samples 1 and 3 vs 2 and 4.

This evidence could suggest that the archaeal aIF5A factor interacts *in vivo* with several protein interacting partners.

Additionally the C-terminal domain is clearly involved in the protein-protein association, since when the His-tag is present in this domain many of these interactions are lost.

In particular, a protein with a molecular weight around 35 kDa, appears to be tightly associated to the factor in all cases (figure 14B) and it is co-purified with Sso-aIF5A even under stringent purification conditions (data not shown).

We determined the identity of this protein by mass spectrometry analysis (figure 15) and the major component identified corresponded to the deoxyhypusine synthase (DHS).

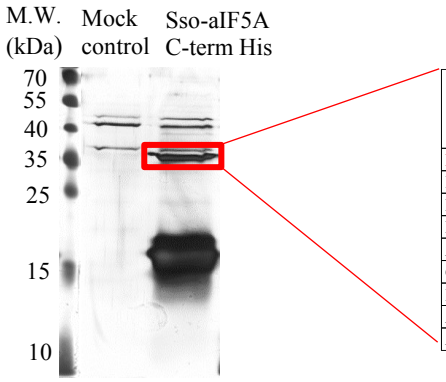

Proteins	*Mol. weight [kDa]*	*Sequence coverage [%]*	*MS/MS count*
Deoxyhypusine synthase (DHS)	35,05	80,8	594
IS605 orfB transposase	32,45	59,9	38
Fructose-1,6-bisphosphate aldolase/ph	42,707	33,8	21
Malate dehydrogenase	36,394	27,8	16
Acetyl-CoA acetyltransferase	42,506	18,4	10
Carbon monoxide dehydrogenase	30,743	28,4	8
Esterase	37,316	14,4	7
Amidohydrolase	30,621	24,7	7
Alcohol dehydrogenase	36,074	14,8	6

Figure 15. SDS-PAGE analysis of mock control and Sso-aIF5A C-terminal His-tagged. 10µl (1/100) of each eluate was analyzed by SDS-PAGE on a 15% gel, silver stained (on the left). Compare to the mock control, the main band of Sso-aIF5A eluate is the recombinant protein aIF5A (around 15 kDa) and the DHS enzyme. The piece of gel marked with the red rectangle was excited and subjected to LC-MS/MS analysis (results show on the right table).

The purified C-terminal His-tagged aIF5A (obtained from *ptf55* promoter), whose final yield was around 1 mg from 1l culture, was used for further experiments.

3.4. The post-translational modification of *Sulfolobus solfataricus* aIF5A

The presence of the hypusine modification of aIF5A has been experimentally confirmed in the crenarchaeon *S. acidocaldarius* [75], suggesting a similar modification pathway in Archaea and Eukarya.

Nevertheless many questions remain unsolved and since we showed that the Sso-DHS enzyme is co-purified with the recombinant aIF5A, we wondered whether the recombinant protein, once produced in *Sulfolobus solfataricus*, is post-translationally modified.

The C-terminal His-tagged aIF5A (theoretical mass: 15472.85 Da), affinity purified from *Sulfolobus solfataricus* PH1-16 [pMJ05 (ptf55)- aIF5A C-terminal His], was, first of all, analyzed to detect the eventual post-translational modification.

Since the modified residue is supposed to be in the N-terminal domain, we decided to analyze, by mass spectrometry, the protein with the His-tag at the C-terminal position, whose location should not affect the activity of enzymes involved in the modification pathway.

The high resolution accurate mass LC-MS/MS analysis detected a mass increase of 87.12 Da, compared to the theoretical mass of the C-terminal His-tagged aIF5A and this increment corresponds exactly to the molecular weight of the hypusine residue.

This is clearly visible in the MS spectrum (figure 16), in which the peak with the highest percentage of relative abundance corresponds to a protein with a mass of 15559.97 Da.

A second peak with a low percentage of relative abundance is also detected, corresponding to the deoxyhypusinated intermediate (15542,48 Da). From this result we concluded that most of the recombinant aIF5A expressed in *Sulfolobus solfataricus* PH1-16 becomes hypusinated.

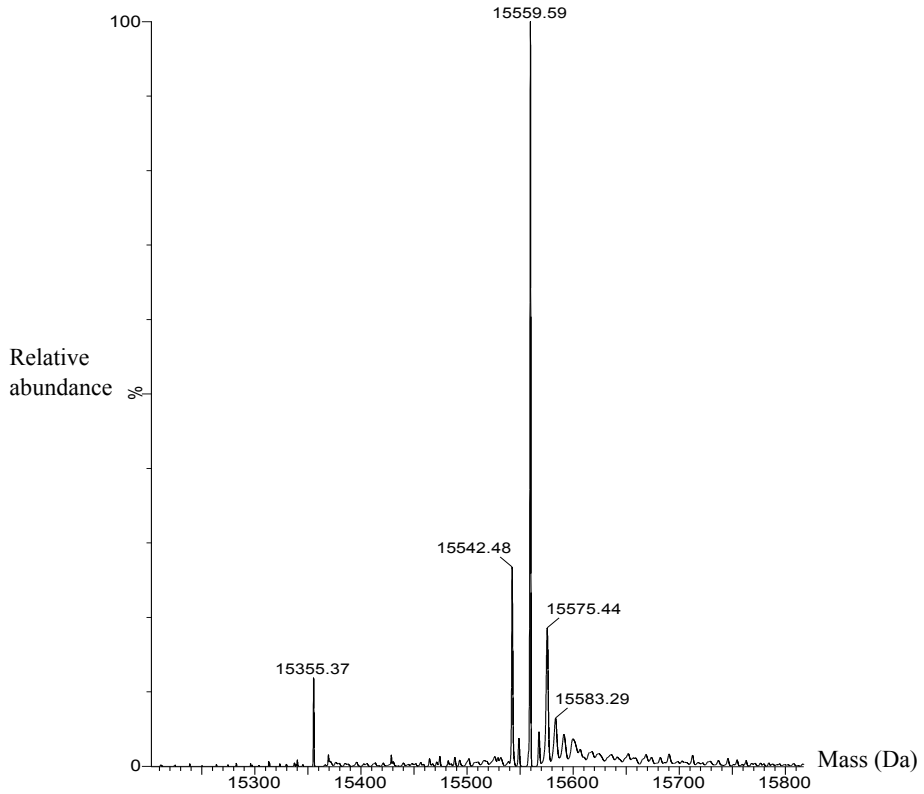

Sample	Expected mass (Da)	Observed mass (Da)	Matching modifications	Delta mass (Da)
Sso-aIF5A C-terminal His-tagged	15472.85	15559.59	Hypusine	- 0.38

Figure 16. The Sulfolobus solfataricus aIF5A factor is hypusinated. MS spectrum of the recombinant Sso-aIF5A C-terminal His-tagged expressed in *Sulfolobus solfataricus* PH1-16.

3.5. Production and purification of *Sulfolobus solfataricus* deoxyhypusine synthase in *E.coli*

The discovery that the recombinant protein produced in *Sulfolobus solfataricus* is hypusinated, and that the DHS enzyme is tightly associated with aIF5A, pressed us to characterize the *Sulfolobus solfataricus P2* post-translational modification pathway, starting from the isolation and characterization of the Sso-Deoxyhypusine synthase (DHS) enzyme.
In the previous MS analysis a low percentage of aIF5A deoxyhypusine intermediate was detected and, as we already mentioned, no deoxyhypusine hydroxylase was found in Archaea, thus we wondered whether the Sso-DHS is the only enzyme involved in the two steps of the hypusination or there is an alternative hydroxylation step, which has to be discovered.
Therefore we decided to clone and express the Sso-DHS in *E.coli*, in order to get a proper amount of recombinant enzyme for structural and functional studies.
A search in the *Sulfolobus solfataricus* P2 genome present in the NCBI database indicated ORF Sso0967 as the putative deoxyhypusine synthase gene.
We, therefore, cloned the ORF Sso0967 in two different expression plasmids (pETM11 and pQE-70), in order to obtain the DHS enzyme His-tagged either at the N-terminal or at the C-terminal position respectively.
We validated the identity and the orientation of the *Sulfolobus solfataricus* P2 DHS insert by sequencing and we aligned it with the eukaryal DHS sequence, as for this homologue enzyme the putative residues responsible for the binding to the NAD+ cofactor and to the spermidine substrate have been identified [12, 13].
The result of the alignment showed that these specific residues are conserved between the archaeal DHS enzyme and the eukaryal one (figure 17).

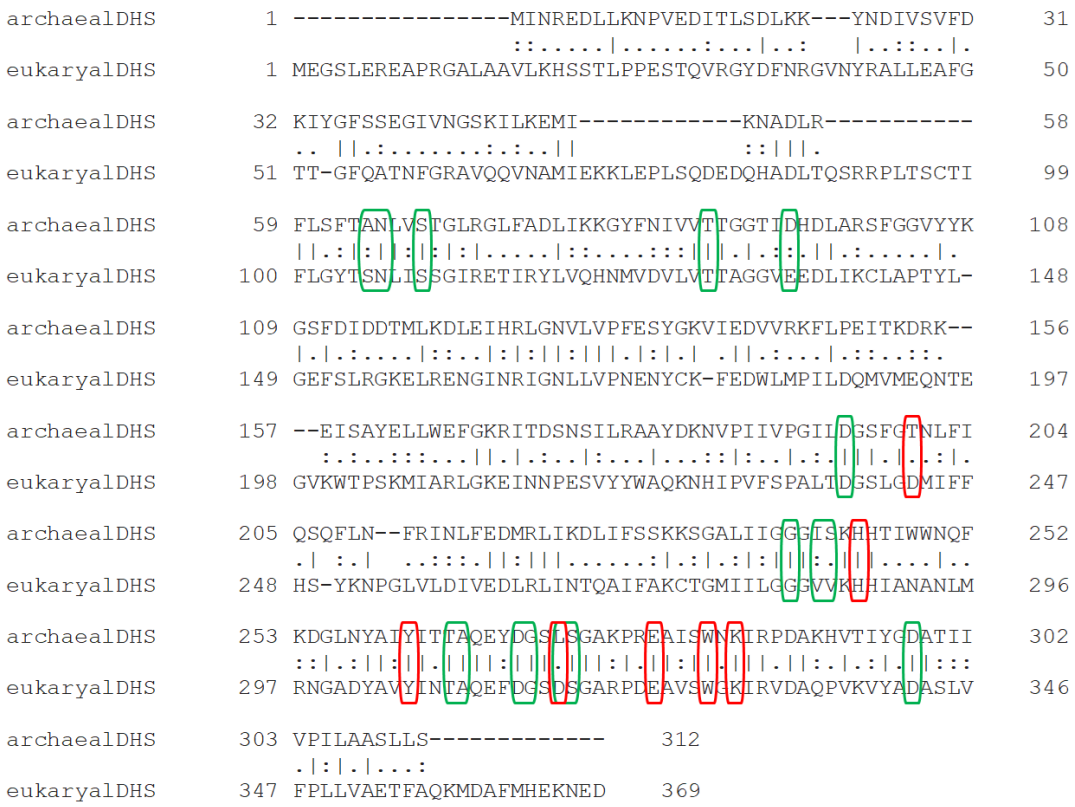

Figure 17. Conserved residues in the DHS enzyme sequence involved in the binding to the NAD+ cofactor and to the spermidine substrate. Pairwise protein sequences alignment of DHS from *Homo sapiens* (gi:1113109) and from *Sulfolobus solfataricus* P2 (gi:13814149). The residues which contact the NAD+ cofactor are marked in green, whereas those related to the spermidine substrate are marked in red.

Since it was reported that the eukaryotic recombinant DHS has solubility problems, the *E. coli* Rosetta strains overproducing the two versions of the protein were first tested in small-scale cultures (50 ml) for DHS expression.

Lysates were subjected to centrifugation and proteins, in pellets and supernatants, were separated by SDS-PAGE, together with the eluate of the DHS affinity purified.

The results (figure 18) show that expression of the protein is rather good in both cases but the Sso-DHS N-terminal His-tagged is insoluble, in fact, the protein produced is found exclusively in the pellet (figure 18 lane 1).

On the other hand, Sso-DHS C-terminal His-tagged (35,9 kDa) was more soluble (figure 18 lane 6) and we successfully purified 3 mg of enzyme from 1l culture.

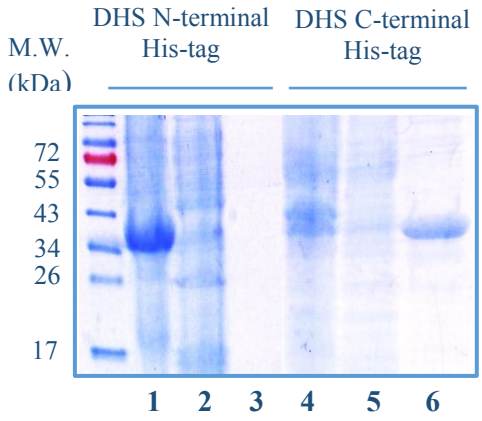

Figure 18. Production and purification of Sso-DHS in E.coli. Lanes 1-3: DHS N-terminal His tagged in *E.coli* ROSETTA (DE3)/ pLysS; lane 1: 1% total proteins in the pellet; lane 2: 1% total proteins in the supernatant; lane 3: 5% of DHS eluate after affinity purification. Lanes 4-6: DHS C-terminal His tagged in *E.coli* BL21 (DE3); lane 4: 1% total proteins in the pellet; lane 5: 1% total proteins in the supernatant; lane 6: 5% of DHS eluate after affinity purification.

3.6. The tetrameric structure of Sso-DHS

From the previous finding, we showed that the His-tag position in the recombinant Sso-DHS has an evident effect on the solubility and proper folding of the protein; however, no structural information related to the archaeal deoxyhypusine synthase has been provided yet. The eukaryotic DHS enzyme has been shown to exist mainly in a tetrameric form therefore, in order to determine the molecular mass and to investigate the oligomeric state in solution of Sso-DHS C-terminal His-tagged affinity purified (theoretical M.W. 35,9 kDa) we performed Analytical Size-Exclusion Chromatography coupled with Multiangle Laser Static Light Scattering.

The elution profile, monitored by absorbance at 280 nm, consisted of a main single peak and the light scattering signal (dots) revealed the mass distribution (figure 19).

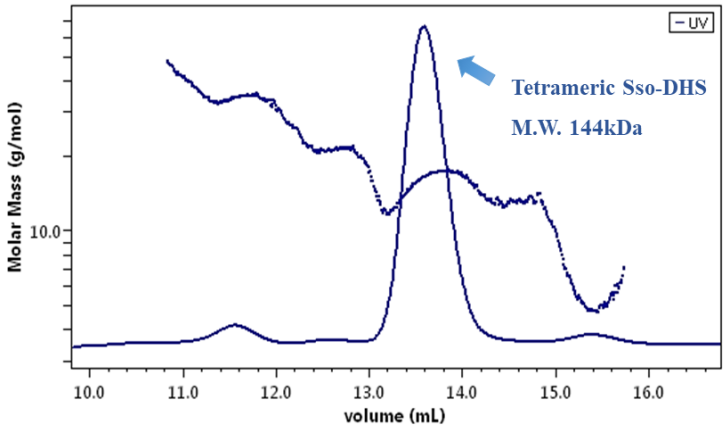

Figure 19. The recombinant Sso-DHS, purified in E.coli, shows a tetrameric structure in solution. The elution profile obtained by Analytical Size-Exclusion Chromatography and Multiangle Laser Static Light Scattering, monitored by absorbance at 280 nm, consists of a single peak and the major population tends to form a tetramer, whose calculated mass is 144 kDa.

The molecular mass related to the major peak was calculated to be 144 kDa, which correlates exactly with the tetrameric protein form.

This result suggests that this might be the active conformation also of the archaeal enzyme and from this finding we can conclude that the His-tag at the N-terminal position hinders the assumption of the functional tetrameric structure.

3.7. Sso-DHS performs the deoxyhypusine synthesis *in vitro*

We demonstrated that Sso-aIF5A is hypusinated and Sso-DHS C-terminal His-tagged, produced in *E.coli*, is a tetramer in solution, as it was shown already for the eukaryotic DHS enzyme [13].

This finding suggested that the recombinant DHS synthesized in *E.coli* could be functionally active. In addition the lack of a DOHH homologue in Archaea, together with the finding that in *Trichomonas vaginalis* hypusination occurs thanks to the catalytic activity of a single bifunctional enzyme (TvDHS), which performs both the DHS and DOHH reactions [18], prompted us to investigate on the enzymatic activity of the DHS trying to discover in which step of the hypusination pathway it might be involved.

For this purpose we performed an *in vitro* hypusination assay in which the recombinant DHS should be able to modify the recombinant unmodified Sso-aIF5A, produced in *E.coli*, using spermidine as substrate, since it is the most abundant polyamine in sulfur-dependent archaea [76] and NAD^+ which is supposed to be the DHS cofactor.

The recombinant DHS was pre-incubated 10 min at 65 °C to allow the formation of the tetrameric complex, then we performed the reaction testing several conditions, like different aIF5A/DHS ratios and incubation times and we assessed the enzyme performance by mass spectrometry (figure 20).

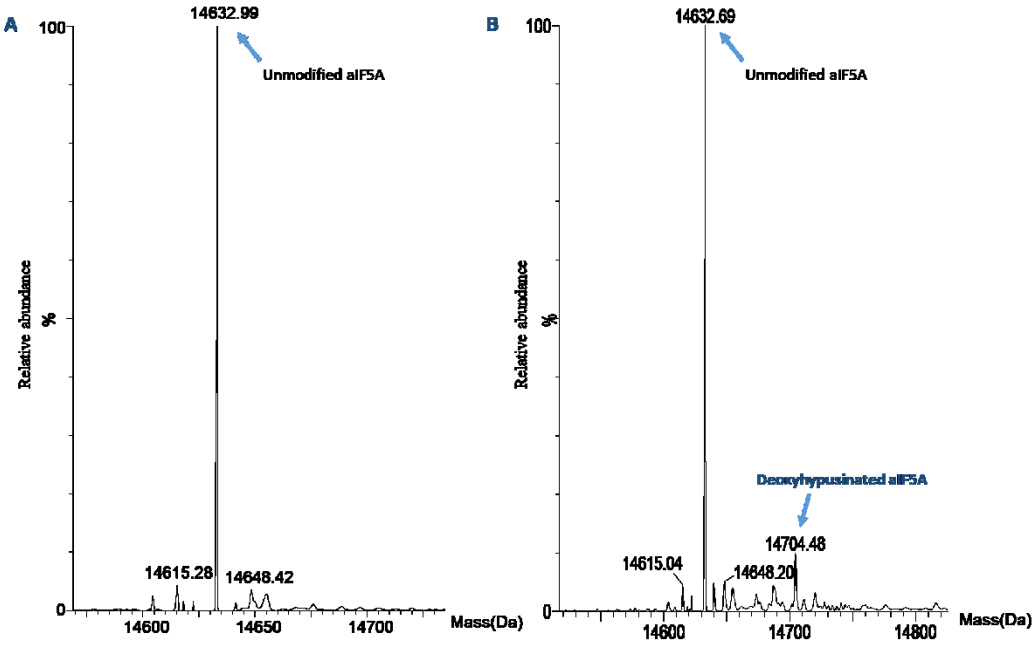

Sample	Expected mass (Da)	Observed masses (Da), Main peak in red	Matching modifications	Delta mass (Da)
Unmodified aIF5A	14632.83	14632.99		+ 0.16
aIF5A from *in vitro* hypusination	Unmodified aIF5A (14632.83)	14632.69		- 0.14
	Deoxyhypusinated aIF5A (14703.83)	14704.56	Deoxyhypusine	+ 0.71
	Hypusinated aIF5A (14719.83)			

Figure 20. The unmodified Sso-aIF5A is in vitro deoxyhypusinated by the recombinant Sso-DHS enzyme. (A) MS control spectrum of the unmodified recombinant Sso-aIF5A; the protein was incubated with all components of the *in vitro* hypusination assay, without the DHS enzyme. (B) MS spectrum of the recombinant Sso-aIF5A subjected to the *in vitro* hypusination assay.

Despite all experimental conditions tested, the main peak in the MS spectrum corresponds to the unmodified protein aIF5A, however we also observed the appearance of another peak (figure 20B), related to the deoxyhypusinated aIF5A, which is not detectable in the control (figure 20A).

The relative abundance of the deoxyhypusinated form is very low (10%), nevertheless its presence allowed us to conclude that, even if the enzymatic reaction is not efficient under these conditions, the recombinant DHS enzyme is able to perform the deoxyhypusine synthesis. Therefore it can be considered functionally homologue to the eukaryal one but not to the *T. vaginalis* one since synthesis of hypusine was not detected.

This result indicates clearly that a second enzyme must exist, therefore, in order to try to isolate a DOHH analogue enzyme but also to investigate whether Sso-aIF5A is involved in other cellular processes we sought to identify proteins interacting with the factor.

3.8. Sso-aIF5A protein interacting partners

There is a rather limited knowledge concerning the aIF5A interactome, however a very recent study identified this archaeal factor among the protein interacting partners of the SmAP1/2 proteins [94], which are involved in different aspects of RNA metabolism.

Therefore, to shed light on the functional role of aIF5A factor in *Sulfolobus solfataricus* we identified the protein interacting partners which were affinity co-purified with the protein of interest, by mass spectrometry analysis.

For this purpose we used the eluate of Sso-aIF5A N-terminal His-tagged (figure 21), since, as already mentioned it is enriched of proteins which are co-eluted with aIF5A, compared to the eluate of Sso-aIF5A C-terminal His-tagged.

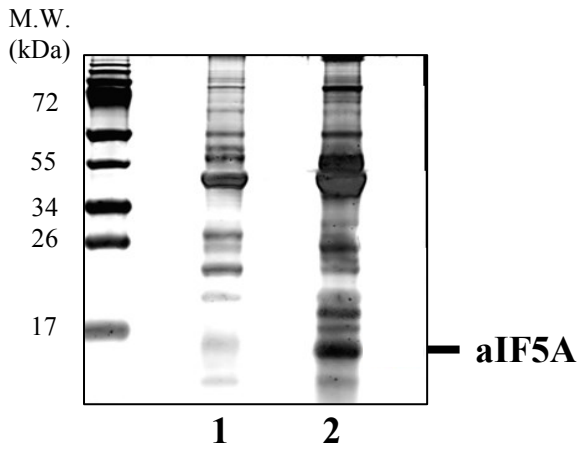

Figure 21. Sso-aIF5A N-terminal His-tagged co-purifying proteins. Lane 1-Mock control: 10 µl (1/100) of the eluate from the mock purification of Sso PH1-16 (pMJ05-ptf55 empty plasmid). Lane 2-SsoaIF5A eluate: 10 µl (1/100) of the eluate from the affinity purification of Sso PH1 [(pMJ05-ptf55)-aIF5A N-terminal His-tagged]. SDS-PAGE gel 12,5%, silver stained.

In parallel unspecific proteins which would bind to the affinity matrix were also analyzed by mass spectrometry, performing a mock purification from Sso PH1-16 (pMJ05-ptf55 empty plasmid) cell lysate (figure 21).

Among the interacting partners, we selected only those that in Sso-aIF5A eluate were enriched over the mock control and with this criterion, we identified 31 proteins (table 5).

Results are presented in table 5 and show proteins which are enriched about more than 1.5 fold in the Sso-aIF5A sample.

Interestingly the protein present with the highest enrichment is the DHS enzyme (122 vs 0 count in the mock control) a result which confirms that also in *Sulfolobus* DHS is the first enzyme in the hypusination pathway.

In addition several dehydrogenase were identified and these may be involved in the deoxyhypusine hydroxylation.

More than half were proteins involved in cell metabolism while one fourth of interacting partners are involved in rRNA/tRNA modification and processing, RNA turnover and translation, whereas the rest of the list include four proteins with unknown functions.

This result suggested the multifunctional role of the aIF5A in *Sulfolobus solfataricus* and allowed us to consider a probable involvement of the factor in the mRNA stability/turnover.

		MS/MS count		
ORF	Mol. weight [kDa]	aIF5A interactıng partners	Mock control	Sso proteins
Cellular methabolism				
SSO0967	**35,05**	**122**	**0**	**deoxyhypusine synthase (DHS)**
SSO0534	42,506	147	63	acetoacetyl-CoA thiolase
SSO1214	23,678	110	0	carbonic anhydrase
SSO2885	35,08	31	0	oxidoreductase
SSO0530	48,508	22	6	serine hydroxymethyltransferase
SSO2779	33,603	21	13	aldo/keto reductase
SSO3006	111,16	20	0	alpha-mannosidase
SSO2356	62,531	16	3	succinate dehydrogenase
SSO2219	27,889	14	3	nad kinase
SSO2747	29,71	13	2	aldose 1-epimerase
SSO0214	34,338	12	0	acetate kinase
SSO0845	27,012	12	1	response regulator aspartyl-phosphate
SSO1067	19,227	11	5	intracellular protease PfpI family
SSO3016	33,011	10	3	amidohydrolase
SSO2514	73,038	9	0	3-hydroxyacyl-CoA dehydrogenase
SSO0989	48,225	7	0	sugar phosphate nucleotydyl transferase
SSO2521	35,508	7	0	lipase, lipP-2
SSO3004	33,096	6	1	3-oxoacyl reductase
SSO1178	20,815	6	1	S-adenosyl-methionine-dependent methyltransferases
rRNA/tRNA modification and processing, RNA turnover, translation				
SSO0176	85,807	157	74	AAA+ ATPAse, mRNA surveillance and transport factors
SSO2509	14,786	83	14	translation recovery factor
SSO2226	24,933	82	53	methyltransfrease Nep1
SSO2363	43,683	40	1	Mox-R like ATPase
SSO0606	17,975	25	14	transcriptional regulator AsnC
SSO0939	46,692	23	16	Nop56, C/D box methylation guide RNP
SSO6454	8,6789	8	6	SmAP1
SSO0221	12,095	6	1	50S ribosomal protein RPL30e
Hypotethical proteins				
SSO1412	23,811	50	4	hypothetical protein
SSO3050	27,012	26	0	hypothetical protein
SSO1413	16,072	23	8	hypotetical protein
SSO1383	20,242	12	0	hypotethical protein

Table 5. Analysis of Sso-aIF5A protein interacting partners by LC-MS/MS. The MS/MS count reveals how often MS/MS spectra of particular peptides of that protein were triggered. Considering this value in the list it is possible to see the clear enrichment in proteins that are co-purified with Sso-aIF5A, compared to the mock control.

3.9. Functional interplay between the factor aIF5A and the translation recovery factor (Trf)

Analysis of Sso-aIF5A interactome (table 5), draw our attention to one of the protein because of its involvement in mRNA translation/turnover: the Translation Recovery Factor (Trf) (Sso2509).

This protein was identified by Märtens et al [88] and found to promote recovery of translation after nutrient stress.

It is known, in fact, that under nutrient limitation conditions the overall protein synthesis ceases and the trimeric translation initiation factor aIF2, normally responsible of recruiting tRNAi on the ribosome, binds, via its γ subunit, to the 5'-PPP end of mRNAs, in particular leaderless mRNAs, preserving their integrity [65, 66].

Upon relief of nutrient stress the Sso-2509 protein binds directly to the aIF2-γ triggering its release from the 5'-PPP end of mRNAs, in this way both the mRNAs and aIF2 are free to reenter translation.

Finding Sso-2509 among the interacting partners of aIF5A lead us to hypothesize a functional role of aIF5A in this scenario.

To demonstrate this we have analyzed more in detail the singular association between aIF5A and Sso-2509.

First we confirmed the interaction between the two proteins by *in vitro* co-immunoprecipitation (Co-IP), using the Sso-2509 and Sso-aIF5A recombinant proteins purified from *E.coli* (figure 22).

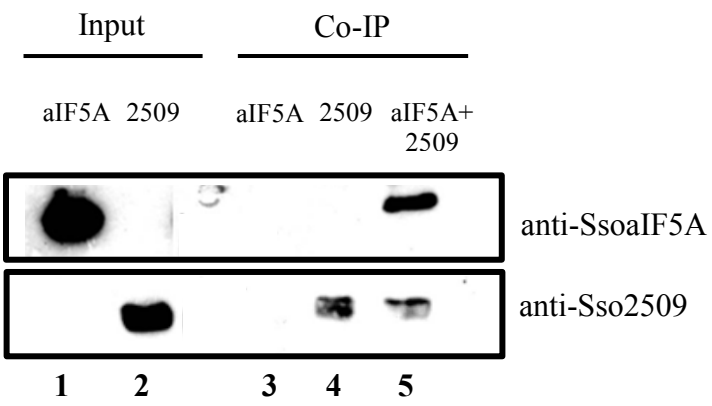

Figure 22. Sso-aIF5A co-immunoprecipitated with Sso-2509. Co-IP with anti-Sso2509 antibody and analysis of immunocomplexes by western blotting, using anti-SsoaIF5A and Sso-2509 specific antibodies. Lanes 1–2: input of aIF5A (lane 1), and 2509 (lane 2) used for the Co-IP assays. Lanes 3–5, Co-IP assays with aIF5A alone (lane 3), 2509 alone (lane 4) and aIF5A in the presence of 2509 (lane 5).

The results in figure 22 confirm that the two proteins can interact *in vitro* (see lane 5).

Having established this, we tried to understand if this interaction is an indication that aIF5A plays a direct role, together with Sso-2509, in the release of aIF2/aIF2-γ from the 5′-P3-end of the RNA.

To do so we performed the same experiment described in [88] but in the presence of aIF5A.

We ligated the 3'-biotinylated 2508sh mRNA to streptavidin beads and the 5'-ends of the RNA were saturated with an excess of trimeric aIF2.

After removal of aIF2 from the supernatant, either Sso-2509, Sso- aIF5A, Sso-2509and Sso-aIF5A together, or buffer were added to the streptavidin-RNA-aIF2 complex.

Then, the supernatant, the wash fraction and the beads (retained fraction) were probed for the presence of the aIF2γ subunit by western blot analysis to detect its release from the 5'end of the mRNA.

As mentioned before it is only the γ subunit, either in the trimeric complex aIF2 or alone, responsible for the binding to the 5' end of mRNAs [66].

We used the recombinant proteins Sso- aIF5A/ Sso-2509 purified in *E.coli*, as we confirmed that they co-immunoprecipitate as previously described.

Result of this assay are showed in figure 23. As expected in the presence of Sso-2509, aIF2γ is released from the mRNA (fig.23 lane 3), when Sso-aIF5A is present in the reaction the release of aIF2γ is impaired (figure 23 lane 6).

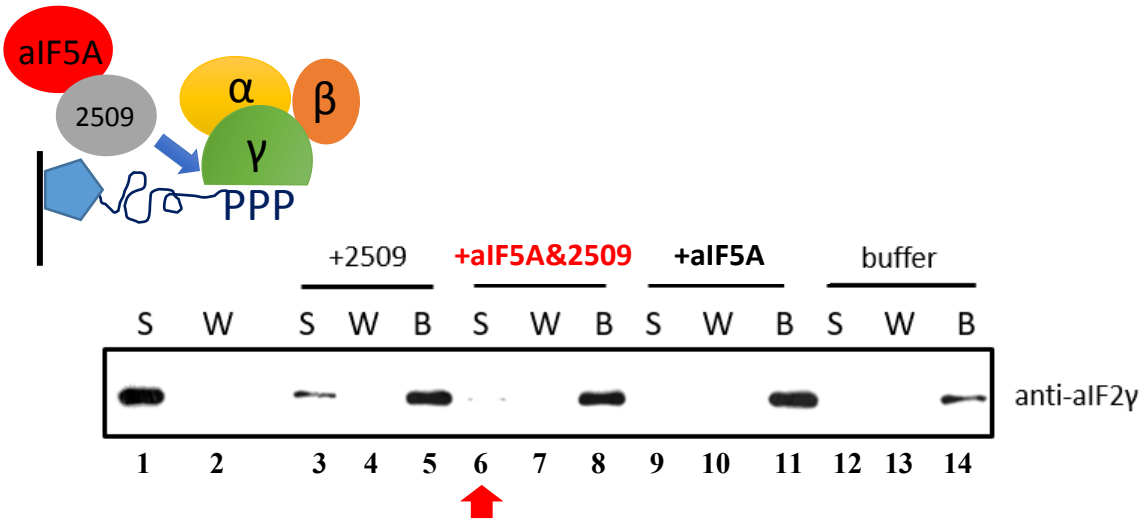

Figure 23: In presence of Sso-aIF5A, Sso2509 is not able to remove aIF2γ from the 5'-P3-end of the RNA. The biotinylated 2508sh RNA was ligated to streptavidin beads and saturated with aIF2. Unbound aIF2γ (S, lane1) was removed by several washing (W, lane 2) steps. The immobilized complex was either incubated with protein 2509 (lanes 3–5; +2509), aIF5A together with 2509 (lanes 6–8; +aIF5A&2509), aIF5A alone (lanes 9-11; +aIF5A) and buffer (lanes 12-14; buffer). The supernatant (S; lanes 3, 6, 9 and 12), wash fractions (W; lanes 4, 7, 10 and 13) and beads (B; lanes 5, 8, 11 and 14) were examined for the presence of aIF2γ by western blot analysis. The red arrow underline that aIF2γ, in presence of aIF5A, was not released in the supernatant (S) by 2509.

This result appears particularly interesting reinforcing the hypothesis of aIF5A involvement in the mRNA stability/turnover. Forming this complex, in fact, aIF5A could behave as a sensor of the cell nutrient conditions regulating when to restart translation and preserving mRNAs integrity during unfavorable environmental conditions.

3.10. Structural characterization of the archaeal factor aIF5A

Results obtained so far indicate that the archaeal aIF5A is associated with ribosomes during the active protein synthesis and this was expected from its conservation as a translation factor. On the other hand, the several protein interacting partners identified, together with the results obtained with one of these partners (Sso-2509) and the RNase activity described for other

archaeal aIF5A proteins, suggest the possibility that the protein might be involved in other, RNA related, cellular processes.

Therefore we decided to investigate the structural conformation of the protein and to investigate the existence of multi-protein complexes.

First of all we questioned whether the archaeal factor can forms oligomers since it has been shown that the eukaryal protein can form dimers.

To assess this we analyzed the Sso-aIF5A recombinant protein (His-tag removed by the cleavage with the TEV protease), purified in *E.coli*, by Analytical Size-Exclusion Chromatography coupled with Multiangle Laser Static Light Scattering.

The size-exclusion chromatography elution profile of the unmodified aIF5A, shown in figure 24, consisted of a single peak and the corresponding molecular weight is 15 kDa, which correlates with the monomeric protein form.

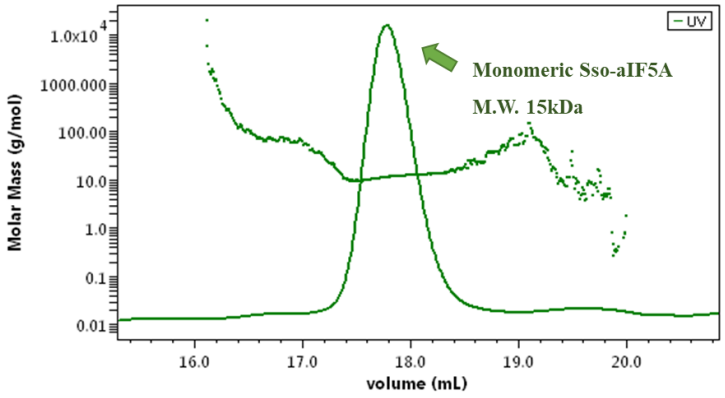

Figure 24. The recombinant Sso-aIF5A produced and purified in E.coli is a monomer in solution. The elution profile shows a single peak and the major population tends to form a monomer, whose calculated mass is 15 kDa.

This result underline that the unmodified Sso-aIF5A is unable to assume any oligomeric conformation and this is consistent with a previous study related to the eukaryotic factor eIF5A, which requires the hypusine modification and the RNA for its dimerization [4].

Since a parallel experiment with the recombinant hypusinated protein expressed in *Sulfolobus* has not been performed yet, due to the difficulty to obtain large amount of the protein, we tried to characterize the structural conformation of the native hypusinated archaeal protein *in vivo*, by fractionating the Sso-S30 extract on a linear 5-15% glycerol gradient, which is a useful tool to study the sedimentation properties of small proteins.

The fractions obtained were analyzed by immunoblotting and the sedimentation profile of aIF5A was compared to that of a mixture of proteins with known molecular weight.
For the western blot analysis we used the anti-SsoaIF5A antibody and since we established that Sso-aIF5A is hypusinated, we decided to use also the eukaryotic anti-hypusine antibody, as we demonstrated that it is able to recognize the archaeal modified protein (figure 25).
The eukaryotic anti-hypusine detected the native archaeal protein aIF5A in a Sso-S30 extract, nevertheless it recognized even the unmodified recombinant protein, when the amount of aIF5A exceeds 40 pmols.

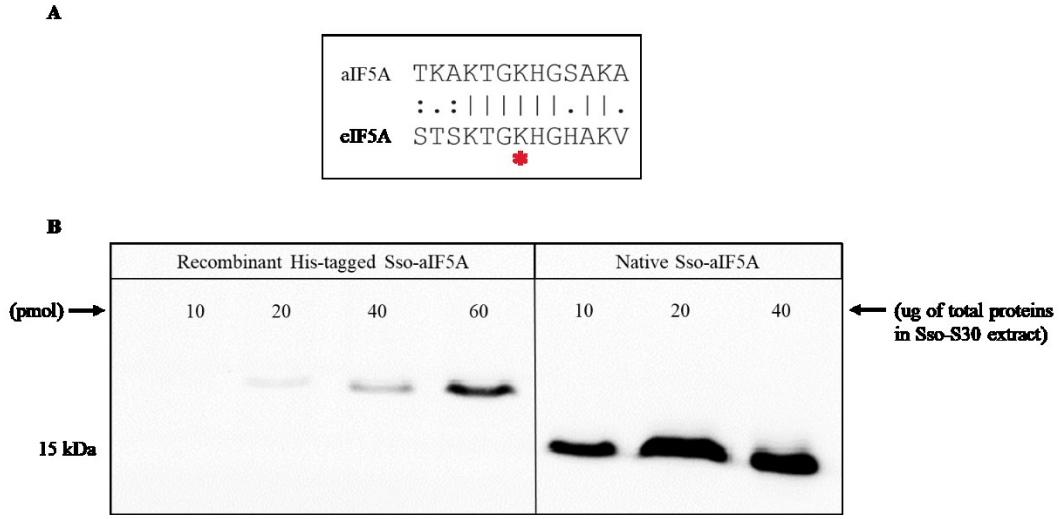

Figure 25. The eukaryotic anti-hypusine antibody recognizes the hypusinated archaeal protein. (A) Sequence alignment between the eukaryotic peptide, used to generate the rabbit polyclonal anti-hypusine antibody [95], and the corresponding peptide in the archaeal aIF5A sequence; the hypusinated lysine is marked by the red asterisk. (B) Detection of the recombinant unmodified N-terminal His-tagged Sso-aIF5A and native hypusinated aIF5A probed, by western blot analysis, with the eukaryotic anti-hypusine antibody.

The *Sulfolobus* S30 extract was either directly loaded on the glycerol gradient or subjected to a previous treatment with the micrococcal nuclease, in order to see if the minimization of nucleic acids content has an effect on the protein sedimentation profile (figure 26).

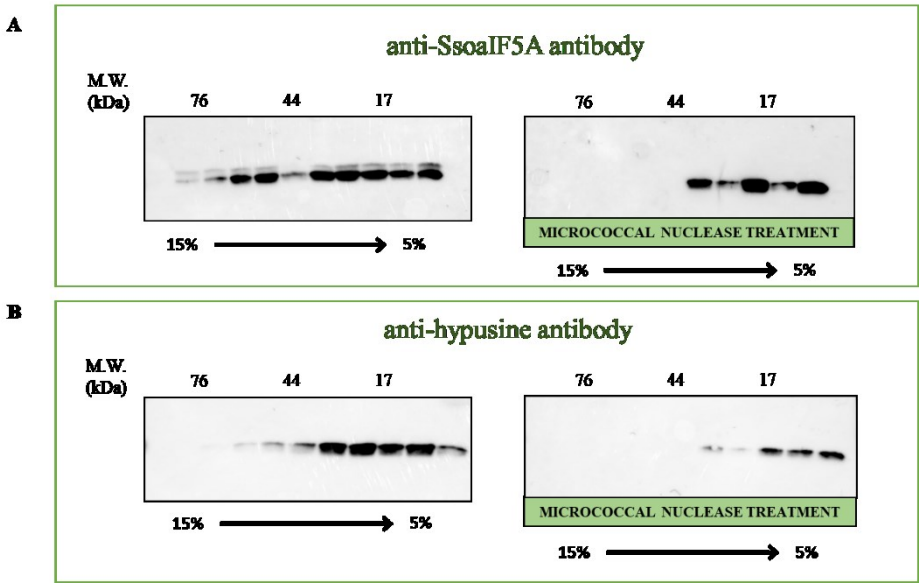

Figure 26. The archaeal aIF5A may forms oligomers or be part of a multi-protein complex. Fractionation of 500 µg (total proteins) *Sulfolobus* S30 extract on glycerol gradients 5-15%, under normal condition or with a previous treatment of the extract with the micrococcal nuclease. (A) Immunoblotting of the fractions with anti-SsoaIF5A antibody. (B) Immunoblotting of the fractions with the eukaryotic anti-hypusine antibody.

Under normal conditions the native aIF5A factor was shown to co-migrate mainly with proteins around 17 kDa, however it was also present in fractions where proteins, with a molecular weight ranging from 44 to 76 kDa, were migrating.

It follows that the protein exists as a monomer *in vivo*, but it is also present in higher molecular weight complexes, which may result from oligomerization or multi-protein complex formation.

When the *Sulfolobus* S30 extract was treated with the micrococcal nuclease the sedimentation scenario of aIF5A was different, the protein is exclusively detectable in fractions related to proteins of 17kDa.

From this is evident that the depletion of nucleic acids leads to the disruption of this oligomeric/multi-protein complex conformation (figure 26A).

Interestingly the western blot analysis performed with the anti-hypusine antibody confirmed that the native protein, as a monomer, is hypusinated.

However, under both conditions tested, this post-translational modification is not detectable in fractions related to proteins with a molecular weight between 44 and 76 kDa (figure 26B).

3.11. The factor aIF5A binds distinct RNA substrates in *Sulfolobus solfataricus*

The previous experiment showed that aIF5A *in vivo* is localized in a complex that becomes dissociated upon nuclease treatment reinforcing the idea of a probable involvement of the protein in the RNA metabolism.

To characterize this complex we decided to isolate and identify, by deep sequencing analysis, RNA molecules that may associated with aIF5A *in vivo* in *Sulfolobus solfataricus*.

To do so we used affinity purification and isolated the RNA bound to Sso-aIF5A C-terminal His-tagged.

We selected this version of the recombinant protein because its production was higher and the eluate from affinity resin looked much pure from proteins than the N-terminal His-tagged one (figure 14B).

As a control we isolated also the RNA co-eluted in a mock purification, using Sso PH1-16 [pMJ05 (ptf55-empty plasmid)] lysate in order to exclude those RNA molecules that may bind to the affinity matrix in a nonspecific way.

The eluates purity was evaluated by SDS-PAGE and the silver staining showed that the eluate of aIF5A was eligible for the deep sequencing analysis, as we already demonstrated that the additional protein around 35 kDa, which is not detectable in the mock control, is the deoxyhypusine synthase (figure 15).

From this finding we can exclude that the presence of the DHS enzyme in the eluate had any effect on the reliability of the RNA_{seq} data.

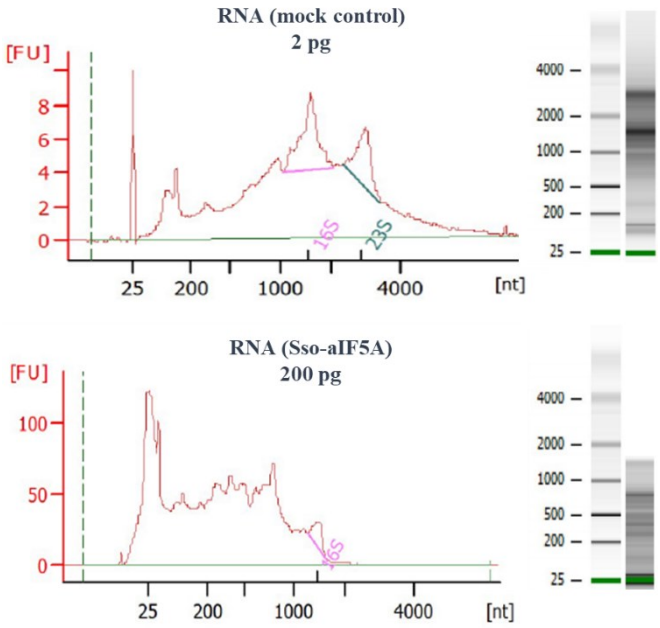

Figure 27. Quality control of RNA samples for the deep-sequencing analysis.

The quality and the quantity of the RNA eluted from the affinity purification of Sso-aIF5A and from the mock purification, was determined with the bioanalyzer (figure 27).

The amount of RNA eluted with Sso-aIF5A was ten-fold enriched with respect to the RNA isolated from the mock purification and the yield was 200 pg from 4l culture, the RNAs size is in the range 20-1500 nt.

The deep-sequencing analysis of co-purifying RNAs (Appendix table A.1 and table A.2) revealed three distinct categories of molecules predominantly bound to Sso-aIF5A, namely non coding RNA, tRNA and protein coding RNA (mRNA) which are presented in tables 6, 7 and 8.

Table 6 shows the group of ncRNAs which have been selected using a threshold of four-fold difference in the TPM values (Ratio: TPM aIF5A/ TPM mock).

Gene	Reads mock	Reads Sso-aIF5A	TPM mock	TPM aIF5A	Ratio (TPM aIF5A/TPM mock)	Homolog name	Group
ncRNA26	3	214	0,2396	124,249	518,5684474	Sso-225	
ncRNA32	0	286	0	433,294	433,294	Sso-125	C/D box targets rRNA
SSOs04	0	156	0	270,106	270,106		snoRNA

ncRNA1	0	146	0	257,387	257,387	Sso-195	C/D box targets rRNA
ncRNA83	41	755	17,637	236,147	13,38929523	Sso-17	
ncRNA36	685	9505	327,415	3303,28	10,08895744	Sso-128	Complementary to tRNA-Pro
ncRNA2	130	1227	86,681	594,856	6,86258811		
ncRNA98	188	1496	278,566	1611,71	5,785727619		
ncRNA99	369	2400	332,489	1572,34	4,728998553		
ncRNA100	882	5312	712,848	3121,56	4,378992436		
ncRNA78	39	230	25,875	110,95	4,287922705		Transposon related

Table 6. ncRNAs co-purifying with Sso-aIF5A. For RNAs highlighted in light blue the value "Ratio (TPM aIF5A/TPM mock)" corresponds to the respective TPM Sso-aIF5A value, since for these RNAs the TPM mock value is 0.

All the ncRNAs presents were previously identified in the *Sulfolobus solfataricus* transcriptome [96] and some were characterized even before as potential antisense regulators [97].

Interestingly some of the RNAs in this group are known to participate in rRNA /tRNA processing: ncRNA32 and ncRNA1 are two C/D box sRNAs, which target the 23S RNA via antisense elements located 5' to D'-boxes, snoRNA Sso04, which recognizes the 23S rRNA target and catalyzes the 2'-*O*-ribose methylation of G2731 predicted site [98].

Another sRNA co-purified with Sso-aIF5A, ncRNA36, is antisense to $tRNA^{Pro}$, which lacks an intron sequence.

The presence of these RNAs strongly suggests the idea that Sso-aIF5A is part of a ribonucleic complex probably involved in rRNA/tRNA processing.

The rest of ncRNAs identified consists of ncRNA98/ncRNA99, which are overlapping, several ncRNAs located in intergenic regions and ncRNA78, which putatively regulate transposition.

The second group, in table 7, is represented by 4 tRNAs whose TPM ratio is rather high being all of them absent in the mock, underlying the involvement of this factor in translation or in the tRNA processing.

Gene	Reads mock	Reads aIF5A	TPM mock	TPM aIF5A	Ratio (TPM aIF5A/TPM mock)	Gene product
SSOt05	3	195	0,5334	252,10	472,6265467	tRNA-Val
SSOt16	0	94	0	121,52	121,52	tRNA-Arg
SSOt20	0	90	0	117,93	117,93	tRNA-Ala
SSOt10	0	83	0	110,24	110,24	tRNA-Asp

Table 7. tRNAs co-purifying with Sso-aIF5A. For RNAs highlighted in light blue the value "Ratio (TPM aIF5A/TPM mock)" corresponds to the respective TPM Sso-aIF5A value, since for these RNAs the TPM mock value is 0.

The mRNA represents the third group. In this group only few RNAs encode for known products (table 8).

Gene	Reads mock	Reads aIF5A	TPM mock	TPM aIF5A	Ratio (TPM aIF5A/TPM mock)	Gene product
SSO-1773	39	944	0,6517	114,70	176,002762	multidrug-efflux transporter
SSO-3226	64	980	10	116,02	11,13348047	fructose-bisphosphate aldolase
SSO-2184	3382	47164	381	3859,13	10,13961676	cell division protein cdc6
SSO-0556	102	1397	23	230,37	9,958284702	CDP-diacylglycerol--glycerol-3-phosphate 3-phosphatidyltransferase
SSO-1896	178	2030	37	308,03	8,291940347	2-haloacid dehalogenase
SSO-0060	0	1293	0	129,38	129,38	UDP-N-acetylglucosamine--dolichyl-phosphate N-acetylglucosaminephosphotransferase (gnptA)

Table 8. mRNAs co-purifying with Sso-aIF5A and encoding for known products. For RNAs highlighted in light blue the value "Ratio (TPM aIF5A/TPM mock)" corresponds to the respective TPM Sso-aIF5A value, since for these RNAs the TPM mock value is 0.

As shown the highest TPM ratio is related to mRNAs encoding a transporter, a cell division protein and proteins involved in different cellular processes.

Nevertheless, most of the mRNAs identified encode for hypothetical proteins (table 9) and for some of them we identified a putative function, using the Sequence Similarity Database of KEGG (Kyoto Encyclopedia of Genes).

Gene	Reads mock	Reads aIF5A	TPM mock	TPM aIF5A	Ratio (TPM aIF5A/TPM mock)	Gene Product
SSO-3164	1	299	0,0361	78,57	2176,371191	hypothetical protein
SSO-8910	1	128	0,0823	76,61	930,8748481	putative transposase
SSO-1196	0	902	0	418,46	418,46	putative ATPase (AAA+ superfamily)
SSO-0175	0	1299	0	346,98	346,98	putative aminoacyl-tRNA hydrolase
SSO-1570	4	172	0,1389	43,43	312,6709863	hypothetical protein
SSO-0620	0	1193	0	294,34	294,34	putative transcriptional regulator (ArsR family)
SSO-3146	34	1357	0,5747	166,76	290,1740038	hypothetical protein
SSO-0123	39	1503	0,7844	219,81	280,2231005	hypothetical protein
SSO-0039	23	872	0,5353	147,56	275,6529049	putative phosphomethylpyrimidine kinase
SSO-0117	0	1099	0	263,11	263,11	hypothetical protein
SSO-0009	30	1072	0,4066	105,63	259,7934088	putative histone deacetylase
SSO-2186	51	1683	0,8039	193,00	240,0796119	hypothetical protein
SSO-3164	0	427	0	226,24	226,24	hypothetical protein
SSO-0253	0	1291	0	223,13	223,13	putative adenylyl cyclase CyaB
SSO-0107	0	746	0	194,44	194,44	putative transcriptional regulator (XRE family)
SSO-2338	45	1156	0,6062	113,22	186,7683933	putative transport protein
SSO-2489	30	658	0,523	83,40	159,4627151	hypothetical protein
SSO-2814	0	459	0	146,88	146,88	hypothetical protein
SSO-2700	33	556	0,4825	59,11	122,5119171	putative transcriptional regulator (TenA family)
SSO-0086	0	804	0	118,66	118,66	hypothetical protein
SSO-1899	0	627	0	115,80	115,80	hypothetical protein
SSO-2395	0	492	0	104,62	104,62	hypothetical protein
SSO-1962	38	509	0,6547	63,76	97,39422636	hypothetical protein
SSO-0581	32	417	0,5308	50,29	94,74189902	putative GTP-binding protein HSR1-related
SSO-2336	0	605	0	94,46	94,46	hypothetical protein
SSO-2230	39	480	0,9795	87,65	89,48238897	hypothetical protein
SSO-0477	110	1299	0,9022	77,46	85,8579029	hypothetical protein
SSO-0108	40	2615	14	645,17	47,53355927	hypothetical protein
SSO-1968	52	2590	18	648,91	36,21362799	hypothetical protein
SSO-0168	67	1660	15	276,56	18,01426524	hypothetical protein
SSO-1160	35	821	10	178,09	17,05487455	hypothetical protein
SSO-0118	173	2890	51	618,58	12,14618677	hypothetical protein
SSO-5209	137	2120	69	778,63	11,25117045	hypothetical protein
SSO-2203	83	1191	16	169,58	10,43345844	hypothetical protein
SSO-3176	154	2151	56	565,21	10,15563741	putative transcriptional regulator (HxlR family)
SSO-1149	122	1642	36	356,17	9,785806523	hypothetical protein
SSO-11020	109	1448	51	492,63	9,658843597	hypothetical protein
SSO-1075	84	1095	30	283,13	9,477972683	hypothetical protein

SSO-2413	91	1165	27	254,41	9,308246744	hypothetical protein
SSO-2310	140	1791	23	212,04	9,301456396	putative beta-lactamase
SSO-12199	162	2009	88	791,85	9,01671601	putative MazG nucleotide pyrophosphohydrolase
SSO-0910	3904	47024	667	5845,50	8,757793316	putative cell division protein

Table 9. mRNAs co-purifying with Sso-aIF5A and encoding for unknown products. For RNAs highlighted in light blue the value "Ratio (TPM aIF5A/TPM mock)" corresponds to the respective TPM Sso-aIF5A value, since for these RNAs the TPM mock value is 0.

The mRNA sequences are being analyzed using different type of software (i.e. MEME) with the aim to verify the presence of a common motif that might mediate recognition by aIF5A protein as it has been proposed for the eukaryotic protein.

Nevertheless the variety of cellular processes to which these mRNA are related and the high amount of hypothetical protein coding mRNAs, does not allow, at the moment, to gather them into functional groups.

3.12. *Sulfolobus solfataricus* aIF5A factor shows ribonucleolytic activity

The results obtained so far indicate that aIF5A in the cell is part of a ribonucleoprotein complex and that this complex might be involved in rRNA-tRNA processing/turnover.

In addition, aIF5A is associated with several mRNAs, which, apparently, do not share any correlation.

Wagner and Klug [78] demonstrated that factor aIF5A from *Halobacterium* sp. NRC-1 is endowed with an RNase activity.

In order to better clarify the nature of this complex and to try to reconcile these findings, we decided to test the eventual RNase activity of Sso-aIF5A.

For this purpose, we set up an *in vitro* RNA cleavage assay to test the RNA degradation activity of both the recombinant unmodified protein purified from *E.coli* and the recombinant hypusinated aIF5A, purified from *Sulfolobus solfataricus*.

The two proteins were incubated at 65°C in the presence of different *in vitro* transcribed mRNA substrates (sh2508, 0118, 0175); the reactions were performed using different

protein/RNA ratios and incubation times. After incubation, the reaction mixtures were analyzed by denaturing Urea-PAGE and/or Native-PAGE. Experiments were repeated at least three times and representative results are shown in figure 28 and 29.

Figure 28 shows results obtained with the unmodified protein, cleavage was observed with all different RNAs although the reactions followed an RNA-specific kinetic (with some RNAs being degraded faster than others (0118 vs 0175), the cleavage is independent on Mg2+ and also independent on the presence of the His tag.

We performed a control assay at 37 °C, to exclude the presence of *E.coli* RNases in the protein preparation, and we also incubated the RNA with another recombinant protein from *Sulfolobus* expressed and purified in *E.coli* (the DHS protein); in both controls no degradation of the RNA substrate was observed.

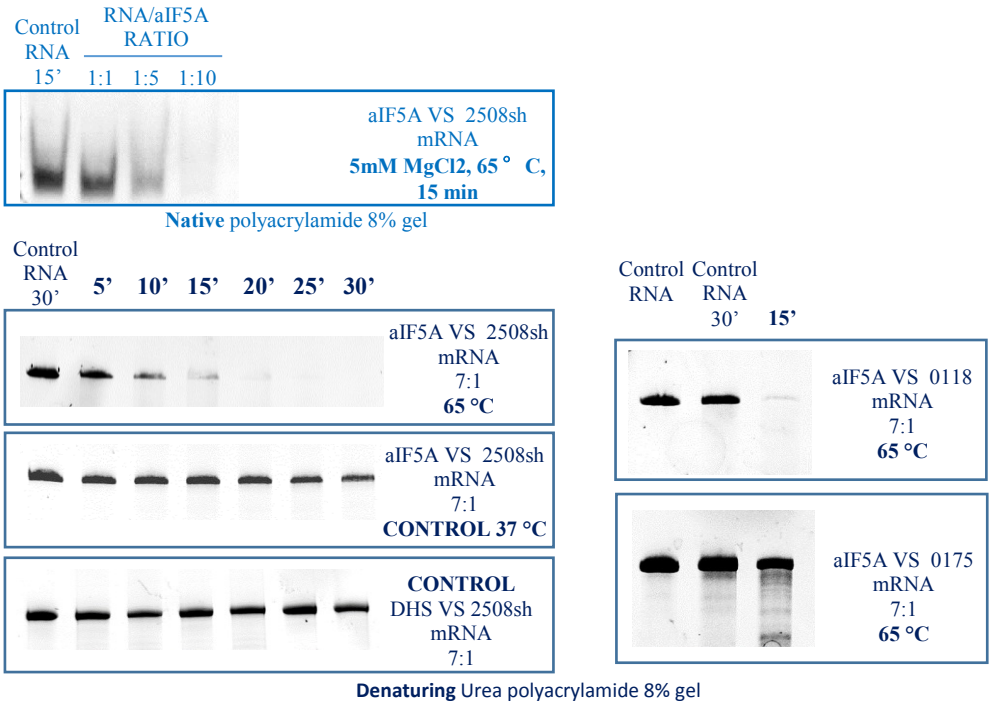

Figure 28. Sso-aIF5A, purified from E.coli, shows ribonucleolytic activity. In the upper panel (light blue) the degradation of sh2508 RNA is shown on a native polyacrylamide gel 8%, testing different RNA/protein ratios (1:1, 1:5, 1:10) in a reaction buffer supplied with 5mM MgCl2. In the other five panels the degradation of 2508sh mRNA (left) and 0118/0175 mRNAs (right) due to aIF5A occurred in a reaction buffer without MgCl2 and the cleavage is visible on a denaturing (8M Urea) 8% polyacrylamide gel.

These results represent a clear indication that unmodified Sso-aIF5A has a ribonucleolytic activity and the cleavage efficiency depends on the RNA substrate.

Figure 29 shows the results obtained with the hypusinated aIF5A C-terminal His-tagged, from *Sulfolobus solfataricus*, which showed also ribonucleolytic activity towards 2508sh mRNA, in a ratio RNA/protein 1:16, after 30 min at 65 °C and, also in this case, independently on the presence of Mg2+ (data not shown).

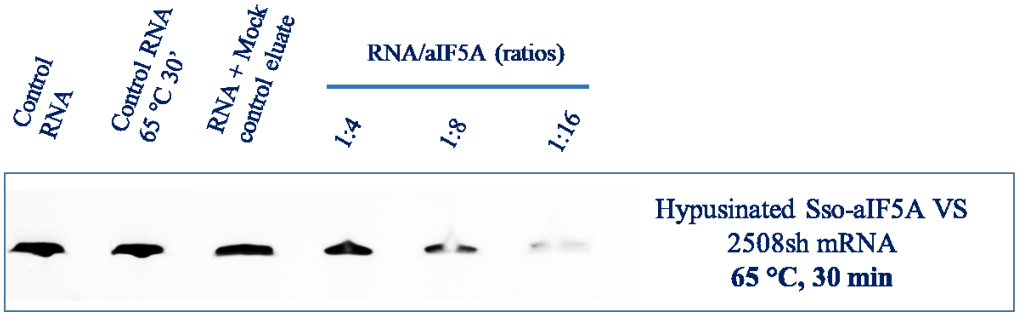

Figure 29. The hypusinated Sso-aIF5A shows ribonucleolytic activity. The degradation of 2508sh mRNA performed by aIF5A, RNA/protein ratios (1:5, 1:8, 1:16) in a reaction buffer without $MgCl_2$, is shown on a denaturing (8M Urea) 8% polyacrylamide gel.

The control, in this case, was the RNA incubated with the eluate obtained from the mock purification, performed with the lysate of Sso PH1-16 [pMJ05 (ptf55-empty plasmid)] and we confirmed that *Sulfolobus* RNases were not present in the protein preparation.

Compared to the unmodified Sso-aIF5A, a double amount of hypusinated Sso-aIF5A C-terminal His-tagged, is required for the cleavage of 2508sh mRNA.

To confirm that Sso-aIF5A definitely has a ribonucleolytic activity we performed the *in vitro* RNA cleavage assay using the native Sso-aIF5A (figure 30), which was purified according the published protocol adopted for the purification of the respective native protein in *Sulfolobus acidocaldarius* [70].

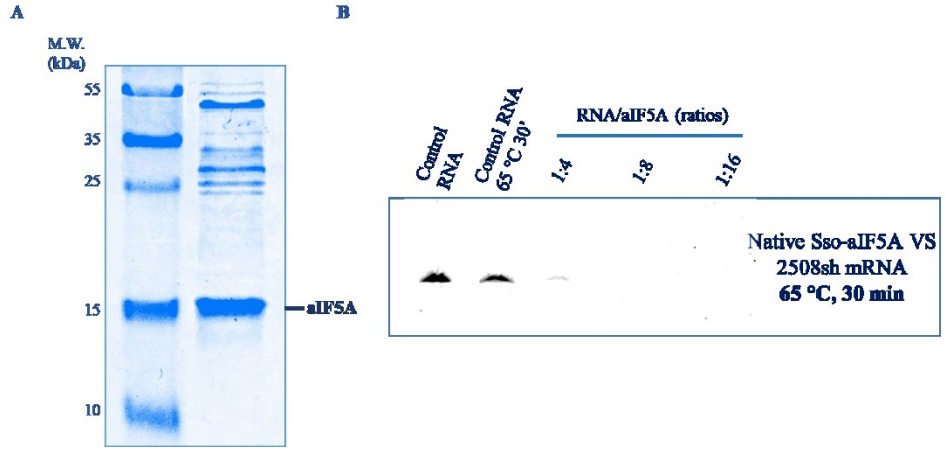

Figure 30. The native Sso-aIF5A shows ribonucleolytic activity. (A) Native Sso-aIF5A, 15% SDS-polyacrilamide gel, coomassie stained. (B) The degradation of 2508sh mRNA performed by aIF5A, RNA/protein ratios (1:4, 1:8, 1:16) in a reaction buffer without $MgCl_2$, is shown on a denaturing (8M Urea) 8% polyacrylamide gel.

The native aIF5A is able to cleave the 2508sh mRNA and appears to be more active compared to the C-terminal His-tagged Sso-aIF5A. However the native Sso-aIF5A is not pure, as it is possible to notice the presence of different contaminants in the protein preparation (figure 30 A).

Therefore, to demonstrate that the ribonucleolytic activity is exclusively related to Sso-aIF5A, a zymogram assay was employed (figure 31).

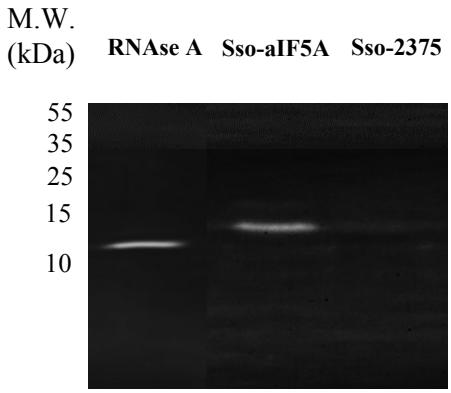

Figure 31. Ribonucleolytic activity of the native Sso-aIF5A showed by the zymogram assay. The white band indicate that the RNA substrate Sso-2508sh, distributed in the entire gel (black colored), is cleaved by RNaseA and Sso-aIF5A. RNaseA: positive control, 10 ng of RNase A from bovine pancreas (13,7 kDa), Native Sso-aIF5A: 3 µg (15 kDa) , Sso-2375: negative control, 5 µg (13 kDa).

The 2508sh mRNA was incorporated in the gel matrix and the native Sso-aIF5A was loaded onto and separated in the gel.

As a positive control we exploited the RNase A and to ensure that the degradation is not due to the large amount of aIF5A used, we also loaded an excess of Sso-2375 (aIF1A).

Degraded RNA was visible as a white band at the position with a corresponding molecular mass of 15 kDa, strongly indicating that the ribonucleolytic activity is conferred by Sso-aIF5A.

Lastly, to provide hints about the residues of Sso-5A involved in the RNA cleavage, we aligned the protein sequence of aIF5A from *Halobacterium* sp. NRC-1 and from *Sulfolobus solfataricus* P2 (figure 32), since Wagner and co-workers showed that specific amino acid exchanges, in the *Halobacterium* aIF5A protein sequence, affect the RNA catalysis [78].

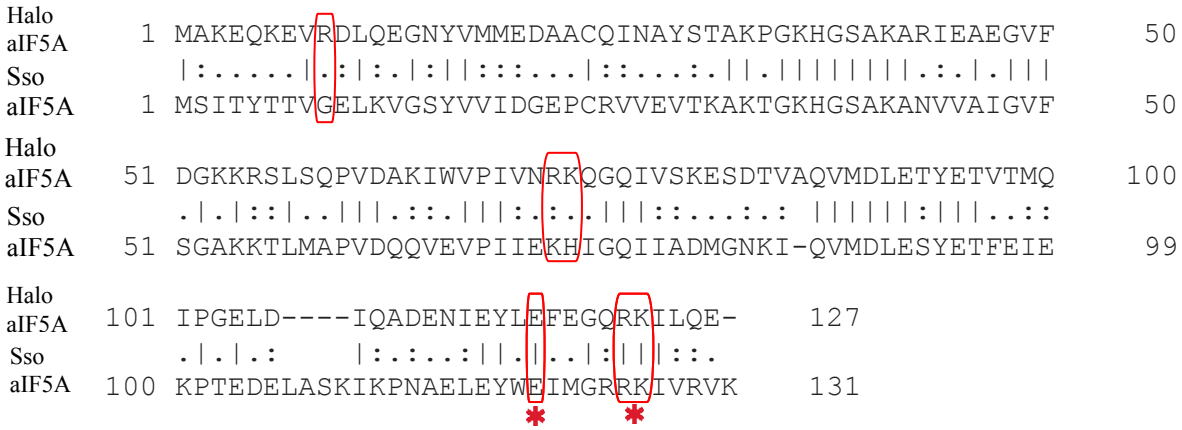

Figure 32. Conservation of aIF5A residues involved in the RNA cleavage. Pairwise protein sequences alignment of aIF5A from *Halobacterium sp*. NRC-1 (HaloaIF5A) and from *Sulfolobus solfataricus* P2 (SsoaIF5A). The residues involved in the RNA cleavage, identified in *Halobacterium* [78], are highlighted by red boxes and among them those that are conserved are marked by red asterisks.

In this study the RNA cleavage activity of aIF5A was reduced when the amino acid at position 9 located in the N-terminal domain, amino acids at position 72/73, which are located in the hinge region, were exchanged or amino acids at position 117 or 122/123 of the C-terminal domain were exchanged.

From the protein sequences alignment the three residue in the C-terminal domain are conserved in Sso-aIF5A and this suggest that they might be involved in the RNA cleavage.

Hitherto we can conclude that the archaeal factor aIF5A is able to cleave diverse RNA substrates, regardless the post-translational modification and binds, in its hypusinated form, a specific subset of RNA molecules.

These two functional aspects are not necessary mutually exclusive, they might be regulated by the structural conformation of the protein, by the modification itself or even by the existence of a multi-protein complex, in which aIF5A might have a specific role.

4. Discussion

The aim of this work was to shed some light on the translation factor aIF5A, in the *crenarchaeon Sulfolobus solfataricus* (Sso-aIF5A).

aIF5A belongs to the small group of universally conserved translation factors: the protein is, in fact, homologous between Eukarya and Archaea while Prokaryotes bear an orthologue protein called EF-P.

The protein is an elongation factor performing a specialized, though essential, function: both eIF5A and EF-P are able to promote the synthesis of proteins containing successive residues of proline.

These type of sequences, in fact, would cause the ribosome to stall, while eIF5A/EF-P bound on the ribosomes would interact with P-site tRNA facilitating in this way Pro-Pro peptide bond formation.

Essential for this activity is the unique post-translation modification typical of these factors: the hypusine residue for eIF5A and lysysl-lysine residue for EF-P.

Since nothing is known concerning the role of the archaeal aIF5A factor in protein synthesis, we performed a series of experiments in order to fill this gap.

First, we used polyclonal anti-SsoaIF5A antibodies to immunolocalize the native Sso-aIF5A protein in different cellular fractions.

The protein, which appears to be quite abundant in *Sulfolobus* cell, is predominantly localized in post-ribosomal fractions (S100 and High Salt Wash fractions), while it appears absent or slightly represented in the ribosomal subunits a result coherent with a translation elongation factor (figure 11, 12A).

We plan then to analyze the behavior of the protein during protein synthesis, to this end we programmed a cell lysate for translation by addition of endogenous mRNA and fractionated it on sucrose density gradients after formaldehyde fixation.

It is known that *S. solfataricus* ribosomes dissociate during centrifugation [81], therefore 70S monosomes or polysomes are usually not detectable.

70S associate more stably only during translation and become detectable upon fixation with formaldehyde.

Results confirmed that in a lysate, Sso-aIF5A is present exclusively in the top low-molecular-weight fractions and it is not associated with ribosomal subunits.

However, if the lysate is programmed for translation (figure 12B) a fraction of aIF5A becomes ribosome bound being detected in the 30S, 50S and 70S fractions.

This represents the first indication of the involvement of an archaeal aIF5A factor in the translation process.

A deeper investigation of the role of aIF5A would require a completely purified *in vitro* translation system that is currently not available for *Sulfolobus*.

This system would also help to verify the hypothesis of a role in translation strictly linked to the rescue of proteins containing polyproline motives since a genome-wide analysis has shown that these proteins are not so common in both Bacteria and Archaea (2.0-2.5%) [99].

As mentioned in the introduction the eukaryotic protein has been related to a variety of cellular processes like apoptosis, retroviral infections, cellular transformation, stress response.

This pleiotropic behavior may be a secondary effect of its role as a translation factor or it may be an indication that aIF5A is involved in functions other than translation.

For example several reports have characterized it as an RNA binding protein and one of the few report available for the archaeal protein indicate that in *Halobacterium* the protein has an RNA binding and degrading activity [78].

Therefore, we planned and performed a series of experiment with the aim to understand which are the functions played by factor aIF5A in *Sulfolobus solfataricus* cells.

We expressed the recombinant Sso-aIF5A in *E.coli* and this gave us the advantage of obtaining a large amount of unmodified protein that could also be used to produce specific antibodies. However, for our purposes, it was best to perform the overproduction of the protein in the native thermophilic host that allowed the characterization of the archaeal factor aIF5A, its post-translational modification and associated partners, under natural conditions of high temperature.

We successfully produced different versions of Sso- aIF5A in *Sulfolobus solfataricus* but a first effect that we could immediately observe was a dramatic slow-down of the growth rate during the exponential phase.

Interestingly this effect, indicating that the expression of the factor is toxic for the cell, was very similar in all the expression strains used, independently of the different level of expression obtained (see below).

This phenomenon suggests that even a small excess of the protein is sufficient to cause a defect in the growth rate.

Significant differences were observed between the proteins bearing the His-tag at the C-terminus compared to the ones with the His-tag at the N-terminus concerning the expression yield and the purity of aIF5A after the affinity purification.

The highest expression yield was achieved with the protein carrying the C-terminal His-tag (figure 14A), whose eluate after the affinity purification looked quite pure with the exception of a 35 kD protein which was always was co-eluted with aIF5A, even under stringent purification conditions.

The identity of this protein was further investigated and, interestingly, it was identified as being the deoxyhypusine synthase (figure 15) the enzyme performing the first reaction of the post-translation modification.

On the other hand, the level of expression of the N-terminal His-tagged protein was rather low, less than half of the native aIF5A (figure 14A) and, in addition, several proteins were co-purified with our protein of interest (figure 14B).

Therefore, we concluded that the position of the His-tag has evidently an effect on the expression level and it influences the binding with protein interacting partners.

Furthermore, according to our findings, the C-terminal domain is clearly involved in protein-protein interactions, even though it is classified as an OB-fold, known to be responsible for the binding to nucleic acids.

However our evidence is coherent with a previous study related to the structural features of *Pyrococcus horikoshii* aIF5A [71], in which the authors speculated that the C-terminal domain, according to its electrostatic potential, is involved in the interaction with protein interacting partners.

Regarding the post-translational modification it was shown already, in *Sulfolobus acidocaldarius*, that the native archaeal factor is an hypusine-containing protein [70]. To

confirm this we performed mass spectrometry analysis of the purified recombinant Sso-aIF5A.

The results confirmed that in the clade of *crenarchaeota*, this factor is hypusinated (figure 16) and, in addition, what is new respect to the previous study is that the recombinant Sso-aIF5A, even when overproduced in *Sulfolobus solfataricus* becomes hypusinated.

We proceeded trying to shed light on the latter aspect starting from the structural and functional analysis of the deoxyhypusine synthase, since no deoxyhypusine hydroxylase enzyme has been identified in any archaeal genomes or proteomes.

The residues involved in the interaction with the NAD+ cofactor and the spermidine substrate have been identified in the active site of the eukaryotic DHS enzyme [12, 13] and the protein sequences alignment between the Sso-DHS sequence and the eukaryal DHS sequence showed that these residues are conserved (figure 17).

Therefore, the enzymatic activity of the DHS enzyme should be an evolutionarily preserved process in Archaea and Eukarya.

While cloning Sso-DHS in *E.coli*, we observed that the DHS enzyme was soluble only if the His-tag resided in the C-terminal position (figure 18).

The eukaryal DHS tetramer consists of two dimers that are tightly associated by their respective N-terminal domains, with the two active sites in the interface between them [13] and this can explain why the His-tag position is important for the solubility of the archaeal enzyme.

The Sso-DHS assumes a tetrameric structure, like the eukaryal enzyme, the His-tag at the N-terminal position can somehow inhibits the formation of the active oligomeric form.

The structural analysis of the recombinant Sso-DHS C-terminal His-tagged revealed that this hypothesis is correct, since we showed that also the archaeal DHS enzyme is a tetramer (figure 19).

All these evidences suggest that the recombinant Sso-DHS, expressed in *E.coli*, should be functionally active and this persuaded us to elucidate its role in the post-translational modification pathway.

In the *in vitro* hypusination assay, the Sso-DHS enzymatic activity is not efficient, however we showed that the enzyme is able to perform the sole deoxyhypusination (figure 20) and we

definitely exclude a bifunctional activity, as it was recently described for the *Trichomonas vaginalis* enzyme [18].

The previous finding, related to the slight detection of the deoxyhypusinated intermediate, together with the weak activity of the recombinant DHS in the *in vitro* hypusination assay, suggest that the archaeal DHS might perform a reversible reaction, like the eukaryal enzyme and the hydroxylation of deoxyhypusine to hypusine blocks this back reaction, stabilizing the hypusinated form.

With the aim to identify the second enzyme performing the hypusination reaction but also to identify the numerous proteins bound to Sso- aIF5A, we performed MS analysis of the eluate from the affinity purification of the N-terminal tagged aIF5A.

Not only the DHS enzyme, but also other proteins involved in cell metabolism, translation, rRNA/tRNA modification and mRNA turnover/processing were part of the Sso-aIF5A interactome (table 5).

Concerning the post-translational modification pathway, no proteins with similarity or functional analogy with DOHH were identified in the aIF5A interactome.

Nevertheless, sequences and structures of some of the proteins are being further analyzed in the attempt to understand if any of them might a probable candidate to perform the deoxyhypusine hydroxylation: carbonic anhydrase, which is the most abundant after DHS, two dehydrogenases (succinate dehydrogenase and 3-hyroxyacyl-CoA dehydrogenase) and one oxidoreductase.

The presence of a group of proteins like the RNA small subunit methyltransferase Nep1, the SmAP1 and the C/D box methylation guide Nop56, reinforce the hypothesis that the protein is involved in RNA metabolism

We focused our attention on one of the proteins in this group: the translation recovery factor (Sso-2509), which was recently characterized for its involvement in mRNA translation/turnover. The Sso-2509 direct interaction with aIF2γ, which counteracts 5’ to 3’ mRNA decay [65], leads to aIF2/aIF2γ release from mRNAs during the cell recovery from nutrient stress [88].

After confirming that the two proteins interact also *in vitro* (figure 22), we discovered that Sso-5 aIF5A interferes with Sso-2509 activity blocking the release of aIF2γ from the 5’-end

of the RNA (figure 23). This result is the first evidence suggesting a possible additional function of aIF5A related to the mRNA translation/turnover. Sso- aIF5A forming a complex with Sso-2509 could act as a sensor of the cell nutrient conditions regulating when to restart translation and preserving mRNAs integrity during unfavorable environmental conditions.

In this regard new hints arose from the structural analysis of the unmodified Sso- aIF5A and from the fractionation of the *S. solfataricus* S30 extract on linear glycerol gradients, followed by immunodetection of the native aIF5A.

The recombinant unmodified Sso- aIF5A shows a monomeric conformation in solution (figure 24). The sedimentation profile (figure 26) of aIF5A, in a cell extract fractionated on glycerol gradients, revealed that the native hypusinated protein is present in a monomeric conformation.

However, its presence is detected even in higher molecular weight fractions (between 44 kDa and 74 kDa), despite in this range the hypusine modification is not detectable.

Hence we state that the native factor aIF5A is not only in a monomeric form, but it might assumes an oligomeric conformation or even be part of a complex.

It remains to be clarified why the hypusine is not detected in this complex and for the first time we might take into consideration the hypothesis that the native protein is not 100% hypusinated. This possibility would offer a new scenario in which the presence or absence of the modification might regulate the function of the protein.

Furthermore, what is really interesting is that the micrococcal nuclease treatment of the S30 extract leads to the disruption of this oligomeric conformation and/or of this complex.

It follows that aIF5A arrangement in any conformation, other than the monomeric one, is somehow regulated by the presence of nucleic acids and this structural versatility is undoubtedly a fundamental element for the multifunctional role of aIF5A, which springs from our experimental evidences.

We anticipated that the C-terminal domain of aIF5A is involved in the interaction with protein interacting partners, even though the structure of this domain is an OB-fold, typical of nucleic acid binding protein.

The binding of nucleic acids (most probably RNA) within the high molecular weight complex might be mediated just by the OB-fold motif in the factor aIF5A.

Hitherto our data suggesting a probable involvement of Sso- aIF5A in the RNA metabolism, are further supported by the richer content of RNA molecules, affinity co-purified with aIF5A, compared to the mock purification (figure 27).

Identification of these RNAs showed that ncRNAs, mRNAs and tRNAs are specifically co-purified with the hypusinated Sso- aIF5A (Appendix table A.1 and table A.2).

In our deep-sequencing analysis of Sso- aIF5A co-purified RNAs, we revealed several ncRNAs and in particular two antisense-box ncRNAs with a typical C/D motif, involved in the 23S rRNA processing, a snoRNA, responsible for the modification of the 23S rRNA and a ncRNA, which is antisense of $tRNA^{Pro}$.

Antisense-box RNAs are associated in stable ribonucleoprotein complexes, with three conserved proteins [100], (the core L7Ae protein, the NOP56 protein and the aFIB methyltransferase protein) and are key players in the modification, processing and dynamic folding of rRNAs/tRNAs.

Interestingly we identified NOP56 as Sso-5 aIF5A protein interacting partner and this finding, together with our RNA_{seq} data, could hint towards a specific role of Sso- aIF5A in these ribonucleoprotein complexes.

Moreover in spite of several mRNAs encoding putative unknown proteins, we revealed several tRNAs, which may derive from translating ribosomes or suggest the involvement of the archaeal aIF5A factor in the processing of the corresponding tRNA.

Part of our investigation was also focused on the involvement of aIF5A in the RNA stability, which is a key element in the regulation of gene expression and its study in Archaea point towards the possible evolutionary conservation of RNA processing and decay in all living cells.

An RNase E-like protein has been identified in Archaea and it shows the same endoribonucleolytic activity of the bacterial enzyme [101].

This study underlines that RNase E is an ancient enzyme, conserved among the primary domains of life, whose processing activity in Archaea is adapted to extreme environmental conditions. Additionally two dehydrogenases have been characterize as archaeal endoribonucleases [102], likewise the eukaryotic and bacterial glyceraldehyde-3-phosphate dehydrogenase (GAPDH).

It followed that archaeal dehydrogenases and dehydrogenase-related proteins are also involved in RNA turnover and this is relevant since we identified two dehydrogenases as Sso- aIF5A protein interacting partners.

Furthermore RNases with exonucleolytic activity has been described in *Sulfolobus solfataricus.*

The archaeal nine-subunits exosome is involved in the mRNA decay and shows 3'-to-5' exonucleolytic activity [103], whereas Sso-RNase J has been recently described as 5'-to-3' directional exonuclease [92].

Recently it was demonstrated by *in vitro* assays, that the *Halobacterium* aIF5A factor is able to bind RNA molecules and the modified and unmodified protein shows also ribonucleolytic activity [78].

Interestingly we proved that the *Sulfolobus solfataricus* aIF5A factor is able to cleave several mRNA substrates, regardless the post-translational modification (figures 28, 29, 30, 31).

The RNA substrates were cleaved by the recombinant unmodified Sso-aIF5A with a different cleavage efficiency, which suggests a possible RNA sequence specificity of this ribonuclease.

A difference in the degradation efficiency was also observed among the recombinant unmodified protein (from *E. coli*), the native protein and the recombinant hypusinated Sso-aIF5A (from *Sulfolobus*) with the first two showing a complete degradation of the substrate with a lower amount compared to the third one.

Such a difference may be due to the presence of the His-tag which is missing in the first two (the recombinant protein was cleaved by TEV protease) but it is present at the C- terminal position in the third one.

Wagner and coworkers showed in fact that both domains are important for the RNA cleavage, since the substitution of charged amino acids at certain positions affects aIF5A ribonucleolytic activity [78].

Additionally we could hypothesize that the association of aIF5A with the translational recovery factor Sso-2509 has important consequences on this RNA cleavage activity.

In fact, in the complex formed between the two proteins Sso-2509 would guarantee the integrity of the mRNAs by maintaining the aIF2 factor bound to the mRNA and at the same

time blocking the RNase activity of aIF5A. We can imagine that, upon release of aIF2, a competition might occur, depending on the cell growth conditions, between the translation apparatus and Sso-aIF5A which, alone or in a complex, would degrade the RNA.

All these findings together support our model (figure 33) in which the Sso- aIF5A, in its monomeric hypusinated form, participate in translation and recognizes specific subsets of RNA substrates and then in an oligomeric state or even in a complex, together with other protein interacting partners, might be responsible of the RNA processing and/or turnover.

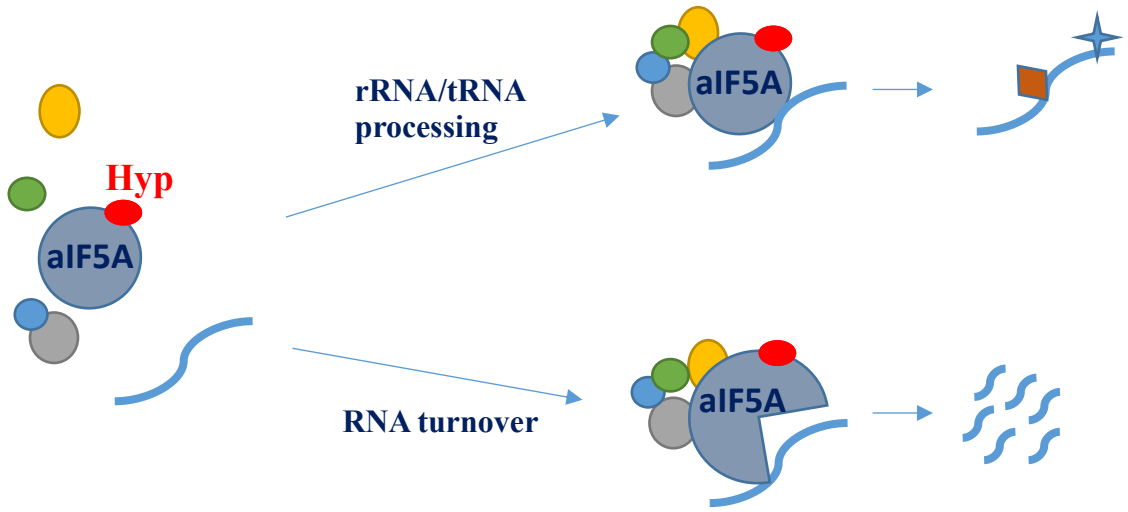

Figure 33. Model of Sso-aIF5A involvement in the RNA metabolism. The monomeric protein, in its hypusinated form, is responsible for the binding to a specific subset of RNA molecules. The protein can interact with other proteins in a complex, which might be responsible of the rRNA/tRNA processing and/or mRNA turnover.

5. Outlook

This thesis shows for the first time unreleased structural and functional features of the *Sulfolobus solfataricus* aIF5A, paving the way for further investigations.

So far there are still many open questions to be answered in order to fully characterize the functional role of this translation factor.

First, the exact involvement of the archaeal aIF5A in the protein synthesis, with particular focus on translation of a specific subset of mRNAs or proteins that contain specific motifs.

Proteins with consecutive polyproline residues are calculated to be around 2%, compared to the 20% in the eukaryal proteome [99].

Considering the abundance of the archaeal aIF5A in the cell, it might be reductive to state that the function of aIF5A regards the sole translation of these proteins, as it was recently showed for the eukaryal homologue and the bacterial orthologue. A possibility that has not been investigated so far, is that the archaeal aIF5A is involved in the translation of leaderless mRNAs, that in *Sulfolobus solfataricus* represent the 69% of all coding transcripts [96].

However if Sso-aIF5A is responsible for the translation of certain mRNAs, our deep sequencing analysis would be useful to identify motifs that are specifically recognized by the protein.

Second, further research should be focused on the hypusination mechanism in *Sulfolobus solfataricus* and on the identification of the enzyme responsible for the deoxyhypusine hydroxylation.

In this regard we anticipate that the LC-MS/MS analysis of aF5A protein interacting partners suggested some candidate, that might be involved in the second step of the hypusination pathway.

Third, the ribonucleolytic activity of the archaeal Sso-aIF5A and its functional association with the translation releasing factor (Sso-2509) have to be further elucidated.

It would be interesting to investigate whether aIF5A is able to perform a 5'-end dependent RNA degradation mechanism, as it was recently shown for the Sso-RNaseJ [92].

The reason for this resides in the association between aIF5A and 2509, since we speculated that aIF5A, under nutrient limitation conditions, might ensures the RNA turnover thanks to its ribonucleolytic activity.

We showed that aIF2γ release by 2509 does not occur in the presence of aIF5A and the γ-subunit bound to the 5' part of mRNAs increases their stability [65], hence if the degradation of mRNAs occurs, this implies a 5' to 3' exonuclease or a 5'-end dependent endonuclease.

In this scenario it is worth to establish also if there is an increase in the expression of Sso-aIF5A during stress conditions, like a prolonged stationary phase and/or a variation of the extent of hypusination.

Oud data highlighted that the archaeal factor aIF5A might be part of a multi-protein complex, which can be involved in the RNA metabolism, therefore insights into protein interacting partners could elucidate this topic.

A recent published study identified aIF5A as a putative interaction partner of the archaeal SmAP1/2 proteins [94], which are involved in different aspects of the RNA metabolism, thus this is an interesting starting point for further investigation.

Appendix

Table A.1: Identity of ncRNAs co-purified with Sso-aIF5A and identified by deep-sequencing analysis. For RNAs highlighted in grey the value "Ratio (TPM aIF5A/TPM mock)" corresponds to the respective TPM Sso-aIF5A value, since for these RNAs the TPM mock value is 0.

Gene	Strand	Size	Start	End	Reads mock	Reads Sso-aIF5A	TPM mock	TPM Sso-aIF5A	Ratio (TPM aIF5A/TPM mock)
ncRNA26	+	167	595577	595744	3	214	0,2396	124,249	518,56
ncRNA32	-	64	837806	837870	0	286	0	433,294	433,294
SSOs04	-	56	2960304	2960360	0	156	0	270,106	270,106
ncRNA1	+	55	22533	22588	0	146	0	257,387	257,387
ncRNA83	-	310	1577360	1577670	41	755	17,637	236,147	13,389
ncRNA36	+	279	898531	898810	685	9505	327,415	3303,276	10,089
ncRNA2	+	200	32667	32867	130	1227	86,681	594,856	6,862
ncRNA98	+	90	2016127	2016217	188	1496	278,566	1611,707	5,786
ncRNA99	-	148	2016089	2016237	369	2400	332,489	1572,34	4,729
ncRNA100	-	165	2020290	2020454	882	5312	712,848	3121,556	4,379
ncRNA78	+	201	1534755	1534956	39	230	25,875	110,95	4,288

Table A.2: Identity of mRNAs/tRNAs co-purified with Sso-aIF5A and identified by deep-sequencing analysis. For RNAs highlighted in grey the value "Ratio (TPM aIF5A/TPM mock)" corresponds to the respective TPM Sso-aIF5A value, since for these RNAs the TPM mock value is 0.

Gene	Strand	Size	Start	End	Reads mock	Reads Sso-aIF5A	TPM mock	TPM Sso-aIF5A	Ratio (TPM aIF5A/TPM mock)
SSO-3164	+	369	2914491	2914859	1	299	0,0361	78,57	2176,371191
SSO-8910	+	162	1619887	1619724	1	128	0,0823	76,61	930,8748481
SSOt05	+	75	114659	114734	3	195	0,5334	252,10	472,6265467
SSO-1196	+	209	1039005	1039213	0	902	0	418,46	418,46
SSO-0175	-	363	146365	146727	0	1299	0	346,98	346,98
SSO-1570	+	384	1416337	1416720	4	172	0,1389	43,43	312,6709863
SSO-0620	-	393	539774	540166	0	1193	0	294,34	294,34
SSO-3146	-	789	2896247	2897035	34	1357	0,5747	166,76	290,1740038
SSO-0123	-	663	103509	104171	39	1503	0,7844	219,81	280,2231005
SSO-0039	-	573	34685	35257	23	872	0,5353	147,56	275,6529049
SSO-0117	-	405	96554	96148	0	1099	0	263,11	263,11
SSO-0009	-	984	5351	6334	30	1072	0,4066	105,63	259,7934088
SSO-2186	+	846	2010928	2011774	51	1683	0,8039	193,00	240,0796119
SSO-3164	+	183	2914914	2915096	0	427	0	226,24	226,24
SSO-0253	+	561	218719	219279	0	1291	0	223,13	223,13
SSO-0107	+	372	87870	88241	0	746	0	194,44	194,44
SSO-2338	+	990	2136182	2137172	45	1156	0,6062	113,22	186,7683933
SSO-1773	+	798	1710446	1711084	39	944	0,6517	114,70	176,002762
SSO-2489	+	765	2260444	2261208	30	658	0,523	83,40	159,4627151
SSO-2814	-	303	2574657	2574959	0	459	0	146,88	146,88
SSO-0060	-	969	50238	51206	0	1293	0	129,38	129,38
SSO-2700	-	912	2452659	2453570	33	556	0,4825	59,11	122,5119171
SSOt16	+	75	246929	247004	0	94	0	121,52	121,52
SSO-0086	-	657	69429	70083	0	804	0	118,66	118,66
SSOt20	+	74	333446	333520	0	90	0	117,93	117,93
SSO-1899	-	525	1713563	1714087	0	627	0	115,80	115,80
SSOt10	-	73	184612	184684	0	83	0	110,24	110,24
SSO-2395	+	456	2181477	2181932	0	492	0	104,62	104,62
SSO-1962	-	774	1777542	1778315	38	509	0,6547	63,76	97,39422636
SSO-0581	-	804	510007	510810	32	417	0,5308	50,29	94,74189902
SSO-2336	+	621	2134538	2135158	0	605	0	94,46	94,46
SSO-2230	+	531	2049579	2050110	39	480	0,9795	87,65	89,48238897
SSO-0477	-	1626	410443	412068	110	1299	0,9022	77,46	85,8579029
SSO-0108	-	393	88218	88610	40	2615	14	645,17	47,53355927
SSO-1968	-	387	1782460	1782846	52	2590	18	648,91	36,21362799
SSO-0168	-	582	139591	140172	67	1660	15	276,56	18,01426524
SSO-1160	-	447	1000636	1001082	35	821	10	178,09	17,05487455
SSO-0118	-	453	97020	96566	173	2890	51	618,58	12,14618677
SSO-5209	+	264	95905	96168	137	2120	69	778,63	11,25117045
SSO-3226	-	819	2972253	2973071	64	980	10	116,02	11,13348047
SSO-2203	+	681	2026970	2027651	83	1191	16	169,58	10,43345844
SSO-3176	+	369	2922727	2923095	154	2151	56	565,21	10,15563741
SSO-0556	+	588	490144	490731	102	1397	23	230,37	9,958284702
SSO-1149	-	447	989495	989941	122	1642	36	356,17	9,785806523
SSO-11020	-	285	2489486	2489770	109	1448	51	492,63	9,658843597
SSO-1075	+	375	933329	933703	84	1095	30	283,13	9,477972683
SSO-2413	-	444	2194603	2195046	91	1165	27	254,41	9,308246744
SSO-2310	+	819	2113415	2114234	140	1791	23	212,04	9,301456396
SSO-12199	-	246	2962893	2962646	162	2009	88	791,85	9,01671601
SSO-0910	-	780	775198	775977	3904	47024	667	5845,50	8,757793316
SSO-1896	-	639	2293961	2294123	178	2030	37	308,03	8,291940347

List of Abbreviations

µg	Microgram
µl	Microliter
µM	Micromolar
µm	Micrometer
2508sh mRNA	Short form of the 2508 messenger RNA
aIF5A	Archaeal Translation Initiation factor 5A
A	Absorbance
ABC	Ammonium bicarbonate
ADP	Adenosindiphosphat
AraP	Arabinose promoter
Arg	Arginine
A-site	Aminoacyl-site
ATP	Adenosine triphosphate
BSA	Bovine serum albumin
CAM	Cysteine Carbamidomethylation
cDNA	Complementary DNA
Co-IP	Co-Immunoprecipitation
cryo-EM	Cryo-Electron Microscopy
Da	Dalton
DEPC	Dietil pyrocarbonate
DHS	Deoxyhypusine synthase
dhs	Gene encoding the deoxyhypusine synthase
DNA	Deoxyribonucleic acid
DNase	Deoxyribonuclease
DOHH	Deoxyhypusine hydroxylase
dohh	Gene encoding the deoxyhypusine hydroxylase
DSSP	Database of protein secondary structure assignments
DTT	Dithiothreitol
E.coli	*Escherichia coli*
EDTA	Ethylenediaminetetraacetic acid
EF	Elongation factor
eif5a1	Gene encoding the isoform 1 of the eukaryotic initiation factor 5A
eif5a2	Gene encoding the isoform 2 of the eukaryotic initiation factor 5A
ESI	Electrospray ionization
E-site	Exit-site

fMet	N-Formylmethionine
GC7	N1-guanyl-1,7-diaminoheptane
Glu	Glutamic acid
GTP	Guanosine triphosphate
H. halobium	*Halobacterium halobium*
H. mediterranei	*Haloferax mediterranei*
HCC	Human hepatocellular carcinoma
HCD	Higher-energy Collisional Dissociation
HEAT	Huntingtin, elongation factor 3, protein phosphatase 2A, Tor1
HeLa cells	Henrietta Lacks cells
HEPES	4-(2-hydroxyethyl)-1-piperazineethanesulfonic acid
Hfx. volcanii	*Haloferax volcanii*
His	Histidine
HIV	Immunodeficiency Virus
HPLC	High-Performance Liquid Chromatography
HRP	Horseradish peroxidase
HSW	High salt wash
Hyp	Hypusine
IF	Translation initiation factor
iNOS	Inducible nitric oxide synthase
IPTG	Isopropyl β-D-1-thiogalactopyranoside
IRES	Iron Responsive ElementS
KEGG	Kyoto Encyclopedia of Genes database
LC-MS	Liquid Chromatography-Mass Spectrometry
LFQ	Label Free Quantification
LUCA	Last Universal Common Ancestor
Lys	Lysine
M.W.	Molecular weight
m/z	Mass to charge ratio
mA	Milliampere
mAID	Mini Auxin-Inducible Degron
MALLS	Multi-Angle Laser Light Scattering
Met	Methionine
mRNA	Messenger RNA
NAD	Nicotinamide-adenin-dinucleotide
NADH	Reduced form of nicotinamide-adenin-dinucleotide
ncRNA	Non coding RNA
ng	Nanogram
NGS	Next Generation Sequencing

nm	Nanometers
NMD	Nonsense-Mediated Decay
NRC	National Research Council
nt	Nucleotide
NTA	Nitrilotriacetic acid
OB-fold	Oligonucleotide/oligosaccharide-Binding fold
OD	Optical Density
ORF	Open Reading Frame
PAGE	PolyAcrylamide Gel Electrophoresis
PCR	Polymerase Chain Reaction
PDB	Protein Data Bank
pg	Picogram
Pmn	Puromycin
pmol	Picomol
PMSF	Phenylmethylsulfonyl fluoride
polyP proteins	Proteins containing polyproline residues
Pro	Proline
P-site	Peptidyl-site
PTC	Peptidyl transferase center
ptf55	Promoter of thermophilic factor 55
P-tRNA	Transfer RNA in the ribosome Peptidyl-site
RF	Releasing factor
RNA	Ribonucleic acid
RNAi	RNA interference
RNase	Ribonuclease
rpm	Revolutions per minute
RRE	Rev Responsive Elements
RSLC	Rapid Separation Liquid Chromatography
rTC	Rotating tilted liquid column
S (unit)	Svedberg unit
S. acidocaldarius	*Sulfolobus acidocaldarius*
S. cerevisiae	*Saccharomyces cerevisiae*
S. solfataricus	*Sulfolobus solfataricus*
SAXS	Small angle X-ray scattering
SD	Shine-Dalgarno
SDS	Sodium Dodecyl Sulphate
SELEX	Systematic Evolution of Ligands by Exponential Enrichment
SH3-domain	SRC Homology 3 Domain
siRNA	Small interfering RNA

SNAAP	Specific Nucleic Acids Associated with Proteins
snoRNA	Small nucleolar RNA
sp.	Species
Sso	*Sulfolobus solfataricus*
SW-480	Human colon carcinoma cell lines
TAE	Tris-Acetate-EDTA
TBE	Tris-Borate-EDTA
TBS	Tris-Buffered Saline
TCA	Trichloroacetic acid
TEV	Tobacco Etch Virus
tif51a/tif51b	Yeast gene pair for the trasnslation initiation factor 5A
TPM	Transcripts Per Million
Trf	Translation recovery factor
tRNA	Transfer RNA
tRNAi	Initiator tRNA
TvDHS	*Trichomonas vaginalis* deoxyhypusine synthase
UTR	Untranslated region
V	Volt
wt	Wild type
ydhs	Gene encoding the yeast deoxyhypusine synthase
Δ	Deletion mutant

References

1. Londei P. (2007) Translation. USA: ASM Press.
2. Gutierrez E, Shin BS, and Dever TE. (2014). The hypusine-containing translation factor eIF5A. Crit Rev Biochem Mol Biol. 49(5): 413–425.
3. Dias CA, Garcia W, Zanelli CF, and Valentini SR. (2013) eIF5A dimerizes not only *in vitro* but also *in vivo* and its molecular envelope is similar to the EF-P monomer. Amino Acids. 44: 631–644.
4. Gentz PM, Blatch GL and Dorrington RA. (2009) Dimerization of the yeast eukaryotic translation initiation factor 5A requires hypusine and is RNA dependent. FEBS J. 276: 695–706.
5. Shiba T, Mizote H, Kaneko T, Nakajima T, Kakimoto Y. (1971) Hypusine, a new amino acid occurring in bovine brain. Isolation and structural determination. Biochim. Biophys. Acta. 244: 523–531.
6. Park MH. (2006) The post-translational synthesis of a polyamine-derived amino acid, hypusine, in the eukaryotic translation initiation factor 5A (eIF5A). J Biochem. (Tokyo) 139:161–169.
7. Park MH, Joe YA, Kang KR. (1998) Deoxyhypusine synthase activity is essential for cell viability in the yeast *Saccharomyces cerevisiae*. J. Biol. Chem. 273:1677–1683.
8. Wolff EC, Folk JE, Park MH. (1997) Enzyme-substrate intermediate formation at lysine 329 of human deoxyhypusine synthase. J. Biol. Chem. 272:15865–15871.
9. Park JH, Wolff EC, Folk JE, Park MH. (2003) Reversal of the deoxyhypusine synthesis reaction. Generation of spermidine or homospermidine from deoxyhypusine by deoxyhypusine synthase. J. Biol. Chem. 278: 32683–32691.
10. Lee YB, Park MH, Folk JE. (1995) Diamine and triamine analogs and derivatives as inhibitors of deoxyhypusine synthase: synthesis and biological activity. Journal of Medicinal Chemistry. 38 (16):3053–3061.
11. Jakus J, Wolff EC, Park MH, Folk JE. (1993) Features of the spermidine-binding site of deoxyhypusine synthase as derived from inhibition studies. Effective inhibition by

bis- and mono- guanylated diamines and polyamines. J. Biol. Chem. 268: 13151–13159.

12. Umland TC, Wolff EC, Park MH, Davies DR. (2004) A new crystal structure of deoxyhypusine synthase reveals the configuration of the active enzyme and of an enzyme NAD inhibitor ternary complex. J. Biol. Chem. 279: 28697–28705.
13. Liao DI, Wolff EC, Park MH, Davies DR. (1998) Crystal structure of the NAD complex of human deoxyhypusine synthase: an enzyme with a ball-and-chain mechanism for blocking the active site. Structure.;6:23–32.
14. Han Z, Sakai N, Bottger LH, Klinke S, Hauber J, Trautwein AX, et al. (2015) Crystal Structure of the Peroxo-diiron(III) Intermediate of Deoxyhypusine Hydroxylase, an Oxygenase Involved in Hypusination. Structure. 23: 882–892.
15. Park JH, Dias CA, Lee SB, Valentini SR, Sokabe M, Fraser CS, Park MH. (2011) Production of active recombinant eIF5A: reconstitution in *E. coli* of eukaryotic hypusine modification of eIF5A by its coexpression with modifying enzymes. Protein Eng Des Sel. 24: 301–9.
16. Sievert H, Pällmann N, Miller KK, Hermans-Borgmeyer I, Venz S, Sendoel A. (2014) A novel mouse model for inhibition of DOHH-mediated hypusine modification reveals a crucial function in embryonic development, proliferation and oncogenic transformation Dis. Model. Mech. 963-976.
17. Park MH, Nishimura K, Zanelli CF, Valentini SR. (2010) Functional significance of eIF5A and its hypusine modification in eukaryotes. Amino Acids. 38:491–500.
18. Quintas-Granados LI, Carvajal-Gamez BI, Villalpando JL, Ortega-Lopez J, Arroyo R, Azuara-Liceaga E, Álvarez-Sánchez ME. (2015) Bifunctional activity of deoxyhypusine synthase/hydroxylase from *Trichomonas vaginalis*, Biochimie. 24
19. Kemper WM, Berry IW, and Merrick WC. (1976) Purification and properties of rabbit reticulocyte protein synthesis initiation factors M2Ba and M2Bß J Biol Chem. 251: 5551–5557.
20. Benne R, Brown-Luedi ML, Hershey JWB. (1978) Purification and characterization of protein synthesis initiation factors eIF-1, eIF-4C, eIF-4D, and eIF-5 from rabbit reticulocytes. J Biol Chem. 253: 3070–3077.

21. Henderson A, Hershey JW. (2011) Eukaryotic translation initiation factor (eIF) 5A stimulates protein synthesis in *Saccharomyces cerevisiae*. Proc Natl Acad Sci USA. 108: 6415–9.
22. Saini P, Eyler DE, Green R, Dever TE. (2009) Hypusine-containing protein eIF5A promotes translation elongation. Nature. 459: 118–21.
23. Dias CA, Gregio AP, Rossi D, Galvao FC, Watanabe TF, Park MH, Valentini SR, Zanelli CF. (2012) eIF5A interacts functionally with eEF2. Amino Acids. 42: 697–702.
24. Gutierrez E, Shin BS, Woolstenhulme CJ, Kim JR, Saini P, Buskirk AR, Dever TE. (2013) eIF5A promotes translation of polyproline motifs. Mol Cell. 51: 35–45.
25. Schmidt C, Becker T, Heuer A, Braunger K, Shanmuganathan V, Pech M, Berninghausen O, Wilson DN, and Beckmann R. (2016) Structure of the hypusinylated eukaryotic translation factor eIF-5A bound to the ribosome. Nucleic Acids Res. 44: 1944–1951.
26. Melnikov S, Mailliot J, Shin BS, Rigger L, Yusupova G, Micura R, Dever TE, and Yusupov M. (2016). Crystal structure of hypusine-containing translation factor eIF5A bound to a rotated eukaryotic ribosome. J. Mol. Biol. 428: 3570–3576.
27. Schuller AP et al. (2017) eIF5A Functions Globally in Translation Elongation and Termination. In: Molecular Cell. 162: 872–884.
28. Nishimura K, and Kanemaki MT. (2014). Rapid depletion of budding yeast proteins via the fusion of an auxin-inducible degron (AID). Curr. Protoc. Cell Biol. 64, 20.9.1–20.9.16.
29. Liu YP, Nemeroff M, Yan Y P, Chen KY. (1997) Interaction of eukaryotic initiation factor 5A with the human immunodeficiency virus type 1 Rev response element RNA and U6 snRNA requires deoxyhypusine or hypusine modification. Biol. Signals. 6: 166–174.
30. Maier B, Ogihara T, Trace AP, Tersey SA, Robbins RD, Chakrabarti SK, Nunemaker CS, Stull ND, Taylor CA, Thompson JE, Dondero RS, Lewis EC, Dinarello CA, Nadler JL, Mirmira RG (2010) The unique hypusine modification of eIF5A promotes islet beta cell inflammation and dysfunction in mice. J Clin Invest. 120: 2156–2170.

31. Xu A, Chen KY. (2001) Hypusine is required for a sequence-specific interaction of eukaryotic initiation factor 5A with postsystematic evolution of ligands by exponential enrichment RNA. J. Biol. Chem. 276: 2555–2561.
32. Xu A, Jao DL, Chen KY. (2004) Identification of mRNA that binds to eukaryotic initiation factor 5A by affinity co-purification and differential display. Biochem J. 384: 585–590.
33. Kim KK, Hung LW, Yokota H, Kim R, Kim SH. (1998) Crystal structures of eukaryotic translation initiation factor 5A from *Methanococcus jannaschii* at 1.8 Å resolution. Proc. Natl. Acad. Sci. U.S.A. 95:10419–10424.
34. Zuk D, Jacobson A. (1998) A single amino acid substitution in yeast eIF-5A results in mRNA stabilization. EMBO J. 17:2914–2925.
35. Valentini SR, Casolari JM, Oliveira CC, Silver PA, McBride AE. (2002) Genetic interactions of yeast eukaryotic translation initiation factor 5A (eIF5A) reveal connections to poly (A)-binding protein and protein kinase C signaling. Genetics. 160: 393–405.
36. Park MH, Lee YB, Joe YA. (1997) Hypusine is essential for eukaryotic cell proliferation. Biol Signals. 6: 115–123.
37. Guan XY, Sham JS, Tang TC, Fang Y, Huo KK, Yang JM. (2001) Isolation of a novel candidate oncogene within a frequently amplified region at 3q26 in ovarian cancer. Cancer Res. 61: 3806–3809.
38. Lee NP, Tsang FH, Shek FH, Mao M, Dai H, Zhang C, Dong S, Guan XY, Poon RT, Luk JM (2010) Prognostic significance and therapeutic potential of eukaryotic translation initiation factor 5A (eIF5A) in hepatocellular carcinoma. Int J Cancer. 15: 968–976.
39. Xie D, Ma NF, Pan ZZ, Wu HX, Liu YD, Wu GQ, Kung HF, Guan XY. (2008) Overexpression of EIF-5A2 is associated with metastasis of human colorectal carcinoma. Human Pathology. 39: 80–86.
40. Hanauske-Abel HM, Slowinska B, Zagulska S, Wilson RC, Staiano-Coico L, Hanauske AR, McCaffrey T, Szabo P (1995) Detection of a sub-set of polysomal

mRNAs associated with modulation of hypusine formation at the G1-S boundary. Proposal of a role for eIF-5A in onset of DNA replication. FEBS Lett. 366: 92–98.

41. Balabanov S, Gontarewicz A, Ziegler P, Hartmann U, Kammer W, Copland M, Brassat U, Priemer M, Hauber I, Wilhelm T, Schwarz G, Kanz L, Bokemeyer C, Hauber J, Holyoake TL, Nordheim A, Bru¨mmendorf TH (2007) Hypusination of eukaryotic initiation factor 5A (eIF5A): a novel therapeutic target in BCR-ABL-positive leukemias identified by a proteomics approach. Blood. 109(4): 1701-1711.
42. Taylor CA, Liu Z, Tang TC, Zheng Q, Francis S, Wang TW, Ye B, Lust JA, Dondero R, Thompson JE. (2012) Modulation of eIF5A expression using SNS01 nanoparticles inhibits NF-κB activity and tumor growth in murine models of multiple myeloma. Mol. Ther. 20: 1305–1314.
43. Schwentke A, Krepstakies M, Mueller AK, Hammerschmidt-Kamper C, Motaal BA, Bernhard T, Hauber J and Kaiser A. (2012) *In vitro* and *in vivo* silencing of plasmodial dhs and eIf-5a genes in a putative, non-canonical RNAi-related pathway. BMC Microbiol. 13: 107.
44. Glick BR, Ganoza MC (1975) Identification of a soluble protein that stimulates peptide bond synthesis. Proc Natl Acad Sci U S A. 72(11): 4257-60.
45. Suetsuzu KH, Sekine SI, Sakai H, Takemoto CH, Terada T, Unzai S, Tame JRH, Kuramitsu S, Shirouzu M, Yokoyama S. (2004) Crystal structure of elongation factor P from *Thermus thermophilus* HB8. Proc. Natl. Acad. Sci. USA. 101: 9595–9600.
46. Aoki H, Xu J, Emili A, Chosay JG, Golshani A, Ganoza MC. (2008) Interactions of elongation factor EF-P with the *Escherichia coli* ribosome. FEBS J. 275: 671–81.
47. Navarre WW, Zou SB, Roy H, Xie JL, Savchenko A, Singer A, Edvokimova E, Prost LR, Kumar R, Ibba M, et al. (2010) PoxA, yjeK, and elongation factor P coordinately modulate virulence and drug resistance in *Salmonella enterica*. Mol Cell. 39: 209–221.
48. Yanagisawa T, Sumida T, Ishii R, Takemoto C, Yokoyama S. (2010) A paralog of lysyl-tRNA synthetase aminoacylates a conserved lysine residue in translation elongation factor P. Nat Struct Mol Biol. 17: 1136–1143.

49. Peil L, Starosta AL, Virumäe K, Atkinson GC, Tenson T, Remme J, Wilson DN. (2012) Lys34 of translation elongation factor EF-P is hydroxylated by YfcM. Nat Chem Biol. 8: 695–697.
50. Roy H, Zou SB, Bullwinkle TJ, Wolfe BS, Gilreath MS, Forsyth CJ, Navarre WW, Ibba M. (2011) The tRNA synthetase paralog PoxA modifies elongation factor-P with (R)-β-lysine. Nat Chem Biol. 7: 667–9.
51. Bullwinkle TJ, Zou SB, Rajkovic A, Hersch SJ, Elgamal S, Robinson N, Smil D, Bolshan Y, Navarre WW, Ibba M. (2013) (R)-β-Lysine-modified elongation factor P functions in translation elongation. J Biol Chem. 288: 4416–23.
52. Lassak J, Keilhauer EC, Fürst M, Wuichet K, Gödeke J, et al. (2015) Arginine-rhamnosylation as new strategy to activate translation elongation factor P. Nat. Chem. Biol. 11:266–70. Corrigendum. Nat. Chem. Biol. 11: 299.
53. Rajkovic A, Hummels KR, Witzky A, Erickson S, Gafken PR et al. (2016) Translation control of swarming proficiency in *Bacillus subtilis* by 5-amino-pentanolylated elongation factor P. J. Biol. Chem. 291: 10976–85.
54. Glick BR, Chladek S, Ganoza MC. (1979) Peptide bond formation stimulated by protein synthesis factor EF-P depends on the aminoacyl moiety of the acceptor. Eur J Biochem. 97: 23–28.
55. Blaha G, Stanley RE, Steitz TA. (2009) Formation of the first peptide bond: the structure of EF-P bound to the 70S ribosome. Science. 325: 966–970.
56. Elgamal S, Katz A,Hersch SJ, Newsom D, White P, et al. (2014) EF-P dependent pauses integrate proximal and distal signals during translation. PLOS Genet. 10: e1004553.
57. Ude S, Lassak J, Starosta AL, Kraxenberger T, Wilson DN, Jung K. (2013) Translation elongation factor EFP alleviates ribosome stalling at polyproline stretches. Science. 339: 82–5.
58. Doerfel LK, Wohlgemuth I, Kothe C, Peske F, Urlaub H, Rodnina MV. (2013) EF-P is essential for rapid synthesis of proteins containing consecutive proline residues. Science. 339: 85–8.

59. Woolstenhulme CJ, Parajuli S, Healey DW, Valverde DP, Petersen EN, Starosta AL, Guydosh NR, Johnson WE, Wilson DN, Buskirk AR. (2013) Nascent peptides that block protein synthesis in bacteria. Proc Natl Acad Sci USA. 110: E878–87.
60. Elgamal S, Artsimovitch I, Ibba M. (2016) Maintenance of transcription-translation coupling by elongation factor P. mBio. 7: e01373-16.
61. Benelli D, Maone E, Londei P. (2003) Two different mechanisms for ribosome/mRNA interaction in archaeal translation initiation. Mol. Microbiol. 50: 635-643.
62. Lecompte O, Ripp R, Thierry J-C, Moras D, Poch O. (2002) Comparative analysis of ribosomal proteins in complete genomes: an example of reductive evolution at the domain scale. Nucleic Acids Research. 30 (24):5382-5390.
63. Benelli D, Londei P. (2009) Begin at the beginning: evolution of translational initiation. Res Microbiol. 160: 493–501.
64. Pedulla N, Palermo R, Hasenöhrl D, Bläsi U, Cammarano P, Londei P. (2005) The archaeal eIF2 homologue: functional properties of an ancient translation initiation factor. Nucleic Acids Res. 33: 1804e1812.
65. Hasenöhrl D, Lombo T, Kaberdin V, Londei P, Bläsi U. (2008) Translation initiation factor a/eIF2 (-gamma) counteracts 5’ to 3’ mRNA decay in the archaeon *Sulfolobus solfataricus*. Proc. Natl. Acad. Sci. U.S.A. 105: 2146e2150.
66. Arkhipova V, Stolboushkina E, Kravchenko O, Kljashtorny V, Gabdulkhakov A, Garber M, Nikonov S, Märtens B, Bläsi U, Nikonov O. (2015) Binding of the 5′-Triphosphate end of mRNA to the γ-subunit of translation initiation factor 2 of the *Crenarchaeon Sulfolobus solfataricus*. J Mol Biol. 427(19):3086–95.
67. Hasenöhrl D, Benelli D, Barbazza A, Londei P, Bläsi U. (2006) *Sulfolobus solfataricus* translation initiation factor 1 stimulates translation initiation complex formation. RNA. 12: 674e682.
68. Guillon L, Schmitt E, Blanquet S, Mechulam Y. (2005) Initiator tRNA binding by e/aIF5B, the eukaryotic/archaeal homologue of bacterial initiation factor IF2. Biochemistry. 44 (47):15594–15601.

69. Benelli D, Marzi S, Mancone C, Alonzi T, la Teana A, Londei P. (2009) Function and ribosomal localization of aIF6, a translational regulator shared by archaea and eukarya. Nucleic Acids Res. 37: 256e267.
70. Bartig D, Lemkemeier K, Frank J, Lottspeich F, and Klink F (1992) The archaebacterial hypusine-containing protein: structural features suggest common ancestry with eukaryotic translation initiation factor 5A. Eur. J. Biochem. 204: 751–758.
71. Yao M, Ohsawa A, Kikukawa S, Tanaka I, Kimura M. (2003) Crystal structure of hyperthermophilic archaeal initiation factor 5A: a homologue of eukaryotic initiation factor 5A (eIF-5A) J Biochem. 133(1): 75–81.
72. Schümann H, and Klink F. (1990) Archaebacterial protein contains hypusine, a unique amino acid characteristic for eukaryotic translation factor 4D. Syst. Appl. Microbiol. 11: 103–107.
73. Bartig D, Schümann H, Klink F. (1990) The unique posttranslational modification leading to deoxyhypusine or hypusine is a general feature of the archaebacterial kingdom. System. Appl. Microbiol. 13: 112–116.
74. Prunetti L, Graf M, Blaby IK, Peil L, Makkay AM, Starosta AL et al. (2016) Deciphering the translation initiation factor 5A modification pathway in halophilic archaea. Archaea. 1–14.
75. Jansson BP, Malandrin L, Johansson HE. (2000) Cell cycle arrest in archaea by the hypusination inhibitor N(1)-guanyl-1,7-diaminoheptane. J Bacteriol. 182: 1158–1161.
76. Friedman M. and Oshima T. (1989) Polyamines of sulfur-dependent archaebacteria and their role in protein synthesis. J Biochem. 105: 1030–1033.
77. Gäbel K, Schmitt J, Schulz S, Näther DJ, Soppa J. (2013) A comprehensive analysis of the importance of translation initiation factors for *Haloferax volcanii* applying deletion and conditional depletion mutants. PLoS One. 8(11): e77188.
78. Wagner S, Klug G. (2007) An archaeal protein with homology to the eukaryotic translation initiation factor 5A shows ribonucleolytic activity. J. Biol. Chem. 282: 13966–13976.

79. Laemmli UK. (1970) “Cleavage of structural proteins during the assembly of the head of bacteriophage T4.” Nature 227, pp. 680–685.
80. Brock TD, Brock KM, Belly RT, Weiss RL. (1972) *Sulfolobus*: a new genus of sulfur-oxidizing bacteria living at low pH and high temperature. Arch. Mikrobiol. 84: 54–68.
81. Londei P, Altamura S, Cammarano P, Petrucci L. (1986) Differential features of ribosomes and of poly(U)-programmed cell-free systems derived from sulphur-dependent archaebacterial species. Eur. J. Biochem.157: 455–462.
82. Condo I, Ciammaruconi A, Benelli D, Ruggero D, Londei P. (1999) Cis-acting signals controlling translational initiation in the thermophilic archaeon *Sulfolobus solfataricus*. Mol. Microbiol. 34: 377–384.
83. Albers SV, Jonuscheit M, Dinkelaker S, Urich T, Kletzin A, Tampe R, Driessen AJ, Schleper C. (2006) Production of recombinant and tagged proteins in the hyperthermophilic archaeon *Sulfolobus solfataricus*. Appl. Environ. Microbiol. 72: 102–111.
84. Märtens B, Bezerra GA, Kreuter MJ, Grishkovskaya I, Manica A, Arkhipova V, Djinovic-Carugo K, Bläsi U. (2015) The heptameric SmAP1 and SmAP2 proteins of the crenarchaeon *Sulfolobus solfataricus* bind to common and distinct RNA targets. Life (Basel). 5: 1264–1281.
85. Schleper C, Kubo K, and Zillig W. (1992) The particle SSV1 from the extremely thermophilic archaeon *Sulfolobus* is a virus: demonstration of infectivity and of transfection with viral DNA. Proc. Natl. Acad. Sci. USA 89: 7645–7649.
86. Rappsilber J, Mann M. and Ishihama Y. (2007) Protocol for micro-purification, enrichment, pre-fractionation and storage of peptides for proteomics using StageTips. Nat. Protoc. 2, 1896–1906.
87. Cox J, Mann M. (2008). MaxQuant enables high peptide identification rates, individualized ppb-range mass accuracies and proteome-wide protein quantification. Nat. Biotechnol. 26 1367–1372.

88. Märtens B, Manoharadas S, Hasenöhrl D, Zeichen L, and Bläsi U. (2014) Back to translation: removal of aIF2 from the 5′-end of mRNAs by translation recovery factor in the crenarchaeon *Sulfolobus solfataricus*. Nucleic Acids Res. 42(4): 2505–2511.
89. Martin M. (2011) Cutadapt removes adapter sequences from high-throughput sequencing reads. EMBnet. J. 17, pp–10.
90. Quinlan AR, Hall IM. (2010) BEDTools: a flexible suite of utilities for comparing genomic features. Bioinformatics. 26: 841–842.
91. Wolfinger MT, Fallmann J, Eggenhofer F, Amman F. (2015) ViennaNGS: a toolbox for building efficient next- generation sequencing analysis pipelines. F1000Research. 4: 50.
92. Hasenöhrl D, Konrat R, Bläsi U. (2011) Identification of an RNase J ortholog in *Sulfolobus solfataricus*: implications for 5′-to-3′ directional decay and 5′-end protection of mRNA in Crenarchaeota. RNA (New York, N.Y.). 17: 99–107.
93. Klier H, Wohl T, Eckerskorn C, Magdolen V, Lottspeich F. (1993) Determination and mutational analysis of the phosphorylation site in the hypusine-containing protein Hyp2p. FEBS Lett. 334: 360–4.
94. Märtens B, Hou L, Amman F, Wolfinger MT, Evguenieva-Hackenberg E, Bäsi U. (2017) The SmAP1/2 proteins of the crenarchaeon *Sulfolobus solfataricus* interact with the exosome and stimulate A-rich tailing of transcripts. Nucleic Acids Res.
95. Nishiki Y, Farb TB, Friedrich J, Bokvist K, Mirmira RG, Maier B. (2013) Characterization of a novel polyclonal anti-hypusine antibody. SpringerPlus. 2: 421.
96. Wurtzel O, et al. (2010) A single-base resolution map of an archaeal transcriptome. Genome Res. 20: 133–141.
97. Tang TH, Polacek N, Zywicki M, Huber H, Brugger K, Garrett R, Bachellerie JP, Hüttenhofer A. (2005) Identification of novel non-coding RNAs as potential antisense regulators in the archaeon *Sulfolobus solfataricus*. Mol. Microbiol. 55, 469–481.
98. She Q, Singh RK, Confalonieri F, Zivanovic Y, Allard G, Awayez MJ, Chan-Weiher CC, Clausen IG, Curtis BA, De Moors A, Erauso G, Fletcher C, Gordon PM, Heikamp-de Jong I, Jeffries AC, Kozera CJ, Medina N, Peng X, Thi-Ngoc HP,

Redder P, Schenk ME, Theriault C, Tolstrup N, Charlebois RL, Doolittle WF, Duguet M, Gaasterland T, Garrett RA, Ragan MA, Sensen CW, Van der Oost J. (2001) The complete genome of the crenarchaeon *Sulfolobus solfataricus* P2. Proc. Natl. Acad. Sci. U.S.A. 98, 7835–7840.

99. Mandal A, Mandal S, Park MH. (2014) Genome-wide analyses and functional classification of proline repeat-rich proteins: potential role of eIF5A in eukaryotic evolution. PLoS One. 9: e111800.

100. Omer AD, Ziesche S, Ebhardt H, Dennis PP (2002) *In vitro* reconstitution and activity of a C/D box methylation guide ribonucleoprotein complex. Proc Natl Acad Sci USA 99: 5289–5294.

101. Franzetti B, Sohlberg B, Zaccai G, von Gabain A. (1997) Biochemical and serological evidence for an RNase E-like activity in halophilic Archaea. J Bacteriol 179: 1180–1185.

102. Evguenieva-Hackenberg E, Schiltz E, Klug G. (2002) Dehydrogenases from all three domains of life cleave RNA. J Biol Chem; 277: 46145-50.

103. Evguenieva-Hackenberg E, Walter P, Hochleitner E, Lottspeich F, Klug G. (2003) An exosome-like complex in *Sulfolobus solfataricus*. EMBO Rep, 4:889–893.

Acknowledgements

Let me premise that my PhD was probably one of the best period of my life and even if I felt like I was running a hurdles final, I enjoyed the support of people, who made me grateful for every single moment.

Prof. Anna LaTeana I don't know the "score of this race" but I hope that you're proud of me, thanks for all your support and mentoring.

Thanks to Prof. Tiziana Cacciamani, you are the most important person who held my hand when I moved my first steps in the research world, I hope you know how much everything you do/did means to me.

Thank you to Alice Romagnoli, I'm always telling you that you're my best creation, but now I know that I'm wrong, you're a great friend for me and you did everything by your own. We just worked together and I couldn't ask for a better colleague.

Thanks to Prof. Paolo Mariani, who believes in me from the beginning and his special coworkers who are helping us in the structural characterization of aIF5A.

Thanks to Prof. Udo Bläsi for this great opportunity at the MFPL institute and for the useful suggestions that he always offered me.

Thank you to Birgit Märtens, I learned a lot from you and from your way of working in the laboratory it's now clear for me which kind of scientist I'd like to be.

Working in Vienna for more than one year was a personal challenge that I won, the reality in which I lived made me strong and this is what I owe to my "Austrian family", that is very numerous.

Thanks to Marlena Rozner, Diego Oxilia Speratti, Muralidhar Tata, Petra Pusic, David Romero and all the people in the laboratory.

I will never forget my "see you soon immediately party" and the moment when you gave me the t-shirt, which is hanging on the wall of my apartment in Italy, as a trophy that I often admire.

Thanks to Armin Resch for all his support, let me tell you once again "What else?".

Thanks to my friends who enjoyed with me every day from a life time, to those who shared with me the university years, stay as you are and keep rocking.

Thank you to Valeria Stefania for being you and the sister I never had. 3.3.2016 is written on my skin and you know what this means for us.

The last words are for my family that is my everything.

Thanks to my parents, I love you both so much today and forever more.

Thank you to my brother Alessandro, when I looked at you carefully I see the best part of me, remember that you are the greatest joy of my life.